

ผลต่อการเพิ่มจำนวนและการเคลื่อนย้ายของเซลล์บุผิวหลอดเลือดดำจากกรรมพันธุ์ของ
โกฐจุฬาลัมพาในพิกัดนาโวโกฐและคุณลักษณะทางเคมีเบื้องต้น

นางสาวศรัณยา ทองอำไพ

วิทยานิพนธ์นี้เป็นส่วนหนึ่งของการศึกษาตามหลักสูตรปริญญาวิทยาศาสตรมหาบัณฑิต
สาขาวิชาชีวเวชเคมี ภาควิชาชีวเคมีและจุลชีววิทยา
คณะเภสัชศาสตร์ จุฬาลงกรณ์มหาวิทยาลัย
ปีการศึกษา 2555

บทคัดย่อและแฟ้มข้อมูลฉบับเต็มของวิทยานิพนธ์นี้พร้อมทั้งเอกสารแนบที่เกี่ยวข้อง
เป็นแฟ้มข้อมูลของนิสิตเจ้าของวิทยานิพนธ์ที่ส่งผ่านทางบัณฑิตวิทยาลัย

The abstract and full text of theses from the academic year 2011 in Chulalongkorn University Intellectual Repository (CUIR)
are the thesis authors' files submitted through the Graduate School.

HUMAN UMBILICAL VEIN ENDOTHELIAL CELL PROLIFERATION AND MIGRATION
OF KOT CHULALUMPA IN PHIKUD NAVAKOT AND
PRELIMINARY CHEMICAL PROFILE

Miss Sarunya Tongumpai

A Thesis Submitted in Partial Fulfillment of the Requirements
for the Degree of Master of Science Program in Biomedical Chemistry

Department of Biochemistry and Microbiology

Faculty of Pharmaceutical Sciences

Chulalongkorn University

Academic Year 2012

Copyright of Chulalongkorn University

ศรัณยา ทองอำไพ : ผลต่อการเพิ่มจำนวนและการเคลื่อนย้ายของเซลล์บุผิวหลอดเลือดดำ
จากรกมนุษย์ของโกลูจุพาลัมพาในพิกัดนว โกลูและคุณลักษณะทางเคมีเบื้องต้น.
(HUMAN UMBILICAL VEIN ENDOTHELIAL CELL PROLIFERATION AND
MIGRATION OF KOT CHULALUMPA IN PHIKUD NAVAKOT AND
PRELIMINARY CHEMICAL PROFILE) อ.ที่ปรึกษาวิทยานิพนธ์หลัก : รศ.ภญ.ดร. ดวง
เดือน เมฆสุริยพันธ์, อ.ที่ปรึกษาวิทยานิพนธ์ร่วม : ดร.สัญญา หกพุดชา, 101 หน้า.

พิกัดนวโกลูเป็นส่วนประกอบเครื่องยาที่สำคัญของยาหอมนวโกลู เพื่อรักษากลุ่มอาการทาง
ระบบไหลเวียนโลหิต วัตถุประสงค์ของการศึกษาครั้งนี้เพื่อประเมินผลของสารสกัดสมุนไพรจากเครื่องยา
ในพิกัดนวโกลูต่อการเพิ่มจำนวนเซลล์และการเคลื่อนย้ายของเซลล์บุผิวหลอดเลือดดำจากรกมนุษย์
ECV304 และจัดทำคุณลักษณะทางเคมีเบื้องต้นของสารสกัดที่มีฤทธิ์ดังกล่าว เครื่องยา 9 ชนิดใน
พิกัดนวโกลูนำมาตรวจสอบคุณภาพตามข้อกำหนดของตำรายาสมุนไพรไทยก่อนสกัดด้วย 50% เอ
ทานอลหรือด้วยน้ำได้สารสกัดสำหรับศึกษาในระดับเซลล์ จากการวิเคราะห์ด้วยวิธี MTT พบว่าเมื่อบ่มเซลล์
ด้วยสารสกัดเอทานอลของโกลูจุพาลัมพานาน 24 ชั่วโมงจำนวนเซลล์บุผิวหลอดเลือดเพิ่มขึ้นอย่างมี
นัยสำคัญทางสถิติและมีความแข็งแรงในการออกฤทธิ์มากที่สุด จึงนำมาศึกษาฤทธิ์การเคลื่อนย้ายเซลล์ด้วยวิธี
scratch พบว่าเมื่อบ่มเซลล์ด้วยสารสกัดโกลูจุพาลัมพาในสภาวะที่ไม่มีซีรัมเป็นเวลา 6 ชั่วโมงสามารถทำ
ให้แผลปิดเร็วขึ้นโดยความแข็งแรงในการออกฤทธิ์สัมพันธ์กับความเข้มข้นของสารสกัด และยังสามารถลด
ปริมาณอนุมูลอิสระภายในเซลล์ได้อย่างมีนัยสำคัญทางสถิติโดยไปกระตุ้นการทำงานของเอนไซม์
superoxide dismutase (SOD) ทั้งนี้ไม่มีผลต่อการทำงานของเอนไซม์ glutathione peroxidase และ catalase
นอกจากนี้สารสกัดโกลูจุพาลัมพายังกระตุ้นการทำงานของ cyclooxygenase (COX) -1 และ COX-2 ได้
อย่างมีนัยสำคัญทางสถิติแต่ไม่มีผลต่อระดับไนตริกออกไซด์ภายในเซลล์เมื่อทดสอบด้วยวิธี 2,3-
diaminonaphthalene จากการศึกษาคุณลักษณะทางเคมีเบื้องต้นของสารสกัดโกลูจุพาลัมพาด้วยเทคนิค
high performance liquid chromatography พบฟลาโวนอยด์ apigenin, eriodictyol, luteolin, quercetin และ
rutin เล็กน้อยซึ่งอาจใช้เป็นสารเทียบสำหรับการควบคุมคุณภาพของสารสกัดโกลูจุพาลัมพา สรุปได้ว่า
สารสกัดเอทานอลของโกลูจุพาลัมพาสามารถเพิ่มจำนวนเซลล์และการเคลื่อนย้ายเซลล์โดยกระตุ้นการ
ทำงานของเอนไซม์ SOD เพื่อลดอนุมูลอิสระภายในเซลล์ และกระตุ้นการทำงานของเอนไซม์ COX ผ่าน
ทางวิถีที่ไม่ขึ้นกับระดับไนตริกออกไซด์ภายในเซลล์บุผิวหลอดเลือดเพื่อเร่งการเพิ่มจำนวนและการ
เคลื่อนย้ายเซลล์บุผิวหลอดเลือด ดังนั้น โกลูจุพาลัมพาซึ่งเป็นหนึ่งในเครื่องยาพิกัดนวโกลูอาจมีศักยภาพ
ไปเร่งการสร้างหลอดเลือดทดแทนหลอดเลือดที่ถูกทำลายสำหรับบรรเทาอาการทางระบบไหลเวียนโลหิต

ภาควิชา.....ชีวเคมีและจุลชีววิทยา.....ลายมือชื่อนิสิต.....
สาขาวิชา.....ชีวเวชเคมี.....ลายมือชื่ออ.ที่ปรึกษาวิทยานิพนธ์หลัก.....
ปีการศึกษา.....2555.....ลายมือชื่ออ.ที่ปรึกษาวิทยานิพนธ์ร่วม.....

5276595233 : MAJOR BIOMEDICINAL CHEMISTRY

KEYWORDS : PHIKUD NAVAKOT / CELL PROLIFERATION / CELL
MIGRATION / ECV304 CELLS / SUPEROXIDE DISMUTASE /
CYCLOOXYGENASE

SARUNYA TONGUMPAI : HUMAN UMBILICAL VEIN ENDOTHELIAL
CELL PROLIFERATION AND MIGRATION OF KOT CHULALUMPA IN
PHIKUD NAVAKOT AND PRELIMINARY CHEMICAL PROFILE.
ADVISOR : ASSOC. PROF. DUANGDEUN MEKSURIYEN, Ph.D., CO-
ADVISOR : SANYA HOKPUTSA, Ph.D., 101 pp.

Phikud Navakot has been recognized as a part of Yahom Navakot for the treatment of circulatory disorder. The present study aimed to evaluate the effects of the ethanol and water extracts of crude drugs in Phikud Navakot on proliferation and migration of human umbilical vein endothelial ECV304 cells. Quality control parameters of nine crude drugs were examined according to Thai Herbal Pharmacopoeia before extraction with either 50% ethanol or water. Treatment of the cells with the ethanol extract of Kot Chulalumpa (*Artemisia pallens*, APES) for 24 h significantly increased cell proliferation using MTT reduction assay. Among nine herbal extracts, APES exhibited the highest activity. An *in vitro* scratch assay showed that treatment with APES for 6 h under serum-free condition significantly promoted endothelial wound closure in a concentration-dependent manner via enhancing cell migration. Furthermore, DCFH-DA assay revealed that APES significantly decreased intracellular reactive oxygen species level *via* activating the activity of superoxide dismutase (SOD) but not glutathione peroxidase and catalase. APES significantly stimulated both cyclooxygenase (COX) -1 and COX-2 activities without affecting intracellular nitric oxide level using 2,3-diaminonaphthalene assay. High performance liquid chromatography profile revealed the presence of flavonoids such as apigenin, eriodictyol, luteolin, quercetin and rutin, which might be used as chemical markers for identification of APES. Thus, the ethanol extract of *A. pallens* enhanced endothelial cell proliferation and migration *via* activating the activities of SOD and COX in a nitric oxide-independent pathway, leading to its potential role in angiogenesis for the treatment of circulatory disorder of Phikud Navakot.

Department : Biochemistry and Microbiology Student's Signature.....

Field of Study : Biomedical Chemistry Advisor's Signature.....

Academic Year : 2012 Co-advisor's Signature.....

ACKNOWLEDGEMENTS

I would like to very grateful to my thesis advisor, Associate Professor Dr. Duangdeun Meksuriyen for her patience, understanding, kindness and encouragement throughout this study. I also deeply thank my co-advisor, Dr. Sanya Hokputsa for his valuable advice on the concept of quality control.

I also sincerely thank the members of thesis examination committee, Assistant Professor Dr. Boonsri Ongpipattanakul, Associate Professor Dr. Sunanta Pongsamart, Associate Professor Dr. Uthai Sotanaphun, for their invaluable time and comment.

I also grateful to Assistant Professor Dr. Surachai Unchern for providing human umbilical vein endothelial ECV304 cells and Associate Professor Dr. Noppamas Soonthornchareonnon for providing the authentic samples of crude drugs in Phikud Navakot and the staffs at Phytochemical Research Group, Research and Development Institute, Government Pharmaceutical Organization for their kindness and assistance.

I would like to thank Pharmaceutical Research Instrument Center and Chulalongkorn University Drug and Health Products Innovation Promotion Center (CU.D.HIP), Faculty of Pharmaceutical Sciences, Chulalongkorn University for supporting laboratory equipments and research instruments.

I wish to grateful thank the 90th Anniversary of Chulalongkorn University Fund (Ratchadapiseksomphot Endowment Fund) for financial supporting and a Grant-in-Aid for Scientific Research from the National Research Council of Thailand (NRCT 2011-33).

I also sincerely thank to all staff members and my friends of Department of Biochemistry and Microbiology, Faculty of Pharmaceutical Sciences, Chulalongkorn University.

Finally, I wish to express my grateful thank to my family for their love, understanding, supporting and encouragement.

CONTENTS

	Page
ABSTRACT IN THAI.....	iv
ABSTRACT IN ENGLISH.....	v
ACKNOWLEDGEMENTS.....	vi
CONTENTS.....	vii
LIST OF TABLES.....	viii
LIST OF FIGURES.....	x
LIST OF ABBREVIATIONS.....	xii
CHAPTER	
I INTRODUCTION.....	1
II LITERATURE REVIEW.....	6
III MATERIALS AND METHODS.....	16
IV RESULTS AND DISCUSSION.....	27
V CONCLUSIONS.....	59
REFERENCES.....	62
APPENDICES	
APPENDIX A.....	76
APPENDIX B.....	79
APPENDIX C.....	91
VITA.....	101

LIST OF TABLES

Table		Page
1	Nine herbs in Phikud Navakot and part used.....	7
2	Biological activities in <i>Artemisia species</i>	8
3	Specification quality control parameters of nine crude drugs in Phikud Navakot.....	30
4	Extract codes and yields of the extracts from nine crude drugs in Phikud Navakot.....	31
5	Summary of the biological activities of APES on ECV304 cells...	51
6	Summary of wavelength at maximum absorbance and retention time obtained from UV spectra and HPLC chromatograms.....	53
7	Flavonoid contents found in APES.....	57
8	The percentage of cell viability of AD at various concentrations for 24 h measured by MTT assay.....	79
9	The percentage of cell viability of AL at various concentrations for 24 h measured by MTT assay.....	79
10	The percentage of cell viability of AP at various concentrations for 24 h measured by MTT assay.....	80
11	The percentage of cell viability of AS at various concentrations for 24 h measured by MTT assay.	80
12	The percentage of cell viability of LC at various concentrations for 24 h measured by MTT assay.....	81
13	The percentage of cell viability of NJ at various concentrations for 24 h measured by MTT assay.....	81
14	The percentage of cell viability of PK at various concentrations for 24 h measured by MTT assay.....	82
15	The percentage of cell viability of SC at various concentrations for 24 h measured by MTT assay.....	82
16	The percentage of cell viability of TC at various concentrations for 24 h measured by MTT assay.....	83

Table	Page
17	Time-dependent study of cell migration of APES with FBS for 6, 12 and 24 h measured by <i>in vitro</i> scratch assay..... 83
18	Time-dependent study of cell migration of APES without FBS for 6, 12 and 24 h measured by <i>in vitro</i> scratch assay..... 84
19	Time-dependent study of cell viability of APES with FBS for 6, 12 and 24 h measured by MTT assay..... 84
20	Time-dependent study of cell viability of APES without FBS for 6, 12 and 24 h measured by MTT assay..... 85
21	The percentage of DCF fluorescence of APES at various concentrations for 6 h measured by DCFH-DA assay..... 85
22	Concentration-dependent study of APES on SOD activity in ECV304 cells for 6 h..... 86
23	Calibration curve of NADPH..... 86
24	Concentration-dependent study of APES on GPx activity in ECV304 cells for 6 h..... 87
25	Calibration curve of H ₂ O ₂ 87
26	Concentration-dependent study of APES on CAT activity in ECV304 cells for 6 h..... 88
27	Calibration curve of NO ₂ ⁻ 88
28	Time-dependent study of APES on NO ₂ ⁻ production for 0.5, 1, 2 and 6 h measured by DAN assay..... 89
29	Concentration-dependent study of APES on COX activity in ECV304 cells for 6 h..... 89
30	Concentration-dependent study of APES on COX-1 and COX-2 activities in ECV304 cells for 6 h..... 90

LIST OF FIGURES

Figure		Page
1	Conceptual framework of the present study.....	3
2	Experimental design of the present study.....	5
3	Macroscopic evaluation of nine crude drugs in Phikud Navakot.....	28
4	Effect of the extracts on viability of ECV304 cells using MTT reduction assay.....	33
5	Effect of APES and LCES on cell proliferation.....	34
6	Effect of APES on cell migration in the presence of FBS.....	36
7	Effect of APES on cell migration in the absence of FBS.....	37
8	Concentration-dependent studies of APES on cell in the absence of FBS.....	38
9	Concentration- and time-dependent studies of APES on cell proliferation.....	39
10	Comparison between cell migration and viability affected by APES.....	40
11	Representative triple-stained microscopic images of endothelial cell culture with or without APES.....	42
12	Concentration- dependent effects of APES-reduced intracellular ROS.....	43
13	Effect of APES on SOD activity.....	45
14	Effect of APES on GPx activity.....	46
15	Effect of APES on CAT activity.....	47
16	Effect of APES on intracellular NO level in ECV304 cells.....	48
17	Effect of APES on cyclooxygenase activity in ECV304 cells.....	50
18	UV spectra of APES and standard flavonoids of rutin, eriodictyol, luteolin, quercetin and apigenin.....	54
19	HPLC chromatogram of rutin, eriodictyol, luteolin, quercetin and apigenin monitored at 270 nm.....	55
20	HPLC fingerprint obtained from APES as compared with standard	

Figure		Page
	flavonoids.....	56
21	Summary of biological activities of APES in ECV304 cells and HPCL chromatogram of APES.....	60
22	Thin-layer chromatograms of AD.....	91
23	Thin-layer chromatograms of AL.....	92
24	Thin-layer chromatograms of AP.....	93
25	Thin-layer chromatograms of AS.....	94
26	Thin-layer chromatograms of LC.....	95
27	Thin-layer chromatograms of NJ.....	96
28	Thin-layer chromatograms of PK.....	97
29	Thin-layer chromatograms of SC.....	98
30	Thin-layer chromatograms of TC.....	99
31	Calibration curve of rutin, eriodictyol, luteolin, quercetin and apigenin.....	100

LIST OF ABBREVIATION

%	percentage
AD	<i>Angelica dahurica</i>
ADES	ethanol extract of <i>Angelica dahurica</i> and further spray-dried
ADWS	water extract of <i>Angelica dahurica</i> and further spray-dried
AGEs	advanced glycation end products
AL	<i>Atractylodes lancea</i>
ALES	ethanol extract of <i>Atractylodes lancea</i> and further spray-dried
ALWF	water extract of <i>Atractylodes lancea</i> and further freeze-dried
ANOVA	analysis of variance
AP	<i>Artemisia pallens</i>
APES	ethanol extract of <i>Artemisia pallens</i> and further spray-dried
APWS	water extract of <i>Artemisia pallens</i> and further spray-dried
AS	<i>Angelica sinensis</i>
ASES	ethanol extract of <i>Angelica sinensis</i> and further spray-dried
ASWS	water extract of <i>Angelica sinensis</i> and further spray-dried
CAT	catalase
CO ₂	carbon dioxide
COX	cyclooxygenase
COX-1	cyclooxygenase-1
COX-2	cyclooxygenase-2
Cu/Zn-SOD	copper/zinc superoxide dismutase
DAN	2,3-diaminonaphthalene
DCF	dichlorofluorescein
DCFH-DA	2',7'-dichlorodihydrofluorescein diacetate
DMSO	dimethyl sulfoxide
DNA	deoxyribonucleic acid
DPPH	2, 2-diphenyl-1-picrylhydrazyl

DuP-697	5-bromo-2-(4-fluorophenyl)-3-(4-(methylsulfonyl)phenyl)-thiophene
EC ₅₀	half maximal effective concentration
ECV304	transformed human umbilical vein endothelial cells
EDTA	ethylenediaminetetraacetic acid
EGF	epidermal growth factor
eNOS	endothelial nitric oxide synthase
<i>et al.</i>	<i>et alii</i> , and others
FBS	fetal bovine serum
GPx	glutathione peroxidase
GR	glutathione reductase
GSH	glutathione reductase
GSSG	oxidized glutathione
h	hour
HCl	hydrochloric acid
HIF-1 α	hypoxia inducible factor-1 alpha
HO-1	heme oxygenase-1
H ₂ O ₂	hydrogen peroxide
HPLC	high performance liquid chromatography
HPTLC	high performance thin layer chromatography
HRP	horseradish peroxidase
IC ₅₀	half maximal inhibitory concentration
IL-1 β	interleukin-1 beta
iNOS	inducible nitric oxide synthase
λ_{\max}	wavelength of maximum absorption
LC	<i>Ligusticum chuanxiong</i>
LCES	ethanol extract of <i>Ligusticum chuanxiong</i> and further spray-dried
LSWS	water extract of <i>Ligusticum chuanxiong</i> and further spray-dried
LSD	least significant difference
5-LOX	5-lipoxygenase
LPS	lipopolysaccharide

M	molar
MAPK	mitogen-activated protein kinase
β -ME	beta-mercaptoethanol
mg	milligram
min	minute
mL	milliliter
Mn-SOD	manganese-superoxide dismutase
MS	mass spectrometry
MTT	3-(4, 5-dimethylthiazol-2-yl)-2, 5-diphenyltetrazolium bromide
NaCl	sodium chloride
NADH	nicotinamide adenine dinucleotide
NADPH	nicotinamide adenine dinucleotide phosphate
NaOH	sodium hydroxide
NJ	<i>Nardostachys jatamansi</i>
NJEF	ethanol extract of <i>Nardostachys jatamansi</i> and further freeze-dried
NJWF	water extract of <i>Nardostachys jatamansi</i> and further freeze-dried
nm	nanometer
NO	nitric oxide
NO_2^-	nitrite
NOS	nitric oxide synthase
O_2^\cdot	superoxide radical
OD	optical density
PBS	phosphate-buffered saline
PDA	photodiode array
PDGF	platelet-derived growth factor
PG	prostaglandin
PGE2	prostaglandin E2
PI	propidium iodide
pH	negative logarithm of hydrogen ion concentration
PK	<i>Picrorhiza kurrooa</i>
PKES	ethanol extract of <i>Picrorhiza kurrooa</i> and further spray-dried

PKWS	water extract of <i>Picrorhiza kurroo</i> and further spray-dried
PMSF	phenylmethanesulfonyl fluoride
RAW 264.7	mouse leukaemic monocyte macrophage cell line
RFU	relative fluorescence units
ROS	reactive oxygen species
SC	<i>Saussurea costus</i>
SC-560	5-(4-chlorophenyl)-1-(4-methoxyphenyl)-3-(trifluoromethyl)-1H-pyrazole
SCES	ethanol extract of <i>Saussurea costus</i> and further spray-dried
SCWF	water extract of <i>Saussurea costus</i> and further freeze-dried
S.E.M.	standard error of mean
SOD	superoxide dismutase
TC	<i>Terminalia chebula</i>
TCES	ethanol extract of <i>Terminalia chebula</i> and further spray-dried
TCWS	water extract of <i>Terminalia chebula</i> and further spray-dried
TMPD	<i>N,N,N',N'</i> -tetramethyl- <i>p</i> -phenylenediamine
TNF- α	tumor necrosis factor alpha
TXA2	thromboxane A2
μ L	microliter
μ M	micromolar
UV	ultraviolet
VEGF	vascular endothelial growth factor
WHO	World Health Organization
WST-1	2-(4-iodophenyl)-3-(4-nitrophenyl)-5-(2,4-disulfophenyl)-2H-tetrazolium, monosodium salt
XO	xanthine oxidase

CHAPTER I

INTRODUCTION

According to the Ministry of Public Health of Thailand, vascular and circulatory disorders play the major role in the top five causes of death in 2008 such as atherosclerosis, hypertension and stroke. The main pathogenesis of the diseases was involved in endothelial dysfunction. Endothelial cells lining in inner vascular wall play a major role in the regulation of vascular tone. The loss of integrity of the inner vascular wall would cause endothelial dysfunction due to oxidative stress, imbalance nitric oxide production or inflammation (Huang *et al.*, 2010). The inflammatory process was associated to pre-atherosclerosis (Libby *et al.*, 2002). Nowadays, the cost of drugs used in treatment of circulatory disorders was relatively high. According to the 10th National Economic and Social Development Plan of Thailand (2550-2554), herbal medicines have been promoted for primary health care. According to Thai traditional knowledge, many herbal medicines have been issued in the List of Herbal Medicinal Products A.D. 2011. Phikud Navakot has been recognized as part of Yahom Navakot and Yahom Tepachit for the treatment of circulatory disorder (Chavalittumrong *et al.*, 2010). However, the lack of scientific evidences to support the use of herbal medicines is still the major concern. Not only efficacy, safety but also quality of herbal medicines is essential to be carried out. Since one of the factors involved in efficacy and safety of herbal medicine is the quality of raw material (Liang *et al.*, 2004). Therefore, the aim of this study was to determine quality control of nine crude drugs in Phikud Navakot followed by evaluation of the selected crude drug on cell proliferation and migration of human endothelial cells.

Conceptual framework

Quality control of nine crude drugs in Phikud Navakot was performed according to Thai Herbal Pharmacopoeia. Each crude drug was extracted with either 50% ethanol or water and was subjected to proliferative study in endothelial cells. The extract with the highest potency was selected to determine cell migration in a model

of wounded endothelial cells. The extract may affect the levels of ROS and nitric oxide (NO) including cyclooxygenase (COX) activity in endothelial cells (Figure 1).

Objectives

1. To study the effect of the selected extract from nine crude drugs in Phikud Navakot on cell proliferation and migration in human umbilical vein endothelial ECV 304 cells.
2. To analyze preliminary chemical profile of the selected bioactive extract.

Scope of study

Quality control of nine crude drugs in Phikud Navakot was performed and their extracts were screened for the proliferative effect on endothelial cells. The selected extract with the highest proliferative potency was subjected to cell migration study. Intracellular ROS affected by the extract was determined under normal condition and wounded endothelial cells. The function of antioxidant enzymes *i.e.* superoxide dismutase (SOD), glutathione peroxidase (GPx) and catalase (CAT) was measured. Intracellular NO level and COX activity influenced by the extract was also determined. The preliminary chemical profile of the bioactive extract was compared with standard flavonoids.

Experimental design

To obtain reproducible results, the assessment of quality control of nine crude drugs in Phikud Navakot was performed according to Thai Herbal Pharmacopoeia including foreign matter, loss on drying, total ash, acid-insoluble ash, ethanol-soluble extractive and water-soluble extractive. The crude drugs which hit acceptance criteria were further extracted with 50% ethanol or water, solvents normally used in Thai traditional medicine. The effect of the extracts on endothelial cell proliferation were investigated by using 3-(4, 5-dimethylthiazol-2-yl)-2, 5-diphenyltetrazolium bromide (MTT) assay. The one which exhibited the highest proliferative effect was selected for further studies. Cell migration was determined using an *in vitro* scratch assay.

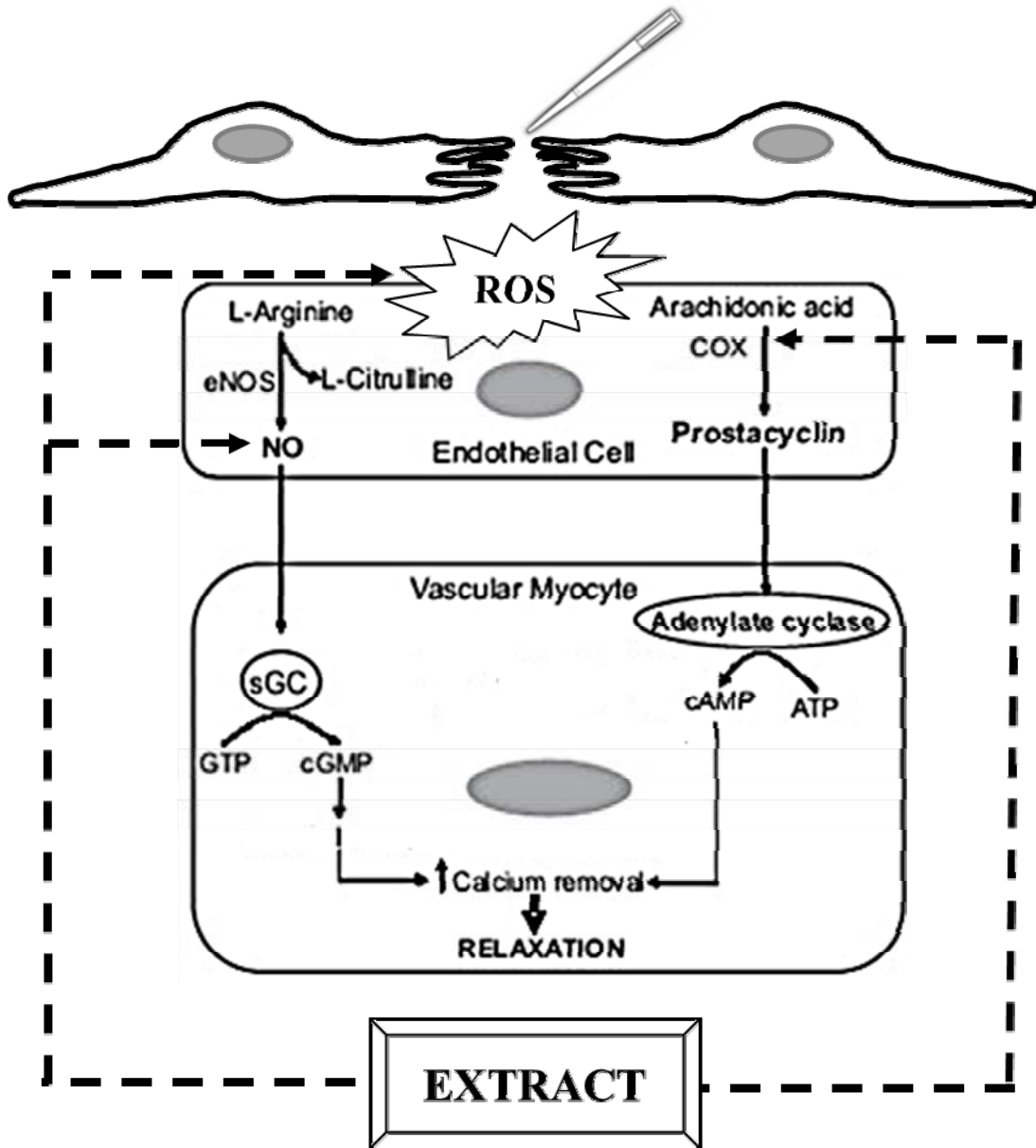


Figure 1. Conceptual framework of the present study.

Measurement of intracellular ROS level was determined using 2',7'-dichlorodihydrofluorescein diacetate (DCFH-DA) assay. Measurement of the antioxidant enzyme activities such as SOD, GPx and CAT were determined using commercial assay kits. Intracellular NO level affected by the extract was determined using 2,3-diaminonaphthalene (DAN) assay. COX activity was determined using a commercial assay kit. The preliminary chemical profile of the bioactive herbal extract was performed using high performance liquid chromatography (HPLC) as compared with standard flavonoids (Figure 2).

Contribution of the study

1. The information about endothelial cell proliferation and migration of the crude drugs in Phikud Navakot might provide a scientific data to support the application of Phikud Navakot for the treatment of circulatory disorder.
2. The information about the preliminary chemical profile of the herbal extract in Phikud Navakot might provide fingerprint comparison in order to obtain reproducible bioactive extract.

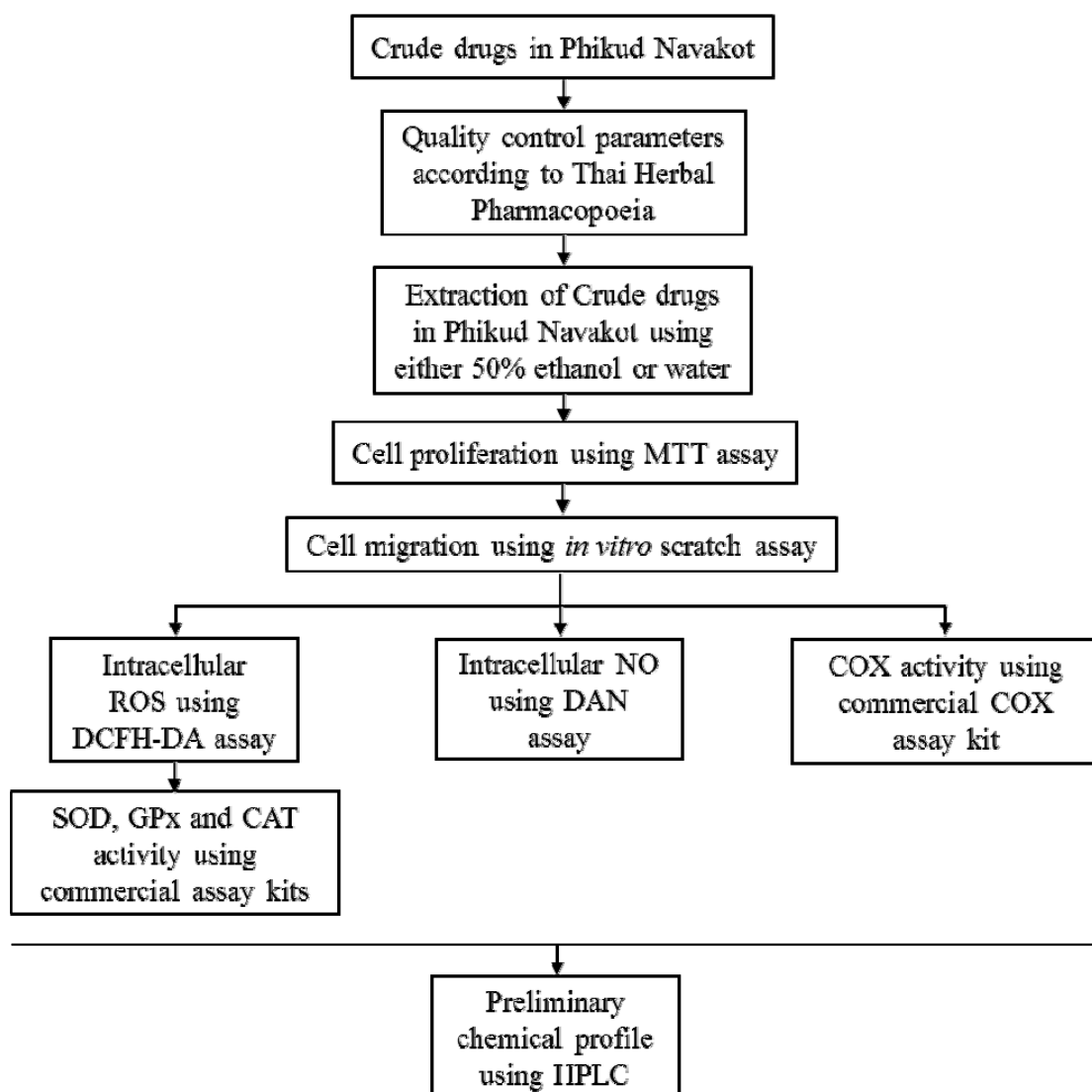


Figure 2. Experimental design of the present study.

CHAPTER II

LITERATURE REVIEW

Crude drugs in Phikud Navakot and biological activities

Phikud Navakot, has been recognized as part of Thai traditional recipes in Yahom Navakot, is composed of nine crude drugs in an equal proportion as shown in Table 1.

Kot Soa is the root of *Angelica dahurica* (AD). Furanocoumarins were considered as its major component. Imperatorin exhibited inhibitory effect on concanavalin A-induced hepatitis in mice (Okamoto *et al.*, 2001). Imperatorin inhibited (COX-2) (Ban *et al.*, 2003) *via* arachidonate metabolism (Abad *et al.*, 2001).

Kot Kamao is the rhizome of *Atractylodes lancea* (AL). Polyacetylenes from *n*-hexane extract of *A. lancea* inhibited 5-lipoxygenase (5-LOX) and cyclooxygenases-1 (COX-1) (Resch *et al.*, 2001), leading to a decrease in phosphoinositide breakdown and inhibition of thromboxane A₂ (TXA₂) (Park *et al.*, 2003).

Kot Chulalumpa is the aerial part of *Artemisia pallens* (AP). Phytochemical investigation of acetone extract showed the presence of pallensin, 4-epipallensin, santonin, valgarin and 4-epivalgarin (Ruikar *et al.*, 2011), sesquiterpene lactones (Catalan *et al.*, 1990), germacranolide (Rojatkarar *et al.*, 1996; Pujar *et al.*, 2000) and furano-sesquiterpenes (Misra *et al.*, 1991). Santonin from AP analyzed by high performance thin layer chromatography (HPTLC) (Ruikar *et al.*, 2010), artemisinin analyzed by LC/MS were quantitatively measured. The amount of artemisinin was 0.1031% w/w in AP (Suresh *et al.*, 2011). Phenolic and flavonoid content of AP in the methanol extract were found.

The methanol extract exhibited radical scavenging activities against DPPH and nitric oxide, giving EC₅₀ values of 292.7 and 204.61 µg/mL (Ruikar *et al.*, 2011). The acetone extract of AP indicated potent anti-inflammatory activity (Ruikar *et al.*, 2011). Hot-water extract of *A. princeps* leaf at the concentration of 5 µg/mL significantly stimulated endothelial cell proliferation *via* activation of basic fibroblast growth factor (Kaji *et al.*, 1990). Several biological activities of *Artemisia* species were summarized in Table 2.

Table 1. Nine crude drugs in Phikud Navakot and plant part used.

Crude drug	Scientific name	Abbreviation	Family	Part used
Kot Soa	<i>Angelica dahurica</i> (Fisch.) Benth. & Hook.f.	AD	Apiaceae	root
Kot Kamao	<i>Atractylodes lancea</i> (Thunb.) DC.	AL	Asteraceae	rhizome
Kot Chulalumpa	<i>Artemisia pallens</i> Walls ex DC.	AP	Asteraceae	aerial part
Kot Chiang	<i>Angelica sinensis</i> (Oliv.) Diels	AS	Apiaceae	root
Kot Huabua	<i>Ligusticum chuanxiong</i> Hort.	LC	Apiaceae	rhizome
Kot Jatamansi	<i>Nardostachys jatamansi</i> (D. Don) DC.	NJ	Valerianaceae	root and rhizome
Kot Kanprao	<i>Picrorhiza kurroa</i> Royle ex Benth.	PK	Scrophulariaceae	rhizome
Kot Kradook	<i>Saussurea costus</i> (Falc.) Lipsch.	SC	Asteraceae	root
Kot Pungpla	<i>Terminalia chebula</i> Retz.	TC	Combretaceae	gall

Table 2. Biological activities in *Artemisia species*

<i>Artemisia</i> species	Part used/ extraction solvent	Constituents	Biological activity	References
<i>A. annua</i>	aerial part/ methanol	quercetin, kaempferol, caffeic or ferulic conjugates and gallic acid (0.74±0.004, 0.74±0.005, 52.49±1.046 and 70.96±1.054 µg g ⁻¹ of dry matter)	antioxidant	Carvalho <i>et al.</i> , 2011
	aerial part/ dichloromethane	essential oil	antibacterial, antifungal and antioxidant	Cavar <i>et al.</i> , 2012
	leaf/water	-	anti-inflammatory	Melillo de Magalhães <i>et al.</i> , 2012
<i>A. arborescens</i>	aerial part/ methanol	kaempferol, caffeic or ferulic conjugates and gallic acid (4.68±0.045, 1275.71±0.788 and 266.46±0.136 µgg ⁻¹ of dry matter)	antioxidant	Carvalho <i>et al.</i> , 2011
<i>A. argentea</i>	aerial part/ alcohol	3,5-O-dicaffeoylquinic acid and 5-O-caffeoylquinic acid (300 mg/100 g dried plant)	antioxidant	Gouveia and Castilho, 2011

Table 2. (continued)

<i>Artemisia</i> species	Part used/ extraction solvent	Constituents	Biological activity	References
<i>A. argyi</i>	leaf/ 95% ethanol	artemilinin A and isoartemisolid	NO inhibitory guaianolide-derived	Wang <i>et al.</i> , 2013
<i>A. campestris</i>	aerial part/ water	-	antioxidant	Saoudi <i>et al.</i> , 2010
	leaf/ water	-	antioxidant	Sefi <i>et al.</i> , 2012
<i>A. capillaris</i>	aerial part/ water	-	antifibrotic	Wang <i>et al.</i> , 2012
<i>A. copa</i>	aerial part/ water	-	anti-inflammatory	Mino <i>et al.</i> , 2004
	aerial part/ water	-	vasorelaxing and hypotensive effects	Gorzalczany <i>et al.</i> , 2013
<i>A. fukudo</i>	leaf	α -thujone (48.28%), β -thujone (12.69%), camphor (6.95%) and caryophyllene (6.01%)	anti-inflammatory	Yoon <i>et al.</i> , 2010
<i>A. herba-alba</i>	aerial part	1,8cineole (18.4%), β -thujone (14.1%), camphor (10.8%) and α -thujone (10.7%)	antimicrobial	Mighri <i>et al.</i> , 2010

Table 2. (continued)

<i>Artemisia</i> species	Part used/ extraction solvent	Constituents	Biological activity	References
<i>A. iwayomogi</i>	aerial part/ water	-	antifibrotic	Wang <i>et al.</i> , 2012
<i>A. ludoviciana</i>	aerial part/ methanol	quercetin, kaempferol, caffeic or ferulic conjugates and gallic acid (7.63±0.123, 1.80±0.123, 798.65±13.056 and 496.32±8.777 µg g ⁻¹ of dry matter)	antioxidant	Carvalho <i>et al.</i> , 2011
<i>A. oleandica</i>	aerial part/ methanol	quercetin, kaempferol, caffeic or ferulic conjugates and gallic acid (4.68±0.145, 47.56±0.345, 730.42±0.034 and 265.39±0.097 µg g ⁻¹ of dry matter)	antioxidant	Carvalho <i>et al.</i> , 2011
<i>A. princeps</i>	trunk/ methanol	-	anti-inflammatory	Chang <i>et al.</i> , 2009
	aerial part/ 80% ethanol	eupatilin and jaceosidin	anti-inflammatory	Min <i>et al.</i> , 2009

Table 2. (continued)

<i>Artemisia</i> species	Part used/ extraction solvent	Constituents	Biological activity	References
	aerial part/ methanol	kaempferol, caffeic or ferulic conjugates and gallic acid (31.60±1.440, 1308.96±22.344 and 334.23±10.555 µg g ⁻¹ of dry matter)	antioxidant	Carvalho <i>et al.</i> , 2011
<i>A. scoparia</i>	leaf/ water	essential oil	antioxidant	Singh <i>et al.</i> , 2010
<i>A. sphaerocephala</i>	seed/ water	polysaccharide	antioxidant	Wang <i>et al.</i> , 2010
<i>A. stelleriana</i>	aerial part/ methanol	quercetin, caffeic or ferulic conjugates and gallic acid (1.25±0.133, 562.95±12.334 and 38.45±0.233 µg g ⁻¹ of dry matter)	antioxidant	Carvalho <i>et al.</i> , 2011
<i>A. sylvatica</i>	aerial part/ methanol	artemininolide B	anti-inflammatory	Jin <i>et al.</i> , 2004
<i>A. vestita</i>	aerial part/ ethanol	cirsilineol, apigenin and 6-methoxytricin	anti-inflammatory	Yin <i>et al.</i> , 2008

Kot Chiang is the root of *Angelica sinensis* (AS). The crude extract of *A. sinensis* significantly promoted epithelial cell migration *via* an increase in epidermal growth factor (EGF) mRNA expression (Ye *et al.*, 2001). The crude extract of *A. sinensis* stimulated proliferation and migration of human endothelial cells *via* S-phase cell cycle and enhancing vascular endothelial growth factor (VEGF) mRNA expression (Lam *et al.*, 2008). The extract of *A. sinensis* stimulated on murine bone marrow mononuclear cells in serum-free culture medium *via* MAPK pathway (Xiaoping *et al.*, 2006).

Kot Huabua is the rhizome of *Ligusticum chuanxiong* (LC). HPLC-UV analysis of *L. chuanxiong* ethanol extract showed the presence of ferulic acid (Yan *et al.*, 2005), which exhibited angiogenic activity both *in vitro* and *in vivo* *via* stimulation of VEGF, platelet-derived growth factor (PDGF) and hypoxia inducible factor 1-alpha (HIF-1 α) pathways (Lin *et al.*, 2010).

Kot Jatamansi is the root and rhizome of *Nardostachys jatamansi* (NJ). The aqueous root extract of *N. jatamansi* significantly increased SOD, GSH and CAT activities in catalepsy-induced rat brain (Rasheed *et al.*, 2010).

Kot Kanprao is the rhizome of *Picrorhiza kurroa* (PK). The methanolic extract of *P. kurroa* exhibited antioxidant and a protective effect on DNA cleavage analyzed by comet assay (Russo *et al.*, 2001). Additionally, apocynin isolated from *P. kurroa* root inhibited ROS generation (van den Worm *et al.*, 2001) and possessed anti-inflammatory property by inhibiting the formation of TXA2 and arachidonic acid-induced aggregation of platelets (Engels *et al.*, 1992).

Kot Kradook is the root of *Saussurea costus* (SC). The ethanol extract of *S. costus* exhibited antioxidant activity, probably as a result of the presence of chlorogenic acid (Pandey *et al.*, 2005). Dehydrocostus lactone inhibited the production of NO in lipopolysaccharide (LPS) activated RAW 264.7 cells (Lee *et al.*, 1999). Cynaropicrin isolated from the extract of *S. costus* inhibited tumor necrosis factor-alpha (TNF- α) release from LPS-stimulated murine macrophage cells (Cho *et al.*, 2000). Costunolide exhibited inhibitory effects of interleukin-1 β (IL-1 β) in LPS-stimulated RAW 264.7 cells (Kang *et al.*, 2004).

Kot Pungpla is the gall of *Terminalia chebula* (TC). The aqueous extract of ripe fruit of *T. chebula* exhibited antioxidant activity using ferric-reducing antioxidant power assay (Lee *et al.*, 2005) including DPPH assay (Klika *et al.*, 2004), probably as a result of the presence of chebulinic acid. Chebulic acid found in *T. chebula* protected endothelial cells against advanced glycation end products (AGEs)-induced endothelial cell dysfunction (Lee *et al.*, 2010). Chebulagic acid showed potent inhibition of COX-2 and 5-LOX, the key enzymes involved in inflammation and carcinogenesis and anti-proliferative activity in cancer cell lines (Reddy *et al.*, 2009).

Quality control of crude drugs

World Health Organization (WHO) guidelines for the assessment of herbal medicines should be consulted when assessment for crude drugs (World Health Organization, 1998). Thai Herbal Pharmacopoeia (1995) prescribes quality control of crude drugs such as foreign matter, raw materials should be entirely free from visible signs of contamination and deterioration by soil, stones, sand, dust, insects and other animal contamination. The ash remaining following ignition of raw materials is determined by the different methods which total ash and acid-insoluble ash measured the total amount of material remaining after ignition such as sand and soil. Loss on drying determines both water and volatile matter, which an excess of water in raw materials will encourage microbial growth, the presence. This extractable method determines the amount of active constituents extracted with solvents from a given amount of raw materials (Singh *et al.*, 2012). Additionally, thin layer chromatography (TLC) and HPLC were used to identify chemical components of crude drugs.

Role of antioxidant enzyme, nitric oxide and cyclooxygenase in endothelial cell function

The endothelial cell is a single cell layer lining the vascular wall and plays an important role in vascular homeostasis, the regulation of blood pressure and blood flow by releasing vasodilators such as NO and prostacyclin, as well as vasoconstrictors, including endothelin (Kitamoto and Egashira, 2004). Cell injury, cell death impairs or prevents conduct of these activities leading to the alterations in

endothelial cell function (Pober *et al.*, 2009; Sitia *et al.*, 2010). Endothelial dysfunction is likely to result from endothelial cell injury including infection, hyperglycemia, obesity, diabetes mellitus and oxidative stress (Abraham *et al.*, 2007). Specifically, endothelial dysfunction is associated with reduced NO production, anticoagulant properties, platelet aggregation, increased expression of adhesion molecules, cytokines and ROS production from endothelium (Al-Isa *et al.*, 2010). Increased production of the superoxide anion can lead to decrease tissue bioavailability of NO *via* several enzymes that involved in generating ROS such as NADH/NADPH oxidase, xanthine oxidase (Turrens, 2003). The ROS are eliminated by antioxidant defense systems of cells including SOD which catalyzes superoxide anions to oxygen and hydrogen peroxide. In mammalian cells, there are 2 isoforms of CuZn-SOD or SOD1 is present in the cytosol and Mn-SOD or SOD2 is present in the mitochondria. Subsequently, GPx and CAT catalyze hydrogen peroxide to oxygen and water (Powers and Jackson, 2008). The imbalance between the production of ROS and limited antioxidant defense of cells induced to oxidative stress. Thereby, the excess ROS can damage cellular lipids, proteins or DNA inhibiting normal cell function (Valko *et al.*, 2007).

The endothelial dysfunction is associated with a decrease in NO bioavailability, (Witting *et al.*, 2007). NO is synthesized by nitric oxide synthase (NOS), convert L-arginine into L-citrulline. The endothelial NOS (eNOS) constitutively synthesizes NO in endothelial cells in response to an increase in intracellular calcium levels, while inducible NOS (iNOS) is not able to respond to changes in calcium level in the cell. As a result the production of NO by iNOS lasts much longer than by eNOS and tends to produce much higher concentrations of intracellular NO (Guzik *et al.*, 2003; Ignarro *et al.*, 2002). NO production can be induced through the up-regulation of iNOS, by factors involved in inflammation, including interleukins, interferon-gamma, TNF-alpha and LPS (Guzik *et al.*, 2003).

Angiogenesis is essential for wound repair. COX catalyzes the conversion of arachidonic acid to prostaglandins and thromboxane. There are 2 isoforms of COX-1 is constitutively expressed in most tissues, such as vascular endothelial cells and is involved in maintenance of cellular homeostasis, whereas the expression of COX-2 is

inducible and present very low level under normal conditions (Marnett, 2000). Previous study revealed that mechanically wound endothelial cell monolayer stimulated COX-2 expression resulting in rapid wound closure. Meanwhile, prostaglandin (PG) E₂, a COX product, enhanced endothelial cell migration to cover wounded area depending on COX-2 activity and expression (Jiang *et al.*, 2004).

CHAPTER III

MATERIALS AND METHODS

Equipments

- Autoclave (HA-300 MD, Hirayama, Japan)
- Biosafety laminar flow hood class II (International Scientific, BV-2225, Thailand)
- Centrifuge (Allegra X-12 R, Beckman, Germany; EBA 12, Hettich Zentrifugen, Germany)
- C₁₈ column (250 mm × 4.6 mm, 5 µm of particle size) with packed guard column (00G-4041-E0, Phenomenex, California, USA)
- CO₂ incubator (3121, Forma Scientific Inc, Massachusetts, USA)
- Hemocytometer (Bright-line, Hausser Scientific, Pennsylvania, USA)
- High performance liquid chromatography (HPLC) coupled with photodiode array (PDA) detector (Shimadzu LC-20A, Kyoto, Japan)
- Hot air oven (Mettler, Germany)
- Microplate reader (Perkin Elmer, Victor 3, Massachusetts, USA)
- Moisture and ash analyzer (CompuTrac MAX 5000XL, USA)
- Phase-contrast inverted microscope (CK30, Olympus, Tokyo, Japan)
- Rotary evaporator (RE120, Buchi, Flawil, Switzerland)
- Sieve number 40 (Retsch, Haan, Germany)
- Thin Layer Chromatography (TLC) plate (Merck, Darmstadt, Germany)
- TLC Scanner (CAMAG, 027.6481, Muttenz, Switzerland)
- Ultrasonic sonicator (Transsonic, Elma, Germany; Sonics Vibra Cell, Connecticut, USA)
- Water bath (Mettler, Germany)

Reagents

- Acetic acid (64-19-7, Lab-Scan Analytical Science, Gliwice, Poland)
- Acetonitrile (75-05-8, Lab-Scan Analytical Science, Gliwice, Poland)
- Apigenin (10798, Sigma, St. Louis, USA)

- Catalase activity assay kit (K773-100, BioVision, California, USA)
- Cyclooxygenase activity assay kit (760151, Cayman Chemical, Michigan, USA)
- 2,3-Diaminonaphthalene (DAN) (88461, Sigma, St. Louis, USA)
- 2',7'-Dichlorodihydrofluorescein diacetate (DCFH-DA) (D6883, Sigma, St. Louis, USA)
- Dimethyl sulfoxide (DMSO) (60153, Merck, Darmstadt, Germany)
- 3-(4,5-Dimethylthiazol-2-yl)-2, 5-diphenyltetrazolium bromide (MTT) (M2128, Sigma, St. Louis, USA)
- Eriodictyol (89061, Sigma, St. Louis, USA)
- Ethanol (H50T05, Mallinckrodt Chemical, Hazelwood, USA)
- Ethylenediaminetetraacetic acid (EDTA) (180, Univar, Sydney, Australia)
- Fetal bovine serum (FBS) (CH30160.02, Hyclone, Utah, USA)
- Glutathione peroxidase activity assay kit (K762-100, BioVision, California, USA)
- Hoechst 33342 (14533, Sigma, St. Louis, USA)
- Hydrochloric acid (AR 1107, Lab-Scan Analytical Science, Gliwice, Poland)
- Hydrogen peroxide (H₂O₂) (H/1750/17, Fisher Scientific, California, USA)
- Luteolin (L9283, Sigma, St. Louis, USA)
- Medium 199 (31100-027, Gibco BRL Life Technologies, New York, USA)
- β -Mercaptoethanol (β -ME) (444203, Merck, Darmstadt, Germany)
- Penicillin-streptomycin (15140, Gibco BRL Life Technologies, New York, USA)
- Phenylmethanesulfonyl fluoride (PMSF) (P7626, Sigma, St. Louis, USA)
- Propidium iodide (P4170, Sigma, St. Louis, USA)
- Quercetin (Q0125, Sigma, St. Louis, USA)
- Rutin (R5143, Sigma, St. Louis, USA)
- Superoxide dismutase activity assay kit (K335-100, BioVision, California, USA)
- Trypsin from porcine pancreas (T4799, Sigma, St. Louis, USA)

- Tris (hydroxymethyl)-methylamine (77-86-1, Fisher Scientific, California, USA)
- Triton X-100 (93420, Fluka, St. Gallen, Switzerland)

Methods

Plant material

Roots of AD, AS, SC, rhizomes of AL, LC, PK, roots and rhizomes of NJ, aerial parts of AP and galls from TC were purchased from Thai herbal drugstores, Bangkok in October 2009, and identified by Dr. Sanya Hokputsa of the Phytochemical Research Group, Research and Development Institute, Government Pharmaceutical Organization, Thailand. The aerial parts of *Artemisia pallens* was identified by Associate Professor Dr. Uthai Sotanaphun of Department of Pharmacognosy, Faculty of Pharmaceutical Sciences, Silpakorn University, Thailand. Voucher specimens have been deposited in the herbarium of the Phytochemical Research Group, Research and Development Institute, Government Pharmaceutical Organization, Thailand.

Quality control of crude drugs according to Thai Herbal Pharmacopoeia

Quality control parameters, including foreign matter, loss on drying, total ash, acid-insoluble ash, ethanol-soluble extractive and water-soluble extractive were examined according to the Thai Herbal Pharmacopoeia (Thai Pharmacopoeia Committee, 1995). All determination was studied repeatedly by 4 experiments and each experiment was performed in duplicate.

Determination of foreign matter

About 100 grams of each crude drug was spread as a thin layer. The foreign matter was detected by inspecting with unaided eyes and separated. The percentage of foreign matter was weighed and calculated with reference to the air-dried crude drug.

Determination of loss on drying

Two grams of each crude drug was accurately taken in a tarred glass-stoppered and dried at 105°C until constant weight. The percentage of loss on drying was calculated with reference to the air-dried crude drug.

Determination of total ash

Two grams of each crude drug was accurately taken in a tarred crucible and incinerated by gradually increasing the temperature, not exceeding 450°C until free from carbon. Cooled and weighed, repeated for constant value. The percentage of total ash was calculated with reference to the air-dried herbal crude.

Determination of acid-insoluble ash

Ash obtained from the total ash was boiled with 25 mL of hydrochloric acid for 5 minutes. The insoluble matter was collected on an ashless filter paper, washed with hot water until the filtrate was neutral, and ignited at about 500°C, then calculated the percentage of acid insoluble ash with reference to the air-dried herbal crude.

Determination of ethanol-soluble extractive

Five grams of each crude drug was macerated with 100 mL of 95% ethanol in a closed flask for 24 h, shaken frequently during the first 6 h and then allowed to stand for 18 h. The filtrate (20 mL) was evaporated to dryness under reduced pressure in a tarred, flat-bottomed, shallow dish and it was further dried at 105°C to constant weight. The percentage of ethanol-soluble extractive was calculated with reference to the air-dried crude drug.

Determination of water-soluble extractive

Accurately weighed about 5 grams of each crude drug was macerated with 100 mL of distilled water in a closed flask for 24 h, shaken frequently during the first 6 h and then allowed to stand for 18 h. The filtrate (20 mL) was evaporated to dryness under reduced pressure in a tarred, flat-bottomed, shallow dish and it was further dried at 105°C to constant weight. The percentage of water-soluble extractive was calculated with reference to the air-dried herbal crude drug.

TLC fingerprint analysis

Accurately weighed about one gram of each crude drug and authentic plant were extracted with 10 mL methanol using reflux apparatus for 30 minutes. The filtrate (20 μ L) was sprayed to a lane on TLC plate. The TLC plate was developed in a chamber containing toluene, ethyl acetate and acetic acid (75:25:5) as the mobile phase for AD, AS and LC; hexane and ethyl acetate (58:42) as the mobile phase for AL; hexane and Acetone (56:44) as the mobile phase for AP; hexane, ethyl acetate and acetic acid (70:30:1) as the mobile phase for NJ and TC; chloroform, ethyl acetate, methanol and

ammonia (50:30:20:1) as the mobile phase for PK; dichloromethane, ethyl acetate, methanol and ammonia (60:20:20:2) as the mobile phase for SC. The developed distance was 10 cm, removed the plate from the chamber and allowed to dry. The dried TLC was then sprayed with an anisaldehyde – sulfuric acid reagent and heated in oven for 10 min for TLC plate of AP. Detection of the chromatogram under UV 254 and 365 nm recorded and photograph.

Preparation of the extracts

The crude drugs were grinded to powder and sieved through No. 40. The powder was extracted with 50% ethanol or water (1 gram of dried powder per 20 mL of 50% ethanol or water) using reflux apparatus for 6 h. The extracts were filtered through Whatman No.1 filter paper. Each extract was evaporated to dryness under reduced pressure by using a rotary evaporator at 40°C and either spray dried or freeze dried. The extracts were stored in capped vials and placed into a desiccator at room temperature until used.

Preparation of a stock solution of the extract for bioassay.

The extracts were dissolved in DMSO to prepare a stock solution at a concentration of 200 mg/mL and were subsequently diluted with complete medium. After appropriate dilutions, the final concentration of DMSO was kept at 0.5% DMSO (v/v).

Preparation of a stock solution of the extract for HPLC analysis.

The extract and standard flavonoids were dissolved in methanol as stock solutions at concentrations of 1 mg/mL and 20 mg/mL, respectively. The stock solution of the extract was further diluted with methanol to make working solutions at the final concentration of 10 mg/mL while the stock solutions of the standard flavonoids were diluted to the final concentrations of 0.1, 0.2, 0.5, 1, 2 and 5 µg/mL. After dilution, the working solutions were filtered through the 0.45 µm membrane filter into the vial before HPLC analysis.

Cell culture

Human umbilical cord endothelial ECV304 cells obtained from Cell Lines Service (Germany) were cultured in M199 medium containing 10% FBS and 1%

penicillin-streptomycin and maintained at 37°C in a humidified 5% CO₂ incubator. The cells were subcultured every 3-4 days using 1 mM EDTA and 0.25% trypsin for trypsinization.

Determination of cell viability using MTT reduction assay

Cell viability was determined by MTT assay as previously described (Carmichael *et al.*, 1987). The cells were seeded into a 96-well plate at a density of 1×10^5 cells/mL and incubated for 24 h. The cells were treated with the extract at the concentrations of 0.001, 0.01, 0.1, 1, 10 and 100 µg/mL in medium with or without FBS for 24 h. The medium was replaced by 0.4 mg/mL MTT in medium. After 4 h incubation, the MTT solution was replaced by 100% DMSO to dissolve purple formazan crystal. The optical density (OD) was measured with a microplate reader using a wavelength of 570 nm. The percentage of cell viability was calculated by the following equation: $(OD_{\text{sample}}/OD_{\text{control}}) \times 100$, where OD_{sample} is the absorbance of the treated cells and OD_{control} is the absorbance of the untreated control.

Determination of cell migration using *in vitro* scratch assay

Cell migration was determined by an *in vitro* scratch assay (Liang *et al.*, 2007) with a slight modification. The cells were seeded into a 24-well plate at 2×10^5 cells/mL and incubated for 24 h until confluence. The cell monolayer was scraped in a straight line to create wound with a p200 pipette tip and washed twice with PBS. The cells were treated with the extract at various concentrations in the presence or absence of FBS for 6, 12 and 24 h. The scratch wounded area was measured using a phase contrast microscope and then analyzed by using Image J 1.41 software (NIH, Bethesda, MD, USA). The percentage of wound closure was calculated by the following equation: $[(A_0 - A_t)/ A_0] \times 100$, where A_0 is the area of wound after scratching at 0 h and A_t is the area of wound at 6, 12 and 24 h.

Determination of intracellular ROS using DCFH-DA assay

Intracellular ROS was determined by DCFH-DA assay as previously described (Wang and Joseph, 1999). The cells were seeded into a 96-well plate at a density of 1×10^5 cells/mL and incubated for 24 h. The cells were treated with the extract at

various concentrations of 12.5, 25, 50, 100 and 200 $\mu\text{g/mL}$ in medium for 24 h. The medium was removed and washed twice with cold-PBS and incubated with 5 μM DCFH-DA for 30 min. After 30 min incubation, the DCFH-DA solution was removed and the treated cells were washed twice with cold-PBS. The fluorescence intensity of DCF was quantified at 485 nm excitation and 535 nm emission. The percentage of DCF fluorescence was calculated by the following equation: $(F_{\text{sample}}/F_{\text{control}}) \times 100$, where F_{sample} is the fluorescence intensity of the treated cells and F_{control} is the fluorescence intensity of control.

The level of intracellular ROS at the scratch wounded area was also determined by co-staining with fluorescence dyes (Bal-Price and Brown, 2001; Li *et al.*, 2009; Saha *et al.*, 2009) with a slight modification. The cells were scraped in a straight line to create wound with a p200 pipette tip and washed twice with PBS. The cells were treated with the extract at various concentrations in the presence of FBS for 6 h. The wounded area was washed with PBS and incubated with 5 μM of DCFH-DA at 37°C for 30 min. The cells were washed with PBS and further incubated with 10 $\mu\text{g/mL}$ of Hoechst 33342 and 10 $\mu\text{g/mL}$ of propidium iodide (PI) at 37°C for 5 min. The images was visualized using an inverted fluorescence microscope.

Determination of SOD activity

The SOD activity was performed using an assay kit according to the manufacturer's instruction as previously described (Mapanga *et al.*, 2012). The commercially SOD assay kit utilizes 2-(4-iodophenyl)-3-(4-nitrophenyl)-5-(2,4-disulfophenyl)-2H-tetrazolium, monosodium salt (WST-1), which produces a water-soluble formazan dye upon reduction with a superoxide anion. The rate of WST-1 reduction with a superoxide anion related to xanthine oxidase (XO) activity, and was inhibited by SOD. The cells were seeded into a 100 mm dish at a density of 2×10^5 cells/mL and incubated for 24 h. The cells were treated with the extract at various concentrations of 25, 50 and 100 $\mu\text{g/mL}$ in culture medium for 6 h. The medium was removed and washed twice with cold-PBS. The cells were collected by scraping and centrifuged at 1,500 x g for 10 min. The cells were lysed in 0.1 M Tris-HCl, pH 7.4 containing 0.5% Triton X-100, 5 mM β -ME, 0.1 mg/mL PMSF and sonicated for 3 x 1s by an ultrasonic sonicator. Thereafter, cell lysates were centrifuged at 14,000 x g

for 5 min and discarded the cell debris. The supernatant was collected and protein concentrations were determined by Bradford assay (Bearden, 1978). The inhibition activity of SOD was measured with a microplate reader using a wavelength of 450 nm. SOD activity was calculated according to the following formula: % inhibition = $[(A_{\text{blank}} - A_{\text{sample}})/A_{\text{blank}}] \times 100$, where A_{blank} is the absorbance of blank and A_{sample} is the absorbance of sample.

Determination of GPx activity

The GPx activity was performed using an assay kit according to the manufacturer's instruction as previously described (Patten *et al.*, 2013). The GPx enzyme reaction was indirectly assessed following the decrease of NADPH. GPx catalyzes the reduction of cumene hydroperoxide while oxidizing reduced glutathione (GSH) to an oxidized glutathione (GSSG). The generated GSSG is reduced to GSH with consumption of NADPH into NADP^+ by glutathione reductase (GR). The decrease of NADPH is proportional to the activity of GPx. The cells were seeded to a 100 mm dish at a density of 2×10^5 cells/mL and incubated for 24 h. The cells were treated with the extract at various concentrations of 25, 50 and 100 $\mu\text{g}/\text{mL}$ in culture medium for 6 h. The medium was removed and the cells were washed twice with cold-PBS. The cells were collected by scraping and centrifuged at $1,500 \times g$ for 10 min. The cells were lysed in cold assay buffer and sonicated for $3 \times 1\text{s}$ by an ultrasonic sonicator. Thereafter, cell lysates were centrifuged at $10,000 \times g$ for 15 min and discarded the cell debris. The supernatant was collected and protein concentrations were determined by Bradford assay. The absorbance was measured with a microplate reader using a wavelength of 340 nm. GPx activity was calculated by the following formula: $\text{GPx activity} = [B / (T2-T1) \times V] \times \text{sample dilution}$, where B is the NADPH amount that was decreased between T1 (time of first reading) and T2 (time of second reading) and V is the sample volume added into the reaction well.

Determination of CAT activity

The CAT activity was performed using an assay kit according to the manufacturer's instruction as previously described (Patten *et al.*, 2013). The CAT enzyme reacts with H_2O_2 to produce water and oxygen. Unconverted H_2O_2 reacts with

the OxiRed probe, which can be detected at 570 nm. The cells were seeded to a 100 mm dish at a density of 2×10^5 cells/mL and incubated for 24 h. The cells were treated with the extract at various concentrations of 25, 50 and 100 $\mu\text{g/mL}$ in culture medium for 6 h. The medium was removed and washed twice with cold-PBS. The cells were collected by scraping and centrifuged at $1,500 \times g$ for 10 min. The cells were lysed in cold assay buffer and sonicated for $3 \times 1\text{s}$ by an ultrasonic sonicator. Thereafter, cell lysates were centrifuged at $10,000 \times g$ for 15 min and discarded the cell debris. The supernatant was collected and protein concentrations were determined by Bradford assay. The absorbance was measured with a microplate reader using a wavelength of 570 nm. CAT activity was calculated by the following formula: $\text{CAT activity} = [B / (30 \times V)] \times \text{sample dilution}$, where B is the decomposed H_2O_2 amount from H_2O_2 standard curve and V is the sample volume added into the reaction well.

Determination of intracellular NO level

Intracellular NO was determined by DAN assay as previously described (Si *et al.*, 1997). NO level was determined by the assay of nitrite (NO_2^-), a relatively stable metabolite of NO. The NO_2^- is reacted with DAN into 2,3-diaminonaphthotriazole, a fluorescent product. The fluorescent intensity is proportional to the NO level, which can be detected with an excitation wavelength of 365 nm and an emission wavelength of 450 nm. The cells were seeded to a 96-well plate at a density of 1×10^5 cells/mL and incubated for 24 h. The cells were treated with the extract at various concentrations of 12.5, 25, 50, 100 and 200 $\mu\text{g/mL}$ in medium for 0.5, 1, 2 and 6 h. The medium was removed and washed twice with cold-PBS and incubated with 0.05 mg/mL DAN for 10 min. Then 0.28 M NaOH was added and incubated for 10 min. The fluorescence intensity was monitored by an excitation wavelength of 365 nm and an emission wavelength of 450 nm. The percentage of NO was calculated by the following equation: $(N_{\text{sample}}/N_{\text{control}}) \times 100$, where N_{sample} is the NO_2^- amount from NO_2^- standard curve of the treated cells and N_{control} is the NO_2^- amount from NO_2^- standard curve of control.

Determination of cyclooxygenase activity

The COX activity was performed using an assay kit according to the manufacturer's instruction as previously described (Guo *et al.*, 2006). The peroxidase activity is assayed calorimetrically by monitoring the appearance of oxidized *N,N,N',N'*-tetramethyl-*p*-phenylenediamine (TMPD). The COX-1 activity was assayed by using of COX-2 specific inhibitor (DuP-697), while the COX-2 activity was determined with using of COX-1 specific inhibitor (SC-560), which can be detected at a wavelength of 590 nm. The cells were seeded to a 100 mm dish at a density of 2×10^5 cells/mL and incubated for 24 h. The cells were treated with the extract at various concentrations of 25, 50 and 100 $\mu\text{g/mL}$ in medium for 6 h. The medium was removed and washed twice with cold-PBS. The cells were collected by scraping and centrifuged at 1,000 x g for 10 min. The cell pellets were lysed in 0.1 M Tris-HCl, pH 7.8 containing 1 mM EDTA and sonicated for 3 x 1s by an ultrasonic sonicator. Thereafter, cell lysates were centrifuged at 10,000 x g for 15 min and discarded the cell debris. The supernatant was collected and protein concentrations were determined by Bradford assay. The enzyme reaction was directly assessed the peroxidase activity of cyclooxygenase. COX activity was calculated according to the following formula: $\text{COX activity} = (((\Delta A_{590}/5 \text{ min})/0.00826) \times (0.21/0.04))/2$, where ΔA_{590} is the absorbance of sample (subtract the background value)

HPLC fingerprint analysis

Chemical profile of the bioactive extract was performed using HPLC system consisting of a binary pump, an autosampler and a column oven and PDA detector. APES was dissolved in methanol as a stock solution (20 mg/mL) and filtered through a 0.45 μm membrane filter before injection (20 μL) to a C_{18} column. Column temperature was set at 25°C. The mobile phase was acetonitrile (solvent A) and 1% acetic acid in water (solvent B) using a gradient elution of 0% A at 0 - 5 min, 0 - 40% A at 5 - 35 min, 40 - 80% A at 35 - 45 min, 80% A at 45 - 50 min, 80 - 0% A at 50 - 55 min and 0% A at 55 - 60 min. The flow rate was 1.0 mL/min. Detection was provided by variable wavelengths at 254, 270 and 350 nm for monitoring apigenin, eriodictyol, luteolin, quercetin and rutin.

Statistical analysis

Each experiment was performed at least three independent experiments and each performed in triplicate. Results were expressed as mean \pm SEM. Data were analyzed by one-way analysis of variance (ANOVA) with LSD post hoc test for statistical difference. The p value < 0.05 were considered statistically significant.

CHAPTER IV

RESULTS AND DISCUSSION

Quality control of crude drug according to Thai Herbal Pharmacopoeia

Nine crude drugs which are called Phikud Navakot were shown in Figure 3. Kot Soa, the root of AD, was conical, externally greyish-brown or yellowish-brown with longitudinal wrinkles. Texture was white and scattered of brown oil in bark, aromatic pungent and bitter (Bauer and Xiao, 2011). Kot Kamao, the rhizome of AL was nodular-cylindrical, somewhat curved greyish-brown with wrinkled. Texture was yellowish-white or greyish-white and scattered of orange-yellow oil cavities, weakly aromatic and bitter (Bauer and Xiao, 2011). Kot Chulalumpa from aerial part of AP, which was a small shrub. The leaf was alternate pinnasect and dark green leaves. The leaves were covered with white silky hairs gives the foliage a grey or white appearance. The flowers were racemose panicles bear numerous small yellow flower heads (Suresh *et al.*, 2011). Kot Chiang, the root of AS, was cylindrical, externally yellowish-brown to brown with longitudinally wrinkled and transversely lenticillate. The texture was flexible yellowish-white or yellowish-brown, strongly aromatic or sweet pungent and slightly bitter (Bauer and Xiao, 2011). Kot Huabua, the rhizome of LC was irregular knotty and fist-like masses yellowish-brown. Texture was yellowish-white or greyish-yellow and scattered with yellowish-brown oil cavities, strongly aromatic and slightly bitter (Bauer and Xiao, 2011). Kot Jatamansi, the root and rhizome of NJ was dark grey color and densely covered with reddish brown silky fibers and typical smell (Singh *et al.*, 2009; Arya *et al.*, 2012). Kot Kanprao, the rhizome of PK was thin, cylindrical, straight or slightly arched, externally greyish-brown with longitudinal wrinkles, dotted scars and characteristic odour and very bitter (Arya *et al.*, 2012; Maharashtra *et al.*, 2012). Kot Kradook, the root of SC was slightly arched, externally brown with longitudinal wrinkles and central pith, which is hollow (Arya *et al.*, 2012). Kot Pungpla, the gall of TC was produced by the plant against insect bite with accompanying microorganism infection and same with fish belly, called 'Pung pla' in Thai (Manosroi *et al.*, 2010).



Figure 3. Macroscopic evaluation of nine crude drugs in Phikud Navakot.

The quality control parameters of crude drugs including foreign matter, loss on drying, total ash, acid insoluble ash, ethanol-soluble extractive and water-soluble extractive of each nine crude drugs (Table 3). The results were well correlated with those of the authentic samples, generous gifts from Associate Professor Noppamas Soonthornchareonnon, Faculty of Pharmacy, Mahidol University. The parameters are useful for setting standards for crude drugs. Assessment of these parameters in crude drugs plays an important role in detecting adulteration and poor quality of the crude drugs. The criterion is that the foreign matter and acid-insoluble ash for controlling the quality of crude drugs should not be more than 2 % w/w (Thai Pharmacopoeia Committee, 1995).

The results are advantageous for the use as a reference crude drug for preparing of the extraction with consistent quality and developing herbal medicine and keep information of extracts with reproducible quality.

Preparation of the extracts

All crude drugs obtaining the criteria of Thai Herbal Pharmacopoeia were then subjected to extraction using either 50% ethanol or water at the ratio of 1:20 using a reflux apparatus. The lowest yield was from NJEF and NJWF (Table 4). Previous study revealed that dried roots and rhizomes of *N. jatamansi* contained 0.5-2% essential oil and 66% sesquiterpenes, jatamansone, jatamol A and B, jatamansic acid and nardostachone (Jadhav *et al.*, 2009; Parekh *et al.*, 2009). Steam-distillation yielded 1.9% of a pale yellow essential oil (Chauhan *et al.*, 2005), which was resemble to our result with 1.43 and 1.71% yield of the ethanolic and water extract of NJ, respectively.

Meanwhile, the highest yield was from TCES, which was 60.00%. From previous reports, *T. chebula* was rich in 33% hydrolysable tannins containing gallic acid, chebulic acid, tannic acid, chebulagic acid and chebulinic acid and flavonoids like luteolin, rutins and quercetin (Juang *et al.*, 2004; Manosroi *et al.*, 2010; Prakash *et al.*, 2012). The water extract of *T. chebula* using HPLC revealed the presence of gallic acid (8.38% w/w) (Kumar *et al.*, 2010). Thus, the highest yield of TCES might be due to solvent used for the extraction. Ethanol was found to be the best solvent for the extraction of chebulinic acid (Prakash *et al.*, 2012).

Table 3. Specification and quality control parameters of nine crude drugs in Phikud Navakot.

Crude drug	Foreign matter (%w/w)	Loss on drying (% w/w)	Total ash (%w/w)	Acid-insoluble ash (% w/w)	Ethanol-soluble extractive (%w/w)	Water-soluble extractive (%w/w)
Kot Soa	0.35	10.37	2.81	0.50	4.18	16.20
Kot Kamao	0.45	8.60	6.45	0.34	12.21	36.85
Kot Chulalumpa	0.30	9.91	5.88	0.15	7.09	26.53
Kot Chiang	0.30	11.83	7.10	1.29	19.35	47.99
Kot Huabua	0.20	11.24	6.41	1.27	17.01	31.53
Kot Jatamansi	0.70	8.17	5.18	0.32	2.43	17.21
Kot Kanprao	0.75	10.67	2.83	0.62	27.95	42.06
Kot Kradook	0.28	11.66	4.74	0.58	9.40	28.54
Kot Pungpla	0.10	12.73	3.11	0.39	43.57	55.13

Table 4. Extract codes and yields of the extracts from nine crude drugs in Phikud Navakot. Codes were assigned as follow: first and second letters are scientific name of plant crude drug; third letter is solvent used for the extraction - either ethanol (E) or water (W); fourth letter is spray-drying (S) or freeze-drying (F).

Crude drug	Scientific name	Extract code (% yield)	
		Ethanol	Water
Kot Soa	<i>Angelica dahurica</i>	ADES (2.44)	ADWS (17.78)
Kot Kamao	<i>Atractylodes lancea</i>	ALES (12.00)	ALWF (7.69)
Kot Chulalumpa	<i>Artemisia pallens</i>	APES (5.00)	APWS (5.66)
Kot Chiang	<i>Angelica sinensis</i>	ASES (3.75)	ASWS (4.70)
Kot Huabua	<i>Ligusticum chuanxiong</i>	LCES (3.75)	LCWS (8.00)
Kot Jatamansi	<i>Nardostachys jatamansi</i>	NJEF (1.43)	NJWF (1.71)
Kot Kanprao	<i>Picrorhiza kurroa</i>	PKES (8.00)	PKWS (12.33)
Kot Kradook	<i>Saussurea costus</i>	SCES (18.44)	SCWF (6.19)
Kot Pungpla	<i>Terminalia chebula</i>	TCES (60.00)	TCWS (41.60)

Effect of the extract on proliferation and toxicity of ECV304 cells

To determine nontoxic concentration of the extract, viability of ECV304 cells was measured by MTT assay. The result showed that the TCES, TCWS and NJEF at the concentrations ranging from 0.001 to 100 $\mu\text{g/mL}$ exhibited significant cytotoxicity. Cell proliferation was observed in the ethanolic extracts but not the water extracts (Figure 4A). Meanwhile, the water extracts tended to be more toxic (Figure 4B).

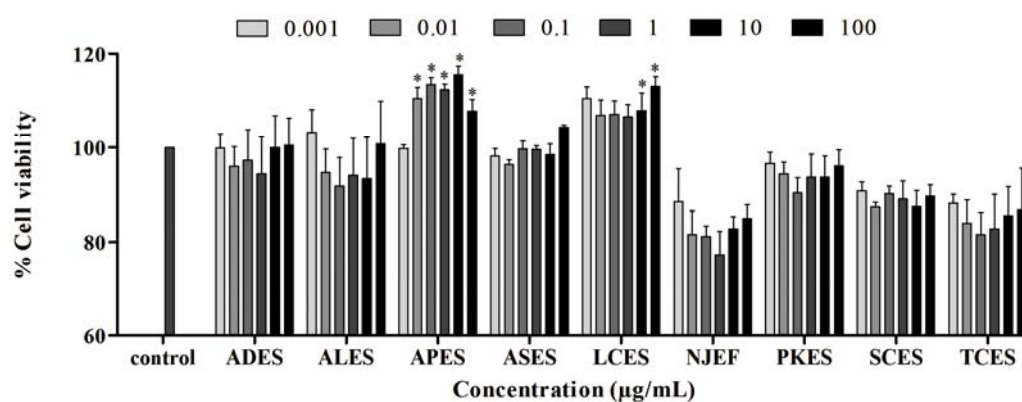
Our result was resemble to a previous report, showing that tannins such as tannic, ellagic acid and gallic acid at the concentrations ranging from 15 to 240 μM decreased cell viability in Chinese hamster cells after 1 h incubation. Our results indicated that TCES and TCWS was cytotoxic due to tannins as the main components in *T. chebula* (Labieniec and Gabryelak, 2003).

Among the extracts, APES at the concentrations of 0.01, 0.1, 1, 10 and 100 $\mu\text{g/mL}$ in the presence of FBS for 24 h exposure significantly increased proliferation in a concentration-dependent manner, showing the percentage of viability at 110.58 ± 2.32 , 113.57 ± 1.45 , 112.45 ± 1.17 , 115.64 ± 1.70 and $107.87 \pm 2.467\%$, respectively (Figure 5A). Meanwhile, LCES only at the concentrations of 10 and 100 $\mu\text{g/ml}$ significantly increased the percentage of viable cells, which were 107.96 ± 3.77 and $105.22 \pm 3.93\%$, respectively (Figure 5B).

Previous study revealed that hot-water extract of *Artemisia princeps* leaf at the concentration of 5 $\mu\text{g/mL}$ significantly stimulated endothelial cell proliferation (Kaji *et al.*, 1990) via activation of basic fibroblast growth factor (Kaji *et al.*, 1990). The cell proliferation of LCES could be partly due to the presence of ferulic acid, which also exhibited angiogenic activity both *in vitro* and *in vivo* via stimulation of VEGF, PDGF and HIF-1 α pathways (Lin *et al.*, 2010).

This study was the first report showing that APES (0.01 $\mu\text{g/mL}$) significantly exhibited endothelial cell proliferation, which might result in a tendency of angiogenesis or endothelial wound repair. Furthermore, cell proliferation of APES was more potent than of LCES. We therefore selected APES for further study in cell migration experiment.

(A)



(B)

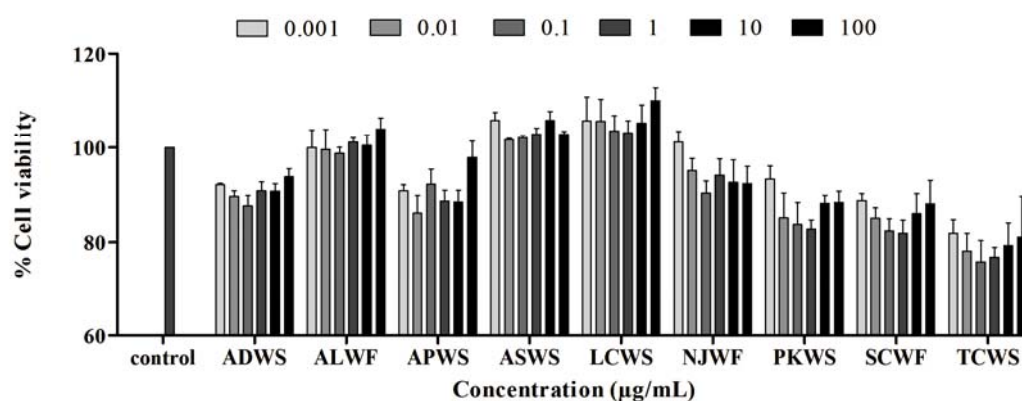
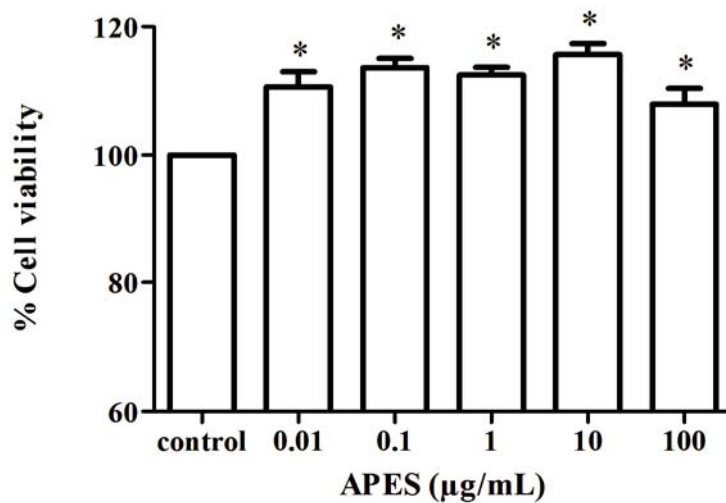


Figure 4. Effect of the extracts on viability of ECV304 cells using MTT reduction assay. The cells were treated with the (A) ethanol or (B) water extracts at the concentrations of 0.001, 0.01, 0.1, 1, 10 and 100 $\mu\text{g/mL}$ and further incubated for 24 h. The cell viability was determined by MTT assay. $*p < 0.05$ compared to the untreated control. The results were expressed as mean \pm S.E.M. (N =3, each performed in triplicate).

(A)



(B)

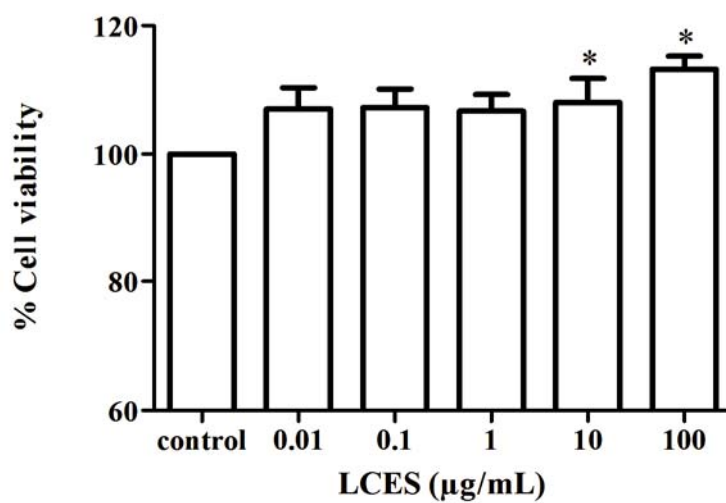


Figure 5. Effect of APES and LCES on cell proliferation. The cells were treated with either (A) APES or (B) LCES at the indicated concentrations for 24 h. The viable cells were assessed using MTT assay. * $p < 0.05$ compared to the untreated control. The results were expressed as mean \pm S.E.M. (N =3, each performed in triplicate).

Effect of APES on cell migration

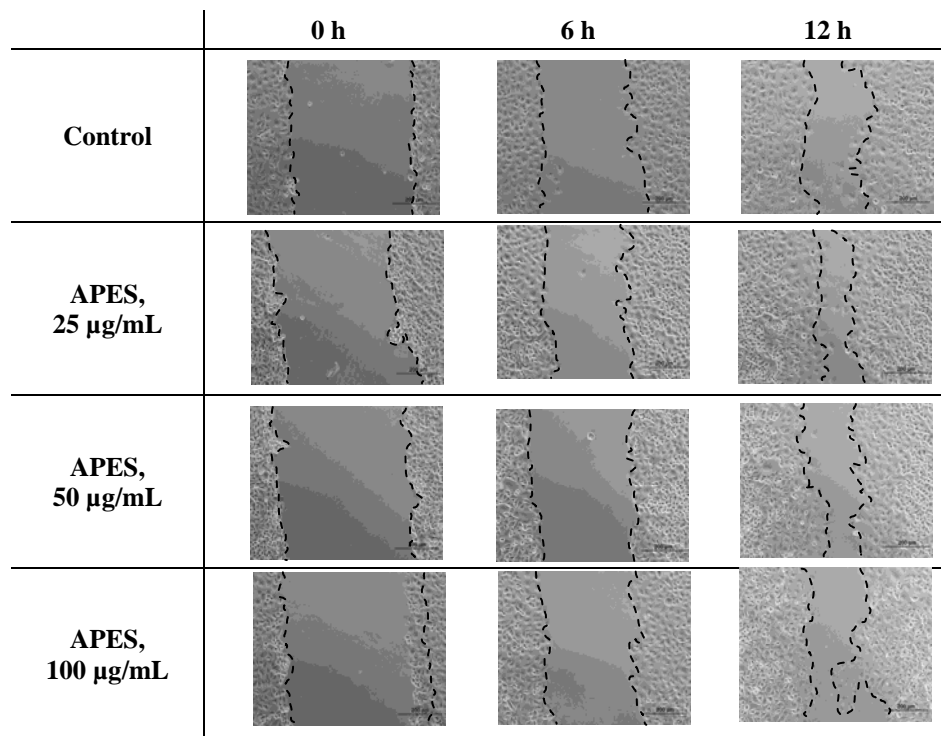
To determine the effect of APES on cell migration, an *in vitro* scratch assay was performed in ECV304 cells. In the presence of FBS, APES at the concentrations of 12.5, 25, 50, 100 and 200 $\mu\text{g/mL}$ for 6, 12 and 24 h did not show significant cell migration, when compared with control (Figure 6). Under serum-free condition to minimize cell proliferation (Yarrow *et al.*, 2004), APES at the concentrations of 25, 50 and 100 $\mu\text{g/mL}$ for 6 h significantly enhanced cell migration in a concentration-dependent manner (Figure 7), exhibiting the percentage of wound closure of 28.62 ± 1.92 , 27.41 ± 1.69 and $26.74 \pm 3.34\%$, respectively (Figure 8).

According to a previous report, *Artemisia anomala*, *A. diffusa*, *A. herba-alba* and *A. tripartita* were used for curing infectious wounds. *A. spicigera* induced more rapid healing of wounds (Martínez *et al.*, 2012).

Both migration and proliferation are often induced during development, angiogenesis and regeneration (Sadanandam *et al.*, 2010). To ascertain whether APES promoted cell migration through proliferation, cell viability affected by APES in both serum free and serum containing media was compared. The result demonstrated that treatment of cells with APES in the media supplement with FBS significantly increased viability in concentration- and time-dependent manner (Figure 9A) while under serum free condition, cell proliferation affected by APES was not observed (Figure 9B). The cells surrounded the wounded area were found to respond by an immediate migration actively within 6 h, while the unaffected cells began to proliferate (Ruszymah *et al.*, 2012). The result suggested that APES induced wound closure through promoting cell migration at the scratch area in addition to an increase in proliferation of normal endothelial cells. Our results demonstrated the ability of APES to migrate in a concentration-dependent manner without affecting viability or proliferation (Figure 10).

Previous study revealed that the level of COX-2 expression increased with the number of lines drawn through the culture in wounding endothelial cell monolayers (Jiang *et al.*, 2004). PGE2 showed to be more important in the early stages of wound healing (Talwar *et al.*, 1996) and involved in proliferation of 3T6 fibroblast cells and promotion of collagen synthesis during wound healing (Sánchez *et al.*, 2001).

(A)



(B)

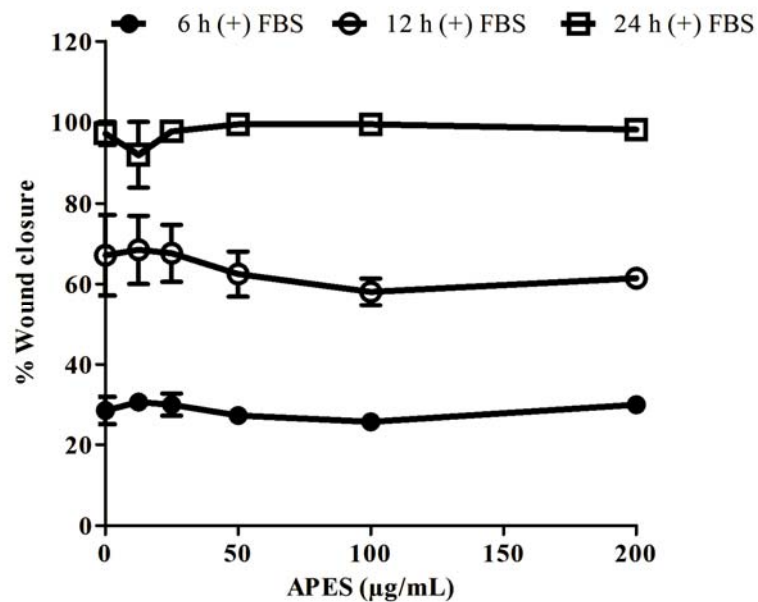


Figure 6. Effect of APES on cell migration in the presence of FBS. Cells were wounded at a p200 pipette tip and incubated with APES for 6, 12 and 24 h. Results were represented as (A) phase contrast microscopy of cells migrating into the denuded area of the scratch wound; 10 x magnification. (B) The percentage of wound closure were expressed as mean \pm S.E.M. (N =3, each performed in triplicate).

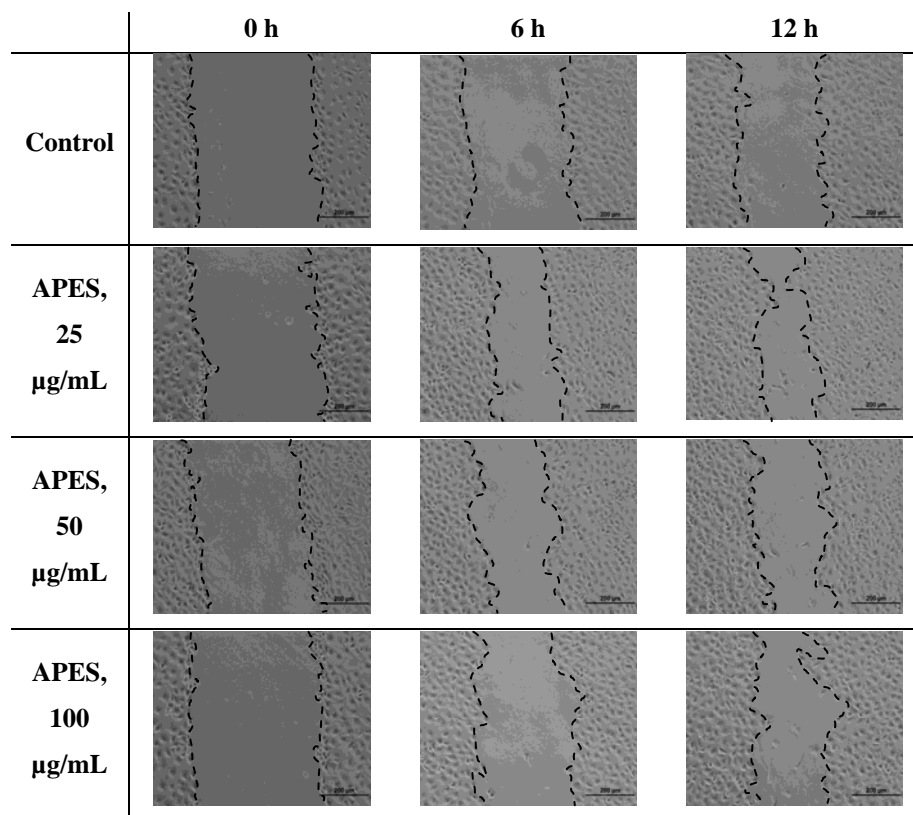


Figure 7. Effect of APES on cell migration in the absence of FBS. The cells were scratched vertically with p200 pipette tips. A phase contrast microscopy of the cells migrating into the denuded area of the scratch wound; 10x magnification. The migration was quantified by the Image J software.

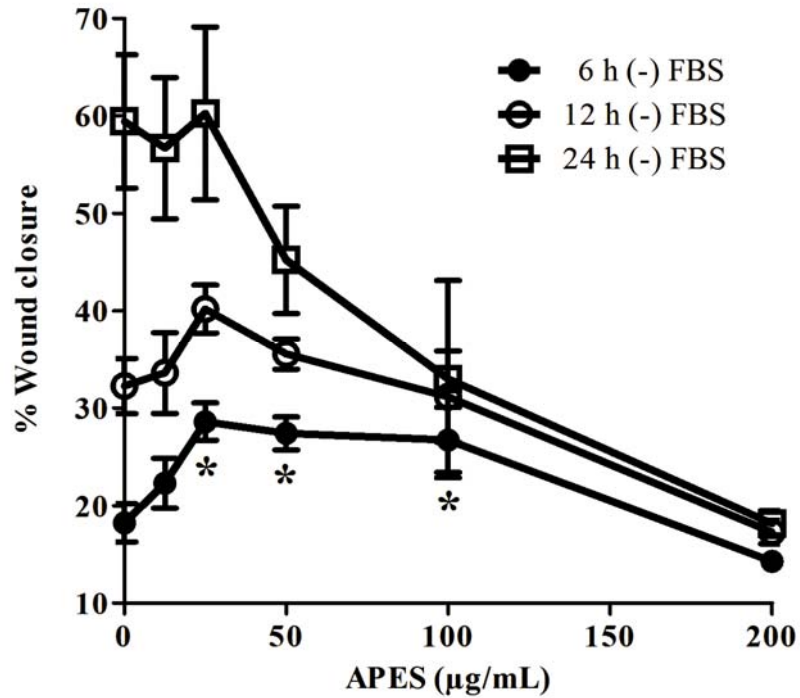
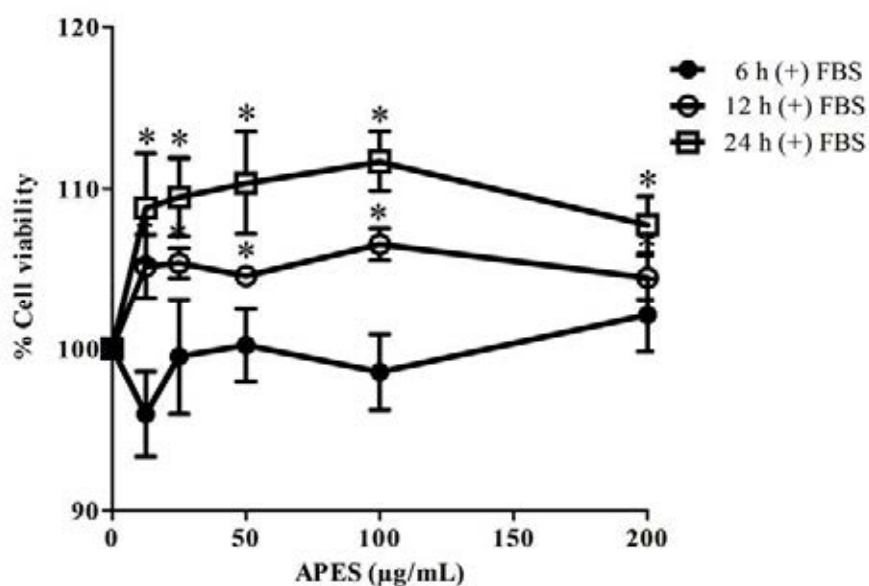


Figure 8. Concentration-dependent studies of APES on cell in the absence of FBS. A confluent monolayer was scratched and then incubated with APES at the concentrations of 12.5, 25, 50, 100 and 200 µg/mL for 6, 12 and 24 h in the absence of FBS. Results were represented as the percentage of wound closure were expressed as mean \pm S.E.M. (N =3, each performed in triplicate). * $p < 0.05$ compared to the untreated control.

(A)



(B)

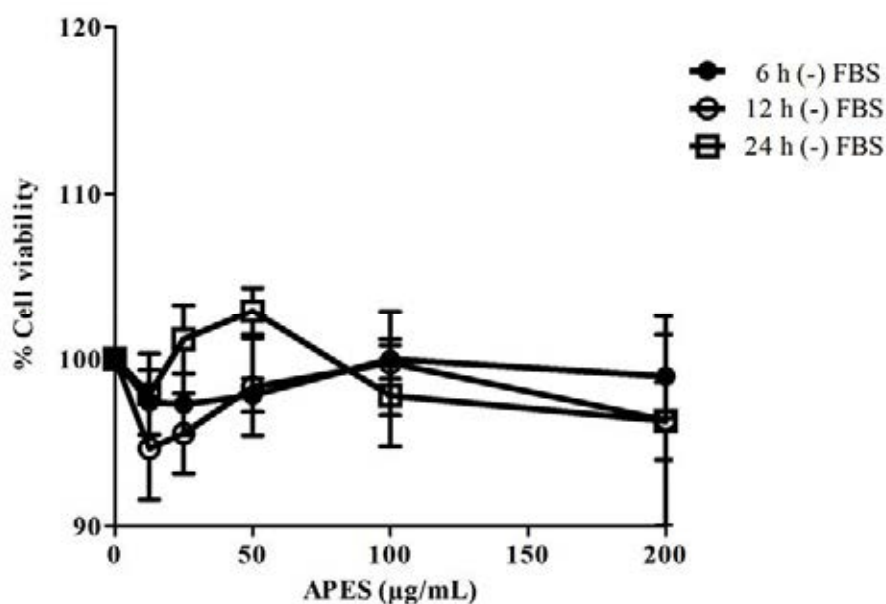


Figure 9. Concentration- and time-dependent studies of APES on cell proliferation. The cells were treated with APES at the concentrations of 12.5, 25, 50, 100 and 200 µg/mL for 6, 12 and 24 h exposure in the (A) presence and (B) absence of FBS. Viable cells were determined by MTT assay. Results were expressed as mean \pm S.E.M. (N =3, each performed in triplicate). * $p < 0.05$ compared to the untreated control.

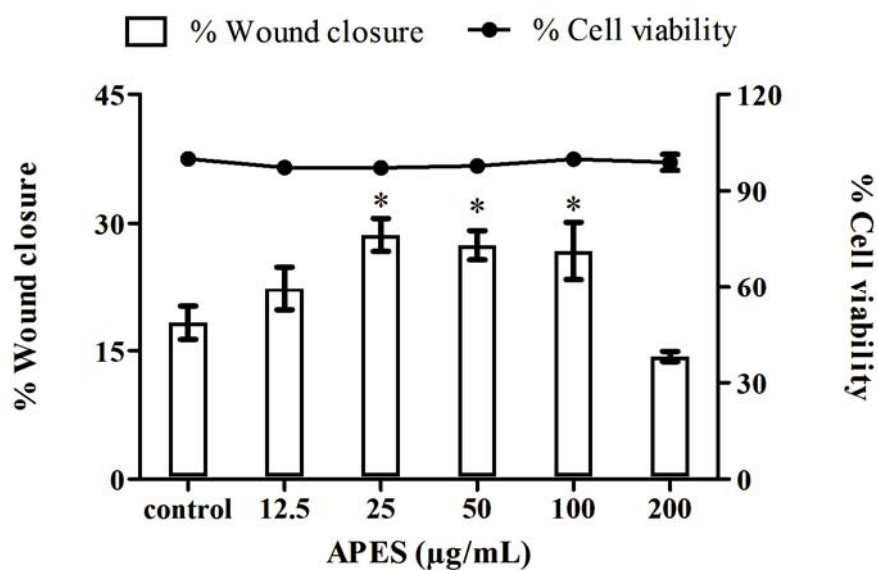


Figure 10. Comparison between cell migration and viability affected by APES in absence of FBS. Treatment with APES at the concentrations of 25, 50 and 100 µg/mL for 6 h, cell migration and viability were determined by *in vitro* scratch and MTT assays. * $p < 0.05$ compared to the untreated control. Results were expressed as mean \pm S.E.M. (N =3, each performed in triplicate).

Effect of APES on intracellular ROS level

Oxidative stress reduces both proliferation and migration of cells at wounded edge by affecting the delay rate of wound repair (Schäfer and Werner, 2008). Our preliminary result by staining with DCFH-DA dye showed that ROS was observed around the wounded area in the untreated control (Figure 11). However, APES did not affect ROS level or cell death as measured by triple staining with DCFH-DA, Hoechst 33342 and PI. We therefore determined the effect of APES on intracellular ROS level under normal cell condition using DCFH-DA assay. Treatment of unwounded cells with APES at the concentrations of 25, 50, 100 and 200 $\mu\text{g/mL}$ for 6 h significantly decreased ROS in a concentration-dependent manner, exhibiting the percentage of DCF fluorescence of 91.54 ± 1.71 , 86.61 ± 0.49 , 74.96 ± 3.39 and $54.54 \pm 2.53\%$, respectively (Figure 12A).

Previous study revealed that the 4',5-dihydroxy-3',6,7-trimethoxyflavone from *Artemisia asiatica* decreased ROS levels in amyloid protein-induced oxidative stress of PC12 cells (Heo *et al.*, 2001). Additionally, the methanolic extract of the aerial part of AP was found to scavenge radicals of DPPH and NO, exhibiting EC_{50} values of 292.7 and 204.61 $\mu\text{g/mL}$, respectively (Ruikar *et al.*, 2011). Hence, a decrease in ROS level was probably due to the presence of phenolic and flavonoid contents. Phytochemical study of the aerial part of AP were found to be phenolic compounds like gallic acid, chlorogenic acid, ferulic acid while flavonoids were kaempferol, quercetin and rutin (Niranjan *et al.*, 2009).

Thus, APES induced cell migration through a reduction of oxidative stress (Figure 12B) leading to endothelial wound repair. We further elucidated whether a decrease in ROS might be due to the activation of antioxidant enzyme activity such as SOD, GPx and CAT.

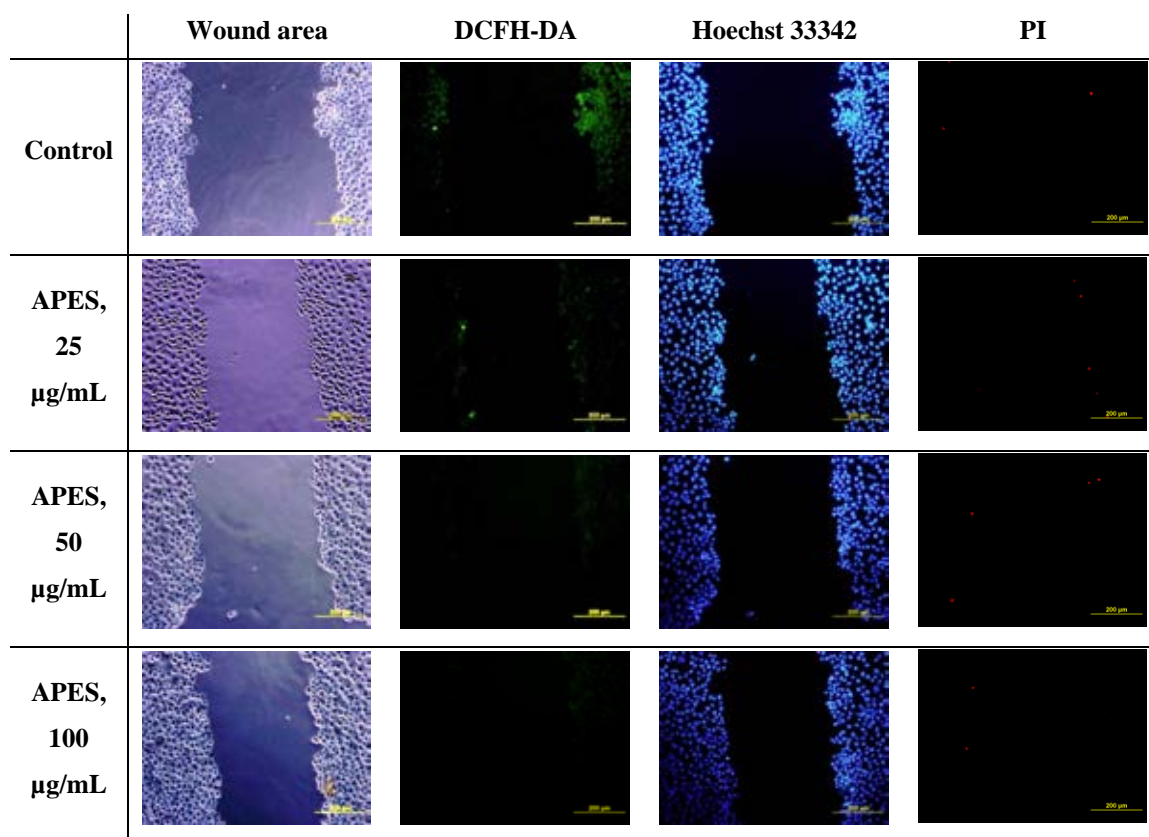
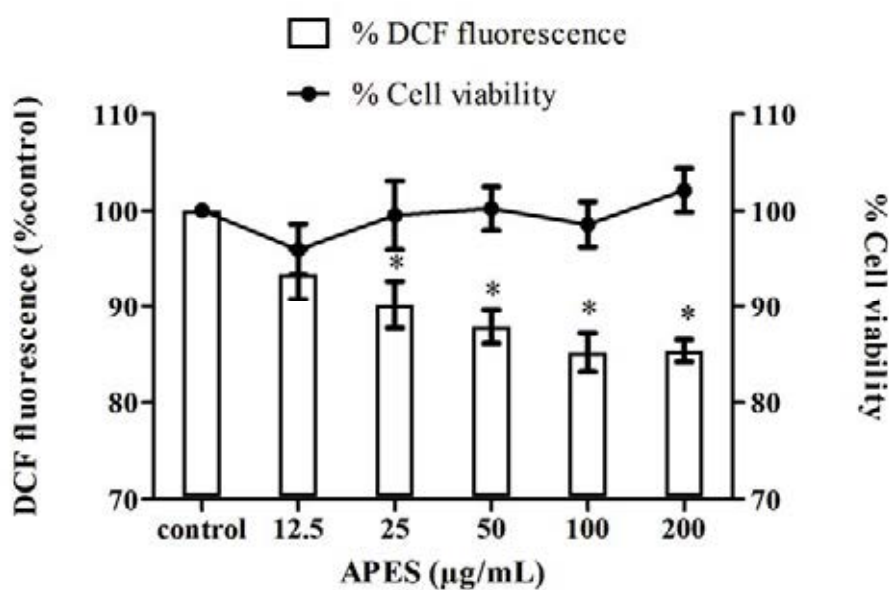


Figure 11. Representative triple-stained microscopic images of endothelial cells with or without APES. The cells were treated with APES (25, 50 and 100 µg/mL) for 6 h in the serum-free medium after wounding. The cells were stained with DCFH-DA (5 µM) at 37°C for 30 min, then washed with PBS and further incubated with Hoechst 33342 (10 µg/ml) and PI (10 µg/ml) at 37°C for 5 min. Photographs were taken around wounded edge at 0 h under inverted microscope (10 x magnification). The wounded area was monitored for repopulation of the void and photographed at 6 h postwounding.

(A)



(B)

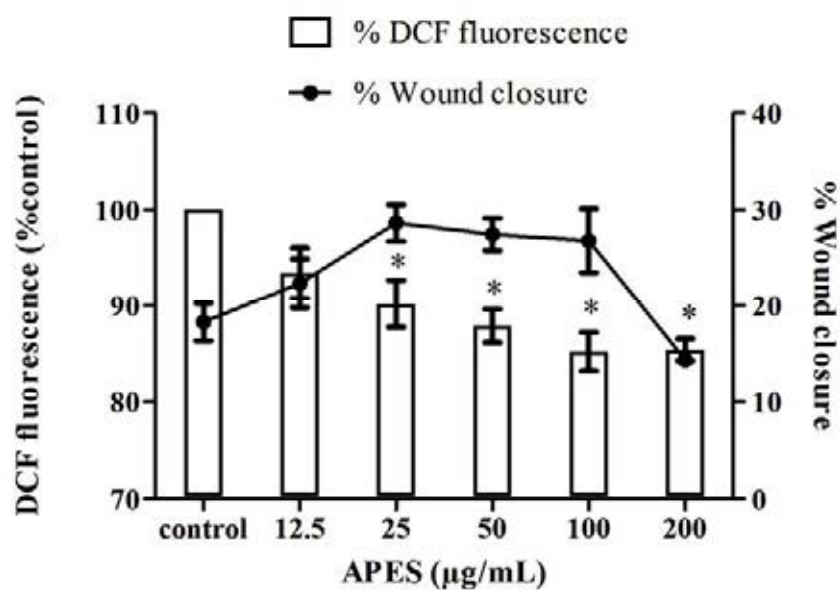


Figure 12. (A) Concentration- dependent effects of APES-reduced intracellular ROS. After 6 h incubation with APES, the cells were incubated with 5 µM DCFH-DA in PBS for 30 min. The fluorescence intensity was monitored at 485 nm excitation and 535 nm emission. (B) Comparison between cell migration and reduction of ROS by APES. * $p < 0.05$ compared to the untreated control. Results were expressed as mean \pm S.E.M. (N =3, each performed in triplicate).

Effect of APES on antioxidant enzyme activity

To verify whether APES could affect antioxidant enzyme function in ECV304 cells, activities of SOD, GPx and CAT were investigated. APES at the concentration of 25 µg/mL significantly enhanced SOD activity after incubation for 6 h, when compared to control (Figure 13). Meanwhile, treatment of the cells with the APES at the concentrations of 25, 50 and 100 µg/mL for 6 h did not change enzyme activities of GPx (Figure 14) and CAT (Figure 15).

The result suggested that the increase of SOD would increase antioxidant activity, the first line of defense against oxidative stress in our body (Rasheed *et al.*, 2010). Free radical scavenging activity of phenolic and flavonoid contents might play a role in the ability of the APES to combat intracellular ROS level as previously reported (Ruikar *et al.*, 2011). The methanolic extract of AP exhibited radical scavenging activities against DPPH (EC_{50} 292.7 µg/mL) due to the presence of phenolic compounds, with EC_{50} value of 150.33 ± 1.5 µg/mL (Suresh *et al.*, 2011).

SOD is a primary and important antioxidant enzyme capable of rapidly reacting with superoxide anion and lowering cellular superoxide radicals. Our unpublished result of cell-free system demonstrated that APES scavenged superoxide radical, exhibiting an EC_{50} value of 75.29 ± 4.65 µg/mL, which might be due to the activation of SOD activity at cellular level. Our finding of APES attenuated intracellular ROS (Figure 12) may thus be attributed to its enhancing superoxide radical scavenging and SOD activities (Figure 13).

Effect of APES on intracellular nitric oxide level

Endothelial cells were shown to release NO, possessing antiplatelet aggregation and vasorelaxation (Widlansky *et al.*, 2003). We also investigated the effect of APES on intracellular NO level using DAN method (Si *et al.*, 1997; Hensley *et al.*, 2003). Analysis of a calibration curve of nitrite standard exhibited no difference on intracellular NO level affected by APES at various antioxidant concentrations and incubation times as compared to untreated control (Figure 16).

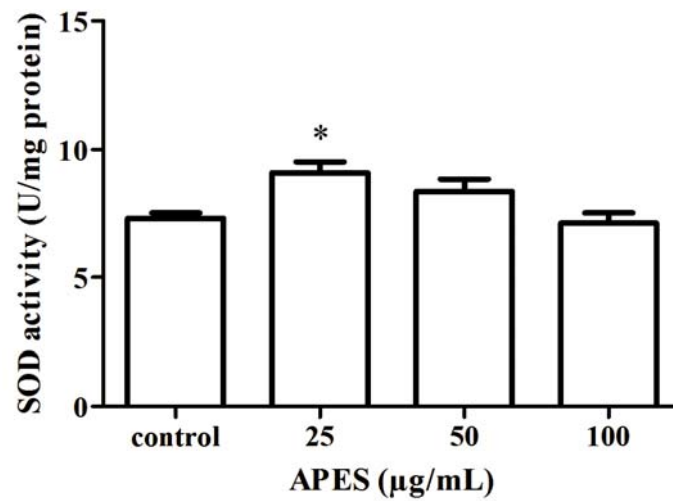
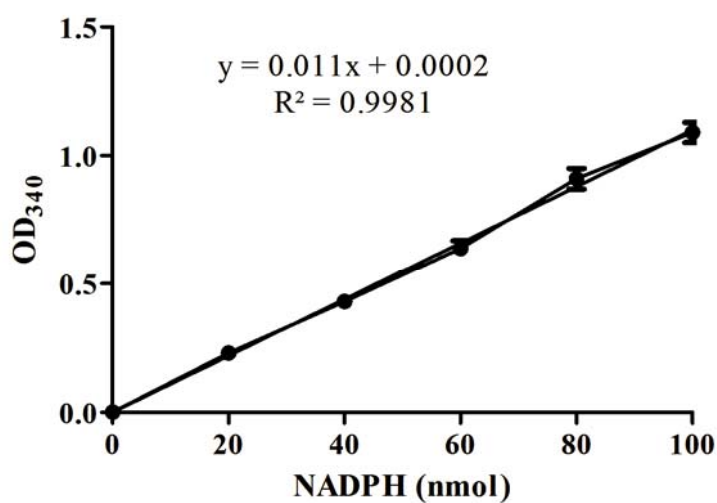


Figure 13. Effect of APES on SOD activity. The cells were treated with APES at the concentrations of 25, 50 and 100 µg/mL for 6 h. SOD activity was performed according of commercially SOD assay kit. Results were expressed as mean \pm S.E.M. (N =3, each performed in triplicate). Significant difference at $*p < 0.05$ compared to the untreated control.

(A)



(B)

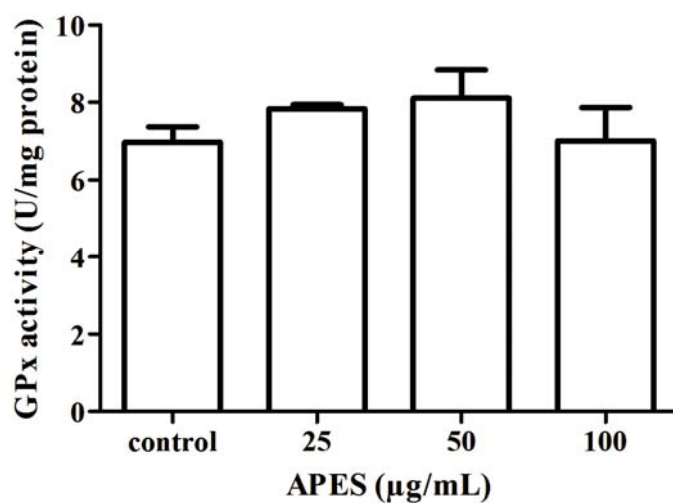
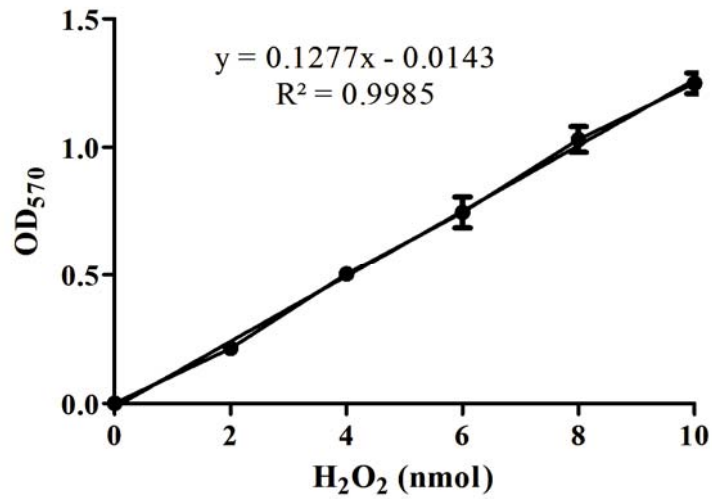


Figure 14. Effect of APES on GPx activity. The cells were treated with APES at the concentrations of 25, 50 and 100 μg/mL for 6 h. (A) Calibration curve of NADPH at the concentrations of 20, 40, 60, 80 and 100 nmol. (B) GPx activity induced by APES. GPx activity was performed according of commercially GPx assay kit. Results were expressed as mean ± S.E.M. (N =3, each performed in triplicate).

(A)



(B)

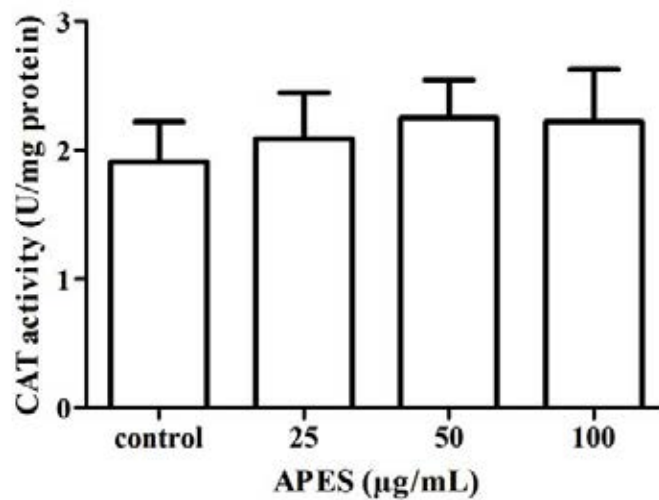
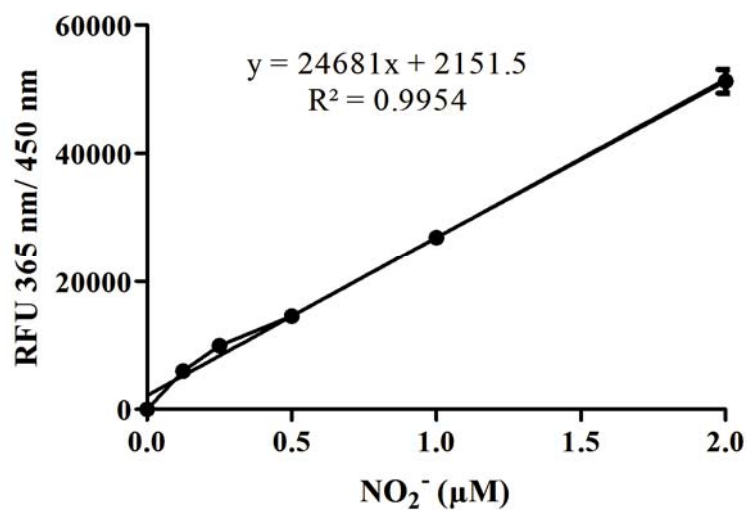


Figure 15. Effect of APES on CAT activity. The cells were treated with APES at the concentrations of 25, 50 and 100 µg/mL for 6 h. (A) Calibration curve of H₂O₂ at the concentrations of 2, 4, 6, 8 and 10 nmol. (B) CAT activity induced by APES. The cells were treated with APES at the indicated concentrations for 6 h. Results were expressed as mean ± S.E.M. (N =3, each performed in triplicate).

(A)



(B)

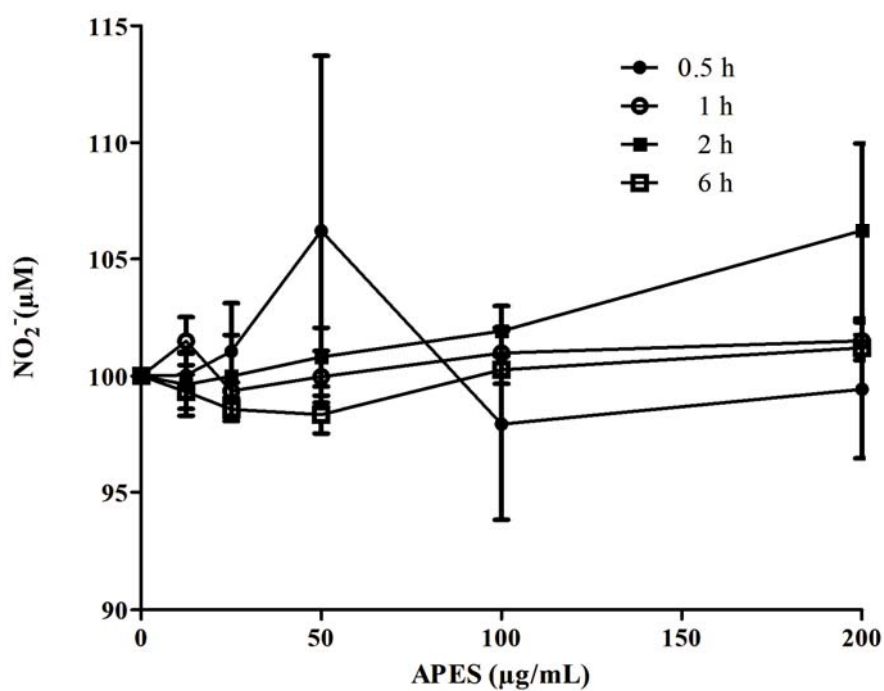


Figure 16. Effect of APES on intracellular NO level in ECV304 cells. The cells were treated with APES at the concentrations of 12.5, 25, 50, 100 and 200 $\mu\text{g/mL}$ for 0.5, 1, 2 and 6 h. (A) Calibration curve of nitrite at the concentrations of 0.125, 0.25, 0.5, 1 and 2 μM . (B) Intracellular NO level induced by APES. Results were expressed as mean \pm S.E.M. (N =3, each performed in triplicate).

Earlier reports showed that chronic treatment of dietary quercetin, also found in the methanolic extract of AP (Niranjan *et al.*, 2009), enhanced vascular eNOS activity leading to an increase in intracellular NO in spontaneously hypertensive rats (Sanchez *et al.*, 2006). However, our result revealed that APES did not affect intracellular NO level.

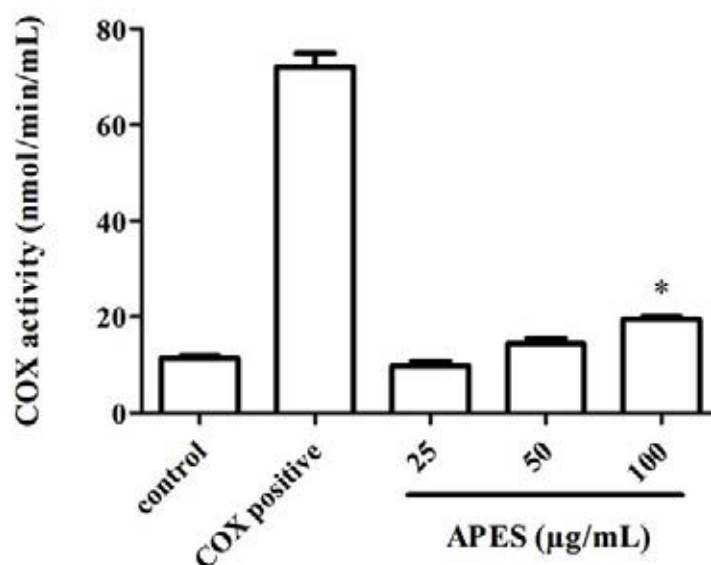
Effect of APES on COX activity

COX-2, a predominant isoform in human cerebral microvessels, is a major contributor to the regulation of cerebral circulation under physiological and pathophysiological conditions (Yakubu *et al.*, 2005). We therefore investigated the effect of APES on COX activity in endothelial cells. APES at the concentration of 100 µg/mL for 6 h significantly activated total COX activity (Figure 17A), which was 4-fold less potent than that enhanced SOD activity (Figure 13). To determine which COX played a role in this activation, specific inhibitors of COX-1 (SC-560) and COX-2 (DuP-697) were then used. The result showed that activation of both COX-1 and COX-2 activities were significantly observed in APES-treated cells (Figure 17B).

Previous study revealed that the COX-2 has a critical role in angiogenesis, while the production of PGE₂ also underlies the angiogenic effects of vascular endothelial cell growth factor and basic fibroblast growth factor (Jiang *et al.*, 2004). Earlier reports showed that several antioxidant bioflavonoids like quercetin served as a physiological cofactor for the stimulation of COX-1 and COX-2 mediated conversion of arachidonic acid to prostaglandins and thromboxanes (Bai *et al.*, 2008). Moreover, the acetone extract of AP indicated potent anti-inflammatory activity in 12-O-tetradecanoyl phorbol-13-acetate induced ear edema in mice (Ruikar *et al.*, 2011).

Taken all together, APES significantly enhanced human endothelial cell proliferation and migration due to the stimulation of COX-1 and COX-2 activities (Table 5). Additionally, APES also modulated intracellular ROS level due to an increase in SOD activity.

(A)



(B)

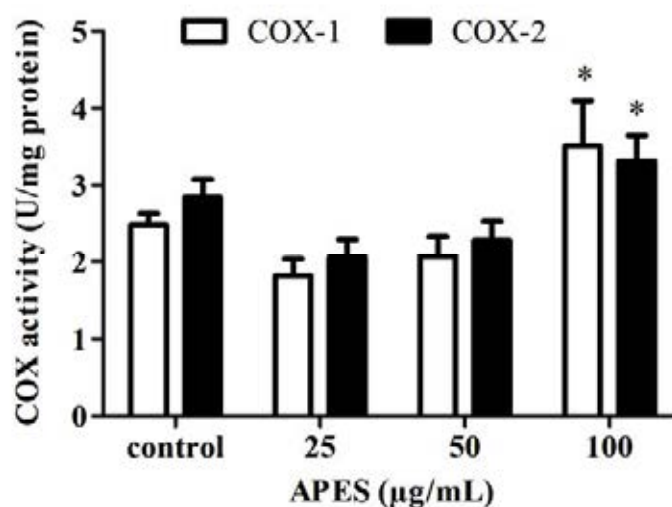


Figure 17. Effect of APES on COX activity. (A) The cells were treated with APES at the indicated concentration for 6 h. (B) The cell lysates were calorimetrically assayed for COX activity using an assay kit in the absence or presence of either COX-1 specific inhibitor (SC-560) or COX-2 specific inhibitor (DuP-697). Results were expressed as mean \pm S.E.M. (N =3, each performed in triplicate). * $p < 0.05$ compared to the untreated control.

Table 5. Summary of the biological activities of APES on ECV304 cells.

Biological activity	APES ($\mu\text{g/mL}$)				
	12.5	25	50	100	200
Endothelial proliferation	+	+	+	+	-
Endothelial wound repair	-	+	+	+	-
Intracellular ROS (decrease)	-	+	+	+	+
SOD activity (activation)	ND	+	-	-	ND
GPx activity	ND	-	-	-	ND
CAT activity	ND	-	-	-	ND
Intracellular NO	-	-	-	-	-
COX-1 activity (activation)	ND	-	-	+	ND
COX-2 activity (activation)	ND	-	-	+	ND

- negative effect; + positive effect; ND not determine

Chemical profile of APES

Overall results revealed that APES induced endothelial wound repair *via* cell migration, proliferation and reduction of oxidative stress. Radical scavenger of DPPH and NO in the methanolic extract of the aerial part of AP was due to the presence of rutin and quercetin (Niranjan *et al.*, 2009) and of *A. vulgaris* was due to eriodictyol, luteolin and apigenin (Lee *et al.*, 1998). We therefore determined the chemical profile of APES as compared with standard flavonoids. The UV/Vis spectroscopic measurements were carried out at the spectral range from 190 to 800 nm. The analysis of APES and standard flavonoids including rutin, eriodictyol, luteolin, quercetin and apigenin were measured in quartz cuvettes at a distance of 1 mm. The UV spectra of APES and standard of rutin, eriodictyol, luteolin, quercetin and apigenin presented the maximum UV absorption (λ_{\max}) at wavelengths of 272, 258, 288, 350, 372 and 268 nm, respectively (Table 6). The majority of λ_{\max} near at 270 nm (Figure 18) was utilized for HPLC analysis. Various retention times of rutin, eriodictyol, luteolin, quercetin and apigenin were 29.18 ± 0.02 , 38.30 ± 0.03 , 38.72 ± 0.02 , 38.96 ± 0.03 and 42.13 ± 0.02 min, respectively (Figure 19, Table 6). HPLC profile of APES compared with the standard flavonoid mixture (Figure 20) showed a minute quantity of flavonoids present in APES (Table 7).

The calibration curve used to calculate the rutin content in the extracts was expressed by the following linear equation: $y = 30,000,000x + 613.3$; $R^2 = 1.00$. Linearity was observed between rutin content and peak height. The result revealed that rutin content in APES was 0.70 ± 0.10 $\mu\text{g}/\text{mg}$ of extract. The calibration curve of eriodictyol was expressed by the following linear equation: $y = 40,000,000x + 83.032$; $R^2 = 1.00$. The result revealed that eriodictyol content in APES was 0.98 ± 0.07 $\mu\text{g}/\text{mg}$ of extract. The calibration curve of luteolin was expressed by the following a linear equation: $y = 60,000,000x - 4010.1$; $R^2 = 0.9997$. The result revealed that luteolin content in APES was 2.51 ± 0.06 $\mu\text{g}/\text{mg}$ of extract. The calibration curve of quercetin was expressed by the following linear equation: $y = 50,000,000x - 817.81$; $R^2 = 0.9997$. The result revealed that quercetin content in APES was 0.68 ± 0.12 $\mu\text{g}/\text{mg}$ of extract. The calibration curve of apigenin was expressed by the following linear equation: $y = 70,000,000x + 4975.5$; $R^2 = 0.9998$. The result revealed that apigenin content in APES was 3.43 ± 0.15 $\mu\text{g}/\text{mg}$ of extract.

Table 6. Summary of wavelength at maximum absorbance and retention time obtained from UV spectra and HPLC chromatograms, respectively.

Sample	λ_{max} (nm)	Retention time (min)
Rutin	206 and 258	29.18 ± 0.02
Eriodictyol	288	38.30 ± 0.03
Luteolin	208, 254 and 350	38.72 ± 0.02
Quercetin	204, 256 and 372	38.96 ± 0.03
Apigenin	210, 268 and 334	42.13 ± 0.02
APES	272 and 328	-

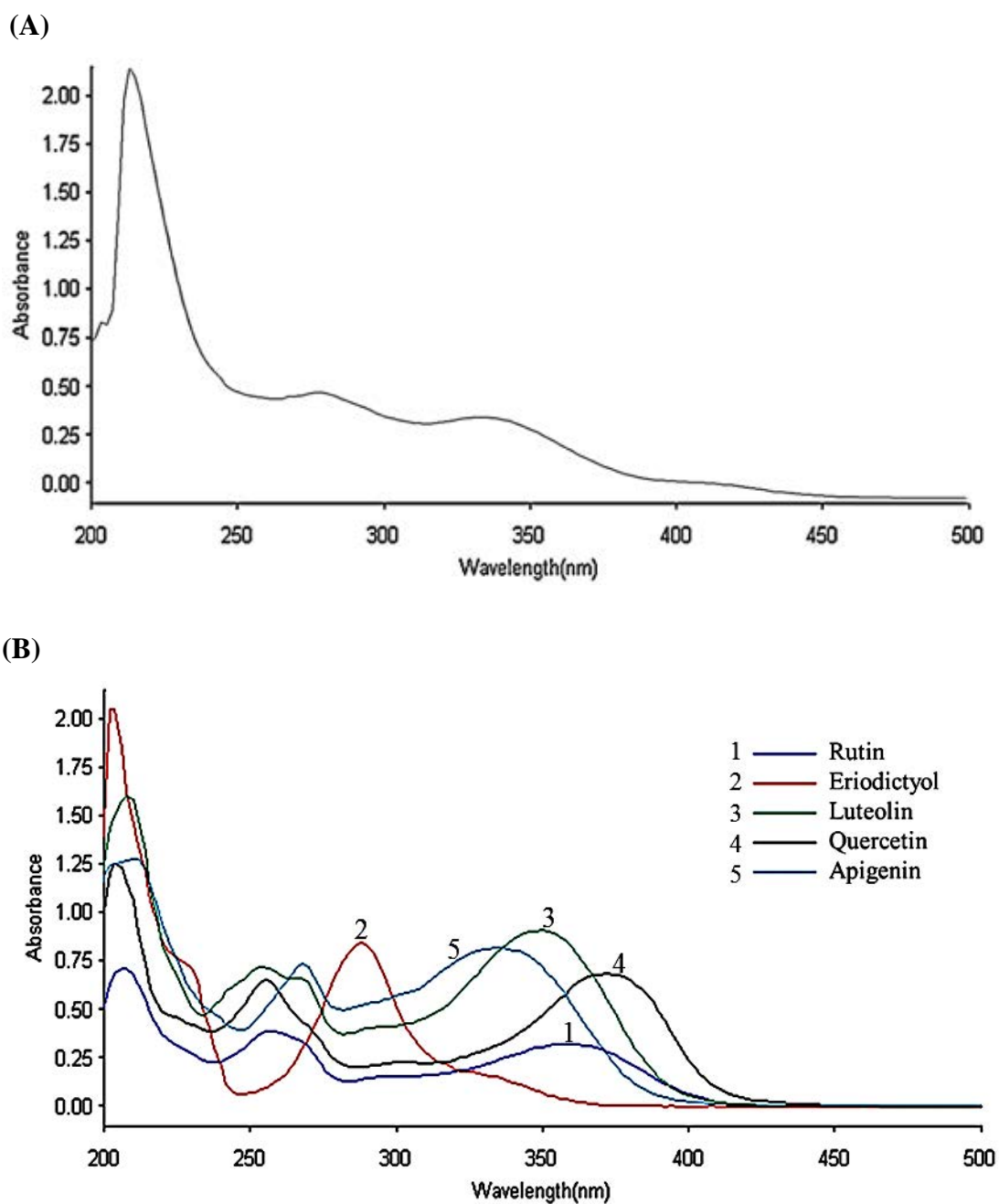
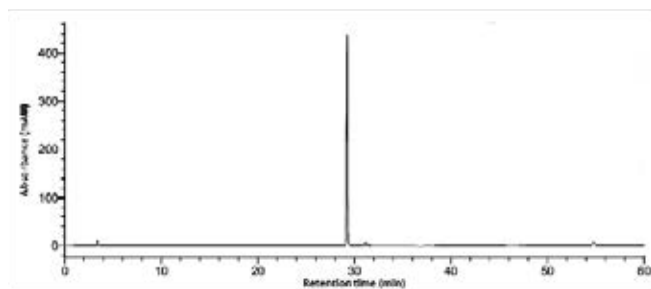
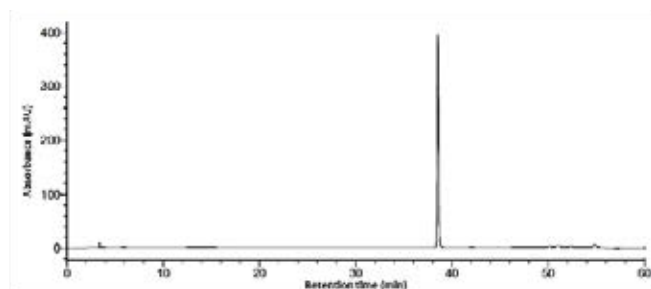


Figure 18. UV spectra of (A) APES and (B) standard flavonoids of (1) rutin, (2) eriodictyol, (3) luteolin, (4) quercetin and (5) apigenin.

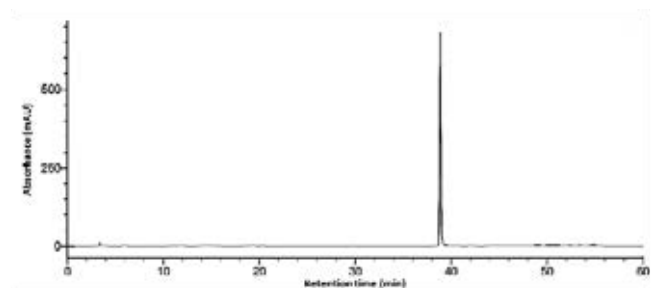
(A)



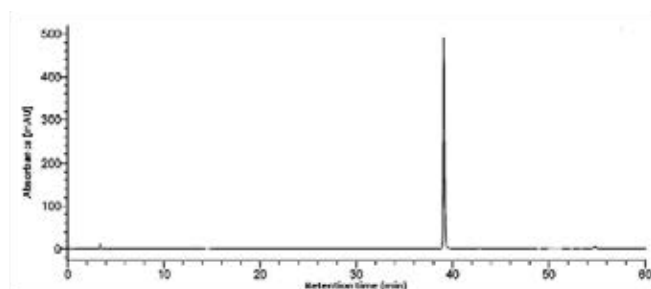
(B)



(C)



(D)



(E)

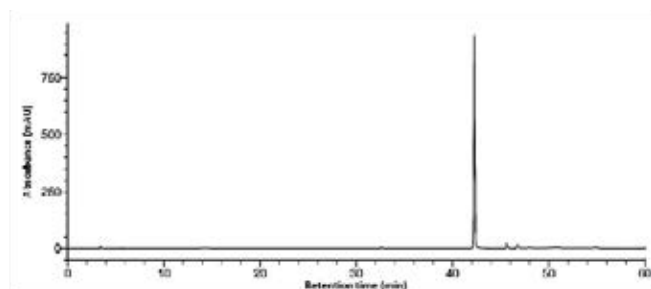
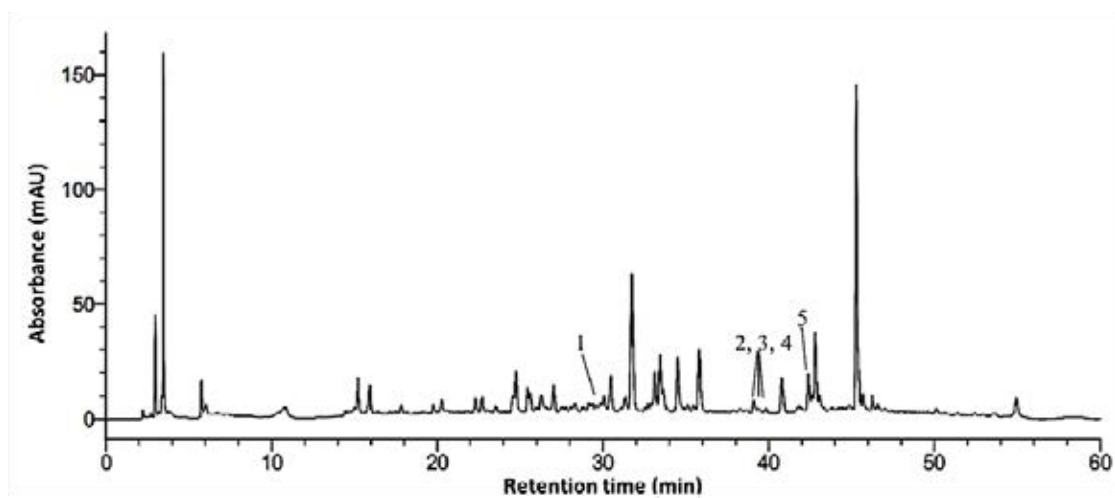


Figure 19. HPLC chromatogram of (A) rutin, (B) eriodictyol, (C) luteolin, (D) quercetin and (E) apigenin monitored at 270 nm.

(A)



(B)

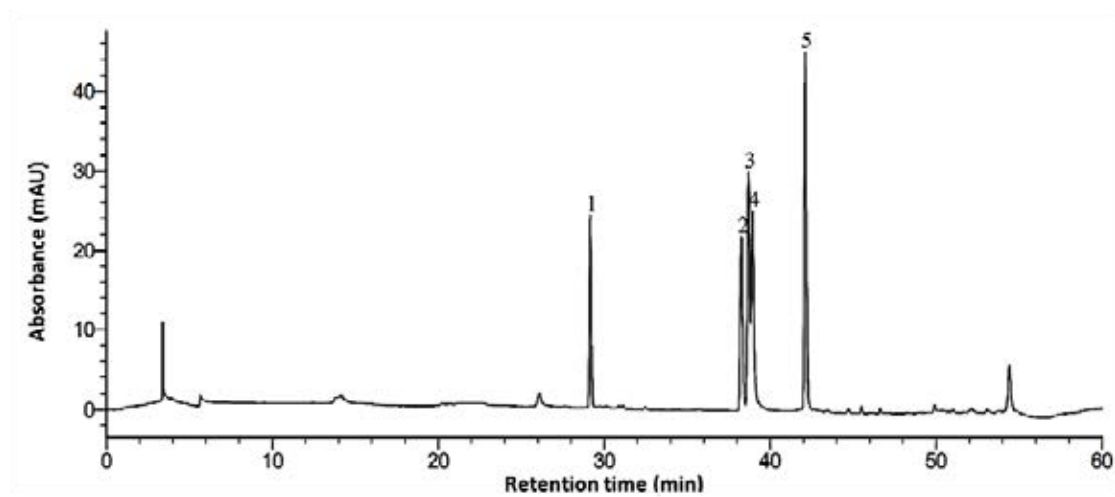


Figure 20. HPLC fingerprint obtained from (A) APES as compared with (B) standard flavonoids of (1) rutin, (2) eriodictyol, (3) luteolin, (4) quercetin and (5) apigenin monitored at 270 nm.

Table 7. Flavonoid contents found in APES.

Flavonoid	Retention time (min)	$\mu\text{g}/\text{mg}$ of extract	$\mu\text{g}/\text{mg}$ of dried crude drug
Rutin	29.15 ± 0.01	0.70 ± 0.10	0.04 ± 0.01
Eriodictyol	38.28 ± 0.01	0.98 ± 0.07	0.05 ± 0.00
Luteolin	38.71 ± 0.02	2.51 ± 0.06	0.13 ± 0.00
Quercetin	39.10 ± 0.01	0.68 ± 0.12	0.03 ± 0.01
Apigenin	42.11 ± 0.01	3.43 ± 0.15	0.17 ± 0.01

Previous study revealed the chemical profile of AP extracted with 50% methanol–water using HPLC–UV/MS/MS. The mobile phase was 1% aqueous with acetic acid and acetonitrile and monitored at 254 nm. The presence of polyphenols such as gallic, protocatechuic acid, chlorogenic acid, caffeic acid, ferulic acids, rutin, quercetin, and kaempferol was observed and the amount of rutin was 0.11% w/w (Niranjan *et al.*, 2009). Additionally, the amount of quercetin in *A. annua* ranged from 0.31 to 0.44 $\mu\text{g/mL}$ using HPLC method (Parial *et al.*, 2009). Eriodictyol and luteolin contents, the most abundant flavonoids in *A. vulgaris*, were 40 mg/kg of dried plant material, while the amount of apigenin was 5 mg/kg of dried plant material (Lee *et al.*, 1998).

Thus, these flavonoids might be used as standard markers for quality control of the herbal formulations containing AP.

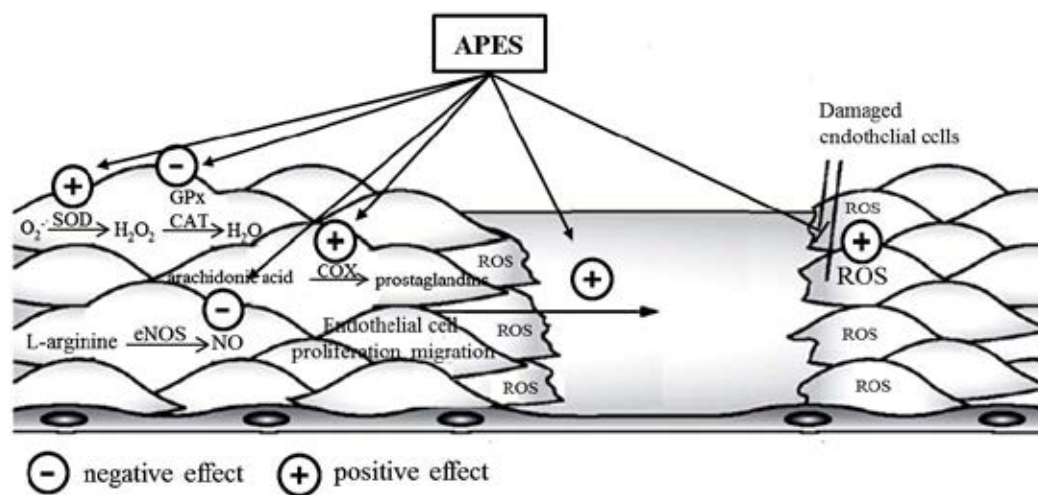
CHAPTER V

CONCLUSION

In the present study, quality control of nine crude drugs in Phikud Navakot, *i.e.* roots of *Angelica dahurica* (AD), *Angelica sinensis* (AS), *Saussurea costus* (SC), rhizomes of *Atractylodes lancea* (AL), *Ligusticum chuanxiong* (LC), *Picrorhiza kurroa* (PK), roots and rhizomes of *Nardostachys jatamansi* (NJ), aerial parts of *Artemisia pallens* (AP) and galls of *Terminalia chebula* (TC) was evaluated according to Thai Herbal Pharmacopoeia. The result was well correlated with those of the authentic samples. The extraction of all nine herbs using either 50% ethanol or water showed that the lowest yield was obtained from both ethanol and water extracts of NJ while the highest yield was from the ethanol extract of TC. Endothelial cell proliferation of each herbal extracts using MTT assay showed that only the ethanolic extracts of AP (0.01 $\mu\text{g/mL}$) and LC (10 $\mu\text{g/mL}$) significantly increased cell proliferation in a concentration-dependent manner. Cell proliferation affected by APES was more potent than LCES. APES was therefore selected for cell migration study using the *in vitro* scratch assay. APES (25 $\mu\text{g/mL}$) in a serum-free condition for 6 h significantly increased cell migrating into wounded area in a concentration-dependent manner (Figure 21A). APES (25 $\mu\text{g/mL}$) for 6 h significantly decreased ROS in a concentration-dependent manner. The result demonstrated that APES enhanced endothelial cell migration into wounded area through the attenuation of ROS while damaged endothelial cells could be replaced through replication treatment of the surrounding endothelial cell. A decrease in ROS level affected by APES (25 $\mu\text{g/mL}$) for 6 h treatment was due to the activation of SOD activity but not GPx or CAT. APES at higher concentration (100 $\mu\text{g/mL}$) for 6-h incubation significantly activated both COX-1 and COX-2 activities without affecting the NO production. HPLC profile of APES showed the presence of apigenin higher than other flavonoid content, *i.e.* eriodictyol, luteolin, quercetin and rutin (Figure 21B).

To the best of our knowledge, this is the first report showing that short exposure to the ethanolic extract of *Artemisia pallens* promoted migration of endothelial cells into

(A)



(B)

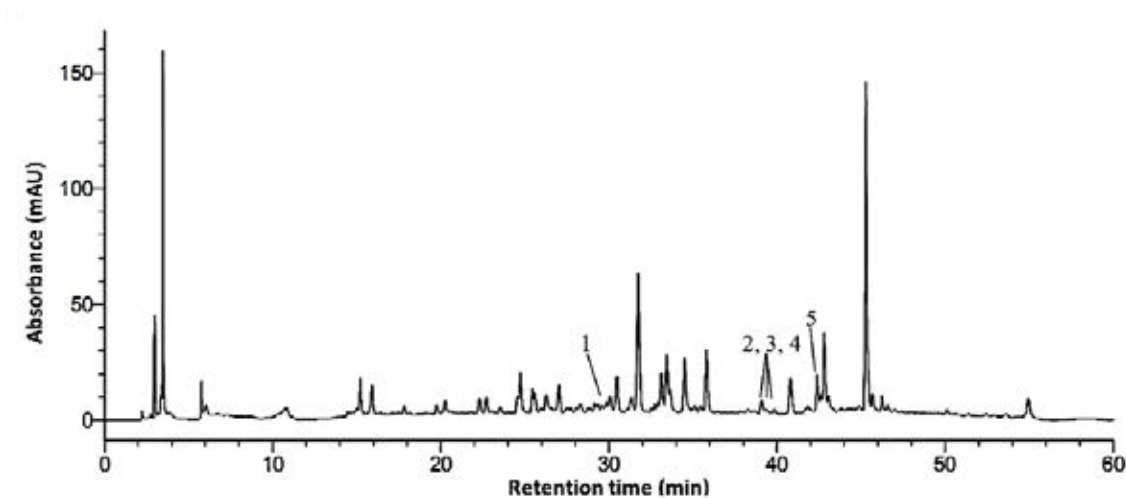


Figure 21. (A) Summary of biological activities of APES in ECV304 cells. (B) HPLC chromatogram of APES showing (1) rutin, (2) eriodictyol, (3) luteolin, (4) quercetin and (5) apigenin.

wounded area probably through the activation of COX-1 and COX-2 activities in a nitric oxide-independent pathway. Meanwhile, long exposure to APES promoted proliferation in normal endothelial cells through activating SOD activity, resulting in oxidative stress relief. Thus, aerial parts of *Artemisia pallens*, one of nine herbs in Phikud Navakot, might play an important role in angiogenesis process for the treatment of circulatory disorder.

REFERENCES

- Abad, M. J., de las Heras, B., Silván, A. M., Pascual, R., Bermejo, P., Rodríguez, B., and Villar, A. M. 2001. Effects of furocoumarins from *Cachrys trifida* on some macrophage functions. Journal of Pharmacy and Pharmacology 53(8): 1163-1168.
- Abraham, N. G., Brunner, E. J., Eriksson, J. W., and Robertson, R. P. 2007. Metabolic syndrome: psychosocial, neuroendocrine, and classical risk factors in type 2 diabetes. Annals of the New York Academy of Sciences 1113: 256-275.
- Al-Isa, A. N., Thalib, L., and Akanji, A. O. 2010. Circulating markers of inflammation and endothelial dysfunction in Arab adolescent subjects: Reference ranges and associations with age, gender, body mass and insulin sensitivity. Atherosclerosis 208(2): 543-549.
- Aruoma, O. I. 1998. Free radicals, oxidative stress, and antioxidants in human health and disease. Journal of the American Oil Chemists' Society 75(2): 199-212.
- Arya, D., Joshi, G. C., and Tiwari, L. M. 2012. Status and trade of crude drug in Uttarakhand. Journal of Medicinal Plants Research 6(18): 3434-3444.
- Bai, H. W., and Zhu, B. T. 2008. Strong activation of cyclooxygenase I and II catalytic activity by dietary bioflavonoids. Journal of Lipid Research 49(12): 2557-2570.
- Bal-Price, A., and Brown, G. C. 2001. Inflammatory neurodegeneration mediated by nitric oxide from activated glia-inhibiting neuronal respiration, causing glutamate release and excitotoxicity. Journal of Neuroscience, 21(17): 6480-6491.
- Ban, H. S., Lim, S. S., Suzuki, K., Jung, S. H., Lee, S., Lee, Y. S., Shin, K. H., and Ohuchi, K. 2003. Inhibitory effects of furanocoumarins isolated from the roots of *Angelica dahurica* on prostaglandin E2 production. Planta Medica 69(5): 408-412.
- Bauer, R., and Xiao, P. G. 2011. Radix *Angelicae sinensis* Danggui. Chromatographic Fingerprint Analysis of Herbal Medicines: 161-170.
- Bauer, R., and Xiao, P. G. 2011. Radix *Angelicae dahuricae* Baizhi. Chromatographic Fingerprint Analysis of Herbal Medicines: 171-179.

- Bauer, R., and Xiao, P. G. 2011. Radix *Ligustici chuanxiong* Chuanxiong. Chromatographic Fingerprint Analysis of Herbal Medicines: 181-190.
- Bauer, R., and Xiao, P. G. 2011. Rhizoma *Atractylodis lanceae* Cangzhu. Chromatographic Fingerprint Analysis of Herbal Medicines: 691-706.
- Bearden, J. C. 1978. Quantitation of submicrogram quantities of protein by an improved protein-dye binding assay. Biochimica et Biophysica Acta 533(2): 525-529.
- Bustos, M., Coffman, T. M., Saadi, S., and Platt, J. L. 1997. Modulation of eicosanoid metabolism in endothelial cells in a xenograft model. Role of cyclooxygenase-2. Journal of Clinical Investigation 100(5): 1150-1158.
- Camacho, M., López-Belmonte, J., and Vila, L. 1998. Rate of vasoconstrictor prostanoids released by endothelial cells depends on cyclooxygenase-2 expression and prostaglandin I synthase activity. Circulation Research 83(4): 353-365.
- Carmichael, J., Degraff, W. G., Gazdar, A. F., Minna, J. D., and Mitchell, J. B. 1987. Evaluation of a tetrazolium-based semi-automated colorimetric assay: assessment of chemosensitivity testing. Cancer Research 47: 936-942.
- Carvalho, I. S., Cavaco, T., and Brodelius, M. 2011. Phenolic composition and antioxidant capacity of six *artemisia* species. Industrial Crops and Products 33(2): 382-388.
- Catalán, C. A. N., Cuenca, M. del R., Verghese, J., Joy, M. T., Gutiérrez, A. B., and Herz, W. 1990. Sesquiterpene ketones related to davanone from *Artemisia pallens*. Phytochemistry 29(8): 2702-2703.
- Ćavar, S., Maksimović, M., Vidic, D., and Parić, A. 2012. Chemical composition and antioxidant and antimicrobial activity of essential oil of *Artemisia annua* L. from Bosnia. Industrial Crops and Products 37(1): 479-485.
- Chang, S.H., Jung, E.J., Park, Y.H., Lim, D.G., Ko, N.Y., Choi, W.S., Her, E., Kim, S.H., Choi, K.D., Bae, J.H., Kim, S.H., Kang, C.D., Han, D.J., and Kim, S.C. 2009. Anti-inflammatory effects of *Artemisia princeps* in antigen-stimulated T cells and regulatory T cells. Journal of Pharmacy and Pharmacology. 61(8):1043-1050.

- Chauhan, R. S., and Nautiyal, M. C. 2005. Commercial viability of cultivation of an endangered medicinal herb *Nardostachys jatamansi* at three different agroclimatic zones. Current Science Bangalore 89(9): 1481-1488.
- Chavalittumrong, P., Chivapat, S., Attawish, A., and Soonthornchareonnon, N. 2010. Chronic toxicity of Yahom Navagoth extract. Journal of Thai Traditional and Alternative Medicine 7(2-3): 134-145.
- Cho, J. Y., Baik, K. U., Jung, J. H., and Park, M. H. 2000. *In vitro* anti-inflammatory effects of cynaropicrin, a sesquiterpene lactone, from *Saussurea lappa*. European Journal of Pharmacology 398(3): 399-407.
- Davidge, S. T., Hubel, C. A., and McLaughlin, M. K. 1993. Cyclooxygenase-dependent vasoconstrictor alters vascular function in the vitamin E-deprived rat. Circulation Research 73(1): 79-88.
- Davidge, S.T. 2001. Prostaglandin H synthase and vascular function. Circulation Research 89(8): 650-660.
- Delgado, V.M., Nugnes, L.G., Colombo, L.L., Troncoso, M.F., Fernández, M.M., Malchiodi, E.L., Frahm, I., Croci, D.O., Compagno, D., Rabinovich, G.A., Wolfenstein-Todel, C., and Elola, M.T. 2011. Modulation of endothelial cell migration and angiogenesis: a novel function for the “tandem-repeat” lectin galectin-8. Federation of American Societies for Experimental Biology Journal 25(1): 242-254.
- Engels, F., Renirie, B. F., ‘T Hart, B. A., Labadie, R. P., and Nijkamp, F. P. 1992. Effects of apocynin, a drug isolated from the roots of *Picrorhiza kurroa*, on arachidonic acid metabolism. Federation of European Biochemical Societies Letters 305(3): 254-256.
- Gorzalczany, S., Moscatelli, V., and Ferraro, G. 2013. *Artemisia copa* aqueous extract as vasorelaxant and hypotensive agent. Journal of Ethnopharmacology [Epub ahead of print]
- Gouveia, S., and Castilho, P. C. 2011. Antioxidant potential of *Artemisia argentea* L'Hér alcoholic extract and its relation with the phenolic composition. Food Research International 44(6): 1620-1631.
- Guo, J. Y., Huo, H. R., Zhao, B. S., Liu, H. B., Li, L. F., Ma, Y. Y., Guo, S. Y., and Jiang, T. L. 2006. Cinnamaldehyde reduces IL-1beta-induced cyclooxygenase-

- 2 activity in rat cerebral microvascular endothelial cells. European Journal of Pharmacology 537(1-3): 174-180.
- Guzik, T., Korbut, R., and Adamek-Guzik, T. 2003. Nitric oxide and superoxide in inflammation. Journal of Physiology and Pharmacology 54: 469-487.
- Heo, H. J., Cho, H. Y., Hong, B., Kim, H. K., Kim, E. K., Kim, B. G., and Shin, D. H. 2001. Protective effect of 4', 5-dihydroxy-3', 6, 7-trimethoxyflavone from *Artemisia asiatica* against A β -induced oxidative stress in PC12 cells. Amyloidosis 8(3): 194-201.
- Huang, J., Wolk, J. H., Gewitz, M. H., and Mathew, R. 2010. Progressive endothelial cell damage in an inflammatory model of pulmonary hypertension. Experimental Lung Research 36(1): 57-66.
- Jadhav, V. M., Thorat, R. M., Kadam, V. J., and Kamble, S. S. 2009. Herbal anxiolyte: *Nardostachys Jatamansi*. Journal of Pharmacy Research 2(8): 1208-1211.
- Jiang, H., Weyrich, A. S., Zimmerman, G. A., and McIntyre, T. M. 2004. Endothelial cell confluence regulates cyclooxygenase-2 and prostaglandin E2 production that modulate motility. Journal of Biological Chemistry 279(53): 55905-55913.
- Juang, L. J., Sheu, S. J., and Lin, T. C. 2004. Determination of hydrolyzable tannins in the fruit of *Terminalia chebula* Retz. by high performance liquid chromatography and capillary electrophoresis. Journal of Separation Science 27(9): 718-724.
- Kaji, T., Kaga, K., Miezi, N., Ejiri, N., and Sakuragawa, N. 1990. A stimulatory effect of *Artemisia* leaf extract on the proliferation of cultured endothelial cells. Chemical and Pharmaceutical Bulletin 38(2): 538-540.
- Kang, J. S., Yoon, Y. D., Lee, K. H., Park, S. K., and Kim, H. M. 2004. Costunolide inhibits interleukin-1 β expression by down-regulation of AP-1 and MAPK activity in LPS-stimulated RAW 264.7 cells. Biochemical and Biophysical Research Communications 313(1): 171-177.
- Kitamoto, S., and Egashira, K. 2004. Endothelial dysfunction and coronary atherosclerosis. Current Drug Targets - Cardiovascular and Haematological Disorders 4(1): 13-22.

- Klika, K. D., Saleem, A., Sinkkonen, J., Kähkönen, M., Loponen, J., Tähtinen, P., and Pihlaja, K. 2004. The structural and conformational analyses and antioxidant activities of chebulinic acid and its thrice-hydrolyzed derivative, 2,4-chebuloyl- β -D-glucopyranoside, isolated from the fruit of *Terminalia chebula*. Arkivoc (7): 83-105.
- Kumar, A., Lakshman, K., Jayaveera, K. N., Mani Tripathi, S. N., and Satish, K. V. 2010. Estimation of gallic acid, rutin and quercetin in terminalia chebula by HPTLC. Jordan Journal of Pharmaceutical Sciences 3(1): 63-68.
- Labieniec, M., and Gabryelak, T. 2003. Effects of tannins on Chinese hamster cell line B14. Mutation Research/Genetic Toxicology and Environmental Mutagenesis 539(1): 127-135.
- Lam, H. W., Lin, H. C., Lao, S. C., Gao, J. L., Hong, S. J., Leong, C. W., Yue, P. Y., Kwan, Y. W., Leung, A. Y., Wang, Y. T., and Lee, S. M. 2008. The angiogenic effects of *Angelica sinensis* extract on HUVEC *in vitro* and zebrafish *in vivo*. Journal of Cellular Biochemistry 103(1): 195-211.
- Lee, H. J., Kim, N. Y., Jang, M. K., Son, H. J., Kim, K. M., Sohn, D. H., Lee, S. H., and Ryu, J. H. 1999. A sesquiterpene, dehydrocostus lactone, inhibits the expression of inducible nitric oxide synthase and TNF- α in LPS-activated macrophages. Planta Medica 65(2): 104-108.
- Lee, H. S., Won, N. H., Kim, K. H., Lee, H., Jun, W., and Lee, K. W. 2005. Antioxidant effects of aqueous extract of *Terminalia chebula* *in vivo* and *in vitro*. Biological and Pharmaceutical Bulletin 28(9): 1639-1644.
- Lee, H.S., Koo, Y.C., Suh, H.J., Kim, K.Y., and Lee, K.W. 2010. Preventive effects of chebulic acid isolated from *Terminalia chebula* on advanced glycation endproduct-induced endothelial cell dysfunction. Journal of Ethnopharmacology 131(3): 567-574.
- Li, M., Firth, J. D., and Putnins, E. E. 2009. An *in vitro* analysis of mechanical wounding-induced ligand-independent KGFR activation. Journal of Dermatological Science 53(3): 182-191.
- Liang, Y.Z., Xie, P., and Chan, K. 2004. Quality control of herbal medicines. Journal of Chromatography B 812: 53-70.

- Liang, C. C., Park, A. Y., and Guan, J. L. 2007. *In vitro* scratch assay: a convenient and inexpensive method for analysis of cell migration *in vitro*. Nature Protocols 2(2): 329-333.
- Libby, P., Ridker, P. M., and Maseri, A. 2002. Inflammation and atherosclerosis. Circulation 105(9): 1135-1143.
- Lin, C. M., Chiu, J. H., Wu, I. H., Wang, B. W., Pan, C. M., and Chen, Y. H. 2010. Ferulic acid augments angiogenesis *via* VEGF, PDGF and HIF-1 alpha. Journal of Nutritional Biochemistry 21(7): 627-633.
- Maharashtra, I., and Usman, M. R. M. 2012. Pharmacognostical Evaluations of Some Herbal Plant. International Journal of Advanced Research in Pharmaceutical and Bio Sciences 2(3): 302-310.
- Manosroi, A., Jantrawut, P., Akazawa, H., Akihisa, T., and Manosroi, J. 2010. Biological activities of phenolic compounds isolated from galls of *Terminalia chebula* Retz.(Combretaceae). Natural Product Research 24(20): 1915-1926.
- Manosroi, A., Jantrawut, P., Akazawa, H., Akihisa, T., Manosroi, W., and Manosroi, J. 2011. Transdermal absorption enhancement of gel containing elastic niosomes loaded with gallic acid from *Terminalia chebula* galls. Pharmaceutical Biology 49(6): 553-562.
- Mapanga, R. F., Rajamani, U., Dlamini, N., Zungu-Edmondson, M., Kelly-Laubscher, R., Shafiullah, M., Wahab, A., Hasan, M. Y., Fahim, M. A., Rondeau, P., Bourdon, E., and Essop, M.F. 2012. Oleanolic acid: a novel cardioprotective agent that blunts hyperglycemia-induced contractile dysfunction. PLoS One 7(10): e47322.
- Marnett, L. J. 2000. Cyclooxygenase mechanisms. Current Opinion in Chemical Biology 4(5): 545-552.
- Martínez, M. J. A., Del Olmo, L. M. B., and Apaza, L. 2012. The *Artemisia* L. Genus: A Review of Bioactive Sesquiterpene Lactones. Studies in Natural Products Chemistry 37: 43-65.
- Melillo de Magalhães, P. M., Dupont, I., Hendrickx, A., Joly, A., Raas, T., Dessy, S., Sergent, T. and Schneider, Y. J. 2012. Anti-inflammatory effect and modulation of cytochrome P450 activities by *Artemisia annua* tea infusions in human intestinal Caco-2 cells. Food Chemistry 134(2): 864-871.

- Mighri, H., Hajlaoui, H., Akrou, A., Najjaa, H., and Neffati, M. 2010. Antimicrobial and antioxidant activities of *Artemisia herba-alba* essential oil cultivated in Tunisian arid zone. Comptes Rendus Chimie 13(3): 380-386.
- Min, S. W., Kim, N. J., Baek, N. I., and Kim, D. H. 2009. Inhibitory effect of eupatilin and jaceosidin isolated from *Artemisia princeps* on carrageenan-induced inflammation in mice. Journal of Ethnopharmacology 125(3): 497-500.
- Mino, J., Moscatelli, V., Hnatyszyn, O., Gorzalczy, S., Acevedo, C., and Ferraro, G. 2004. Antinociceptive and antiinflammatory activities of *Artemisia copa* extracts. Pharmacological Research 50(1): 59-63.
- Misra, L. N., Chandra, A., and Thakur, R. S. 1991. Fragrant components of oil from *Artemisia pallens*. Phytochemistry 30(2): 549-552.
- Moncada, S., Palmer, R. M. J., and Higgs, E. A. 1991. Nitric oxide: Physiology, pathophysiology, and pharmacology. Pharmacological Reviews 43(2): 109-142.
- National Drug Committee of Thailand. 2011. List of Herbal Medicinal Products A.D. 2011. Bangkok: 2011: 19-28.
- Niranjan, A., Barthwal, J., Lehri, A., Singh, D. P., Govindraj, R., Rawat, A. K. S., and Amla, D. V. 2009. Development and validation of an HPLC-UV-MS-MS method for identification and quantification of polyphenols in *Artemisia pallens* L. Acta Chromatographica 21(1): 105-116.
- Okahara, K., Bing, S., and Kambayashi, J. I. 1998. Upregulation of prostacyclin synthesis-related gene expression by shear stress in vascular endothelial cells. Arteriosclerosis, Thrombosis, and Vascular Biology 18(12): 1922-1926.
- Okamoto, T., Yoshida, S., Kobayashi, T., and Okabe, S. 2001. Inhibition of concanavalin A-induced mice hepatitis by coumarin derivatives. Japanese Journal of Pharmacology 85(1): 95-97.
- Pandey, M. M., Govindarajan, R., Rawat, A. K., and Pushpangadan, P. 2005. Free radical scavenging potential of *Saussurea costus*. Acta Pharmaceutica 55(3): 297-304.

- Parial, S., Jain, D. C., and Joshi, S. B. 2009. Identification and quantification by RP-HPLC analysis of secondary metabolites in extracts of *Artemisia annua*. Journal of Pharmacy Research 2(9): 1552-1556.
- Park, W. H., Kim, S. H., Chang, Y. C., Lee, Y. C., and Kim, C. H. 2003. The antiplatelet activity of Danggijakyaksan by inhibition of phospholipase C. Immunopharmacology Immunotoxicology 25(4): 561-571.
- Parente, L., and Perretti, M. 2003. Advances in the pathophysiology of constitutive and inducible cyclooxygenases: Two enzymes in the spotlight. Biochemical Pharmacology 65(2): 153-159.
- Patten, A.R., Brocardo, P.S., and Christie, B.R. 2013. Omega-3 supplementation can restore glutathione levels and prevent oxidative damage caused by prenatal ethanol exposure. Journal of Nutritional Biochemistry 24(5): 760-769.
- Pober, J. S., Min, W., and Bradley, J. R. 2009. Mechanisms of endothelial dysfunction, injury, and death. Annual Review of Pathology Mechanisms of Disease 4: 71-95.
- Powers, S. K., and Jackson, M. J. 2008. Exercise-induced oxidative stress: Cellular mechanisms and impact on muscle force production. Physiological Reviews 88(4): 1243-1276.
- Parekh, A., and Jadhav, V. M. 2009. Development of validated HPTLC method for quantification of jatamansone in jatamansi oil. Journal of Pharmacy Research 2(5): 975-977.
- Prakash, S. D. V., Satyendra Dinesh, G., Sree Satya, N., Sumalatha, M., Venkateswara Kumar, S., and Vangalapati, M. 2012. Determination of partition coefficient for chebulinic acid extraction from various extracts of *Terminalia chebula* species. International Journal of Chemical Sciences 10(4): 2111-2116.
- Pujar, P. P., Sawaikar, D. D., Rojatkar, S. R., and Nagasampagi, B. A. 2000. A new germacranolide from *Artemisia pallens*. Fitoterapia 71(5): 590-592.
- Rasheed, A. S., Venkataraman, S., Jayaveera, K. N., Fazil, A. M., Yasodha, K. J., Aleem, M. A., Mohammed, M., Khaja, Z., Ushasri, B., Pradeep, H. A., and Ibrahim, M. 2010. Evaluation of toxicological and antioxidant potential of

- Nardostachys jatamansi* in reversing haloperidol-induced catalepsy in rats. International Journal of General Medicine 26(3): 127-136.
- Reddy, D. B., Reddy, T. C. M., Jyotsna, G., Sharan, S., Priya, N., Lakshmipathi, V., and Reddanna, P. 2009. Chebulagic acid, a COX-LOX dual inhibitor isolated from the fruits of *Terminalia chebula* Retz., induces apoptosis in COLO-205 cell line. Journal of Ethnopharmacology 124(3): 506-512.
- Resch, M., Heilmann, J., Steigel, A., and Bauer, R. 2001. Further phenols and polyacetylenes from the rhizomes of *Atractylodes lancea* and their anti-inflammatory activity. Planta Medica 67(5): 437-442.
- Rojatkar, S. R., Pawar, S. S., Pujar, P. P., Sawaikar, D. D., Gurunath, S., Sathe, V. T., and Nagasampagi, B. A. 1996. A germacranolide from *Artemisia pallens*. Phytochemistry 41(4): 1105-1106.
- Ruikar, A., Jadhav, R., Tambe, A., Misar, A., Mujumdar, A., Puranik, V., and Deshpande, N. 2010. Quantification of santonin from *Artemisia pallens* Wall by HPTLC. International Journal of Pharma and Bio Sciences 1(1): 1-3.
- Ruikar, A. D., Khatiwora, E., Ghayal, N. A., Misar, A. V., Mujumdar, A. M., Puranik, V. G., and Deshpande, N. R. 2011. Studies on aerial parts of *Artemisia pallens* Wall for phenol, flavonoid and evaluation of antioxidant activity. Journal of Pharmacy and Bioallied Sciences 3(2): 302-305.
- Russo, A., Izzo, A. A., Cardile, V., Borrelli, F., and Vanella, A. 2001. Indian medicinal plants as antiradicals and DNA cleavage protectors. Phytomedicine, 8(2): 125-132.
- Ruszymah, B. H. I., Chowdhury, S. R., Manan, N. A. B. A., Fong, O. S., Adenan, M. I., and Saim, A. B. 2012. Aqueous extract of *Centella asiatica* promotes corneal epithelium wound healing *in vitro*. Journal of Ethnopharmacology 140(2): 333-338.
- Sadanandam, A., Rosenbaugh, E. G., Singh, S., Varney, M., and Singh, R. K. 2010. Semaphorin 5A promotes angiogenesis by increasing endothelial cell proliferation, migration, and decreasing apoptosis. Microvascular Research 79(1): 1-9.

- Saha, T., Rih, J. K., and Rosen, E. M. 2009. BRCA1 down-regulates cellular levels of reactive oxygen species. Federation of European Biochemical Societies Letters 583(9): 1535-1543.
- San Miguel, S. M., Opperman, L. A., Allen, E. P., Zielinski, J., and Svoboda, K. K. 2011. Bioactive antioxidant mixtures promote proliferation and migration on human oral fibroblasts. Archives of Oral Biology 56(8): 812-822.
- Sanchez, T., and Moreno, J. J. 2001. The effect of high molecular phospholipase A2 inhibitors on 3T6 fibroblast proliferation. Biochemical Pharmacology 61(7): 811-816.
- Saoudi, M., Allagui, M. S., Abdelmouleh, A., Jamoussi, K., and El Feki, A. 2010. Protective effects of aqueous extract of *Artemisia campestris* against puffer fish *Lagocephalus lagocephalus* extract-induced oxidative damage in rats. Experimental and Toxicologic Pathology 62(6): 601-605.
- Schäfer, M., and Werner, S. 2008. Oxidative stress in normal and impaired wound repair. Pharmacological Research 58(2): 165-171.
- Sefi, M., Fetoui, H., Soudani, N., Chtourou, Y., Makni, M., and Zeghal, N. 2012. *Artemisia campestris* leaf extract alleviates early diabetic nephropathy in rats by inhibiting protein oxidation and nitric oxide end products. Pathology-Research and Practice 208(3): 157-162.
- Si, Q. S., Nakamura, Y., and Kataoka, K. 1997. Hypothermic suppression of microglial activation in culture: inhibition of cell proliferation and production of nitric oxide and superoxide. Neuroscience 81(1): 223-229.
- Singh, a., kumar, a., and duggal, s., 2009. *Nardostachys Jatamansi* DC. potential herb with cns effects. Journal of Pharmaceutical Research and Health Care 1(2): 276-290.
- Singh, H. P., Kaur, S., Mittal, S., Batish, D. R., and Kohli, R. K. 2010. *In vitro* screening of essential oil from young and mature leaves of *Artemisia scoparia* compared to its major constituents for free radical scavenging activity. Food and Chemical Toxicology 48(4): 1040-1044.
- Singh, M., Mukhtar, H. M., and Vashishth, D. 2012. Standardization of stem bark of *ficus bengalensis*. International Journal of Research in Pharmacy and Chemistry 2(3): 790-793.

- Sitia, S., Tomasoni, L., Atzeni, F., Ambrosio, G., Cordiano, C., Catapano, A., Tramontana, S., Perticone, F., Naccarato, P., Camici, P., Picano, E., Cortigiani, L., Bevilacqua, M., Milazzo, L., Cusi, D., Barlassina, C., Sarzi-Puttini, P., and Turiel, M. 2010. From endothelial dysfunction to atherosclerosis. Autoimmunity Reviews 9(12): 830-834.
- Suresh, J., Singh, A., Vasavi, A., Ihsanullah, M., and Mary, S. 2011. Phytochemical and pharmacological properties of *Artemisia pallens*. International Journal of Pharmaceutical Sciences and Research 2(12): 3081-3090.
- Suresh, J., Vasavi Reddy, A., Rajan, D., Ihsanullah, M., and Nayeemmullah Khan, M. 2011. Antimicrobial activity of *Artemisia abrotanum* and *Artemisia pallens*. International Journal of Pharmacognosy and Phytochemical Research 3(2): 18-21.
- Talwar, M., Moyana, T. N., Bharadwaj, B., and Tan, L. K. 1996. The effect of a synthetic analogue of prostaglandin E2 on wound healing in rats. Annals of Clinical and Laboratory Science 26(5): 451-457.
- Thai Pharmacopoeia Committee. 1995. Department of Medical Sciences. Ministry of Public Health. Thai Herbal Pharmacopoeia Vol I. Nonthaburi: Prachachon Co., Ltd.
- Turrens, J. F. 2003. Mitochondrial formation of reactive oxygen species. Journal of Physiology 552(2): 335-344.
- Valko, M., Leibfritz, D., Moncol, J., Cronin, M. T., Mazur, M., and Telser, J. 2007. Free radicals and antioxidants in normal physiological functions and human disease. International Journal of Biochemistry and Cell Biology 39(1): 44-84.
- Van den Worm, E., Beukelman, C.J., and Van den Berg, A.J. 2001. Effects of methoxylation of apocynin and analogs on the inhibition of reactive oxygen species production by stimulated human neutrophils. European Journal of Pharmacology 433:225–230.
- Wang, H., and Joseph, J. A. 1999. Quantifying cellular oxidative stress by dichlorofluorescein assay using microplate reader. Free Radical Biology and Medicine 27: 612-616.
- Wang, J., Guo, H., Zhang, J., Wang, X., Zhao, B., Yao, J., and Wang, Y. 2010. Sulfated modification, characterization and structure–antioxidant relationships

- of *Artemisia sphaerocephala* polysaccharides. Carbohydrate Polymers 81(4): 897-905.
- Wang, Z., Pan, Z., Ma, H., and Atungulu, G. G. 2011. Extract of Phenolics From Pomegranate Peels. The Open Food Science Journal 5: 17-25.
- Wang, J. H., Choi, M. K., Shin, J. W., Hwang, S. Y., and Son, C. G. 2012. Antifibrotic effects of *Artemisia capillaris* and *Artemisia iwayomogi* in a carbon tetrachloride-induced chronic hepatic fibrosis animal model. Journal of Ethnopharmacology 140(1): 179-185.
- Wang, S., Li, J., Sun, J., Zeng, K. W., Cui, J. R., Jiang, Y., and Tu, P. F. 2013. NO inhibitory guaianolide-derived terpenoids from *Artemisia argyi*. Fitoterapia 85: 169-175.
- Widlansky, M. E., Gokce, N., Keaney Jr., J. F., and Vita, J. A. 2003. The clinical implications of endothelial dysfunction. Journal of the American College of Cardiology 42(7): 1149-1160.
- Witting, P. K., Rayner, B. S., Wu, B. J., Ellis, N. A., and Stocker, R. 2007. Hydrogen peroxide promotes endothelial dysfunction by stimulating multiple sources of superoxide anion radical production and decreasing nitric oxide bioavailability. Cellular Physiology and Biochemistry 20(5): 255-268.
- World Health Organization. 1998. Quality Control Methods for Medicinal Plant Materials. World Health Organization.
- Xiaoping, C., Jianghua, C., Ping, Z., and Jizeng, D. 2006. Angelica stimulates proliferation of murine bone marrow mononuclear cells by the MAPK pathway. Blood Cells, Molecules, and Diseases 36(3): 402-405.
- Yakubu, M. A., and Leffler, C. W. 2005. Regulation of cerebral microvascular endothelial cell cyclooxygenase-2 message and activity by blood derived vasoactive agents. Brain Research Bulletin 68(3): 150-156.
- Yan, R., Li, S. L., Chung, H. S., Tam, Y. K., and Lin, G. 2005. Simultaneous quantification of 12 bioactive components of *Ligusticum chuanxiong* Hort. by high-performance liquid chromatography. Journal of Pharmaceutical and Biomedical Analysis 37(1): 87-95.

- Yarrow, J. C., Perlman, Z. E., Westwood, N. J., and Mitchison, T. J. 2004. A high-throughput cell migration assay using scratch wound healing, a comparison of image-based readout methods. BMC Biotechnology 4(1): 1-9.
- Ye, Y. N., Koo, M. W. L., Li, Y., Matsui, H., and Cho, C. H. 2001. *Angelica sinensis* modulates migration and proliferation of gastric epithelial cells. Life Sciences 68(8): 961-968.
- Yin, Y., Gong, F. Y., Wu, X. X., Sun, Y., Li, Y. H., Chen, T., and Xu, Q. 2008. Anti-inflammatory and immunosuppressive effect of flavones isolated from *Artemisia vestita*. Journal of Ethnopharmacology 120(1): 1-6.

APPENDICES

APPENDIX A

PREPARATION OF REAGENTS

Bradford reagent

To prepare 1,000 mL of Bradford reagent, the ingredients including 50 mg Coomassie Brilliant Blue G-250, 50 mL of 85% phosphoric acid and 25 mL of methanol were mixed and adjusted volume to 500 mL with ultrapure water. Store the solution in the dark at 4° C.

0.05 mg/mL DAN solution

DAN was freshly prepared before used. 0.05 mg of DAN was dissolved in 0.62 M HCl and protected from light.

5 µM DCFH-DA solution

To prepare 1 mL of 5 µM DCFH-DA, 0.49 mg of DCFH-DA was dissolved in DMSO and then aliquot into 0.1 mL/tube and store the solution at -20 °C.

1 mM EDTA solution

To prepare 20 mL of 1 mM EDTA, 7.44 mg of EDTA was dissolved in 20 mL of ultrapure water and store the solution at room temperature.

Growth medium of ECV304 cells

M199 medium powder was dissolved with ultrapure water and the 2.2 g sodium hydrogen carbonate was added. The medium was mixed and adjusted pH to 7.2 - 7.4 with HCl. After that, the medium was then adjusted volume to 1,000 mL with ultrapure water. The medium was sterilized by filtration with 0.22 µm Bottle-Top Vacuum Filters. Before using, the medium was supplement with 1% penicillin and streptomycin and 10% FBS or 0% FBS under serum-free condition.

Hoechst 33342 staining solution

Hoechst 33342 was dissolved in PBS and then aliquot into 0.1 mL/tube and store the solution at -20 °C.

0.62 M HCl solution

To prepare 100 mL of 0.62 M of HCl, 6.11 mL of HCl was mixed with 93.89 mL of ultrapure water and store the solution at room temperature.

0.4 mg/mL MTT solution

MTT was freshly prepared before used. 0.4 mg of MTT was dissolved in the incomplete medium and protected from light.

0.28 M NaOH solution

To prepare 50 mL of 0.28 M of NaOH, 5.6 g of NaOH was dissolved in ultrapure water and store the solution at room temperature.

Phosphate Buffer Saline (PBS)

To prepare 1,000 mL of PBS, The ingredients of PBS solution including 8.00 g of NaCl, 0.20 g of KCl, 1.15 g of Na₂HPO₄ and 0.20 g of KH₂PO₄ were dissolved in ultrapure water and adjusted the pH to 7.2-7.4 with NaOH. The solution was adjusted the volume to 1,000 mL and sterilized by autoclave.

Propidium iodide staining solution

Propidium iodide was dissolved in PBS and then aliquot into 0.1 mL/tube and store the solution at -20 °C.

Sodium nitrite standard

Sodium nitrite was freshly prepared before used. 0.69 mg of sodium nitrite was dissolved in ultrapure water. Dilute known amount of sodium nitrite with ultrapure water to make a series of sodium nitrite.

0.1 M Tris-HCl, pH 7.8

To prepare 100 mL of 0.1 M Tris-HCl pH 7.8 buffer, 12.11 g of Tris-base was dissolved in 80 mL of ultrapure water. Adjust to pH 7.8 with HCl and adjust the total volume to 100 mL. Store the buffer at 4° C.

0.25% Trypsin/ 0.038% EDTA solution

To prepare 100 mL of trypsin/EDTA solution, 0.250 g of trypsin and 0.038 g of EDTA were dissolved in PBS. The solution was sterilized by filtration with 0.22 μm syringe filter.

APPENDIX B
TABLE OF EXPERIMENTAL RESULTS

Table 8. The percentage of cell viability of AD at various concentrations for 24 h measured by MTT assay. Each value represented the mean \pm S.E.M. of three independent experiments. Each performed in triplicate.

concentration ($\mu\text{g/mL}$)	% cell viability	
	ADES	ADWS
0.001	99.91 \pm 3.06	92.1 \pm 0.34
0.01	96.02 \pm 4.18	89.57 \pm 1.22
0.1	97.25 \pm 6.61	87.59 \pm 2.22
1	94.4 \pm 7.91	90.85 \pm 1.82
10	100.01 \pm 6.79	90.72 \pm 1.62
100	100.51 \pm 5.79	93.76 \pm 1.77

Table 9. The percentage of cell viability of AL at various concentrations for 24 h measured by MTT assay. Each value represented the mean \pm S.E.M. of three independent experiments. Each performed in triplicate.

concentration ($\mu\text{g/mL}$)	% cell viability	
	ALES	ALWF
0.001	103.31 \pm 4.82	100.02 \pm 3.83
0.01	94.65 \pm 5.03	99.61 \pm 4.3
0.1	91.79 \pm 6.08	98.77 \pm 1.31
1	94.12 \pm 7.88	101.16 \pm 0.92
10	93.38 \pm 8.84	100.47 \pm 2.18
100	100.84 \pm 9.14	103.99 \pm 2.38

Table 10. The percentage of cell viability of AP at various concentrations for 24 h measured by MTT assay. Each value represented the mean \pm S.E.M. of three independent experiments. Each performed in triplicate. * $p < 0.05$ compared to the untreated control.

concentration ($\mu\text{g/mL}$)	% cell viability	
	APES	APWS
0.001	99.81 \pm 0.75	90.81 \pm 1.25
0.01	110.58 \pm 2.32*	86.20 \pm 3.56
0.1	113.57 \pm 1.45*	92.16 \pm 3.25
1	112.45 \pm 1.17*	88.64 \pm 2.29
10	115.64 \pm 1.70*	88.45 \pm 2.42
100	107.87 \pm 2.467	97.95 \pm 3.48

Table 11. The percentage of cell viability of AS at various concentrations for 24 h measured by MTT assay. Each value represented the mean \pm S.E.M. of three independent experiments. Each performed in triplicate.

concentration ($\mu\text{g/mL}$)	% cell viability	
	ASES	ASWS
0.001	98.2 \pm 1.59	105.88 \pm 1.68
0.01	96.36 \pm 1.07	101.65 \pm 0.37
0.1	99.73 \pm 1.67	102.11 \pm 0.46
1	99.63 \pm 0.79	102.9 \pm 1.33
10	98.51 \pm 2.27	105.82 \pm 1.95
100	104.41 \pm 0.41	102.87 \pm 0.61

Table 12. The percentage of cell viability of LC at various concentrations for 24 h measured by MTT assay. Each value represented the mean \pm S.E.M. of three independent experiments. Each performed in triplicate. * $p < 0.05$ compared to the untreated control.

concentration ($\mu\text{g/mL}$)	% cell viability	
	LCES	LCWS
0.001	110.54 \pm 2.52	105.73 \pm 5.12
0.01	106.99 \pm 3.3	105.62 \pm 4.77
0.1	107.16 \pm 2.91	103.57 \pm 3.25
1	106.63 \pm 2.61	103.17 \pm 2.63
10	107.96 \pm 3.77*	105.22 \pm 3.93
100	113.18 \pm 2.04*	110.07 \pm 2.81

Table 13. The percentage of cell viability of NJ at various concentrations for 24 h measured by MTT assay. Each value represented the mean \pm S.E.M. of three independent experiments. Each performed in triplicate.

concentration ($\mu\text{g/mL}$)	% cell viability	
	NJEF	NJWF
0.001	88.53 \pm 6.93	101.16 \pm 2.34
0.01	81.62 \pm 4.96	95.09 \pm 2.62
0.1	81.22 \pm 2.2	90.25 \pm 2.61
1	77.37 \pm 4.88	94.14 \pm 3.5
10	82.77 \pm 2.59	92.58 \pm 4.83
100	84.96 \pm 2.95	92.31 \pm 3.7

Table 14. The percentage of cell viability of PK at various concentrations for 24 h measured by MTT assay. Each value represented the mean \pm S.E.M. of three independent experiments. Each performed in triplicate.

concentration ($\mu\text{g/mL}$)	% cell viability	
	PKES	PKWS
0.001	93.25 \pm 2.86	96.62 \pm 2.41
0.01	85.17 \pm 5.12	94.43 \pm 2.48
0.1	83.75 \pm 4.6	90.36 \pm 3.26
1	82.78 \pm 1.95	93.71 \pm 4.93
10	88.12 \pm 1.69	93.72 \pm 4.48
100	88.31 \pm 2.4	96.07 \pm 3.42

Table 15. The percentage of cell viability of SC at various concentrations for 24 h measured by MTT assay. Each value represented the mean \pm S.E.M. of three independent experiments. Each performed in triplicate.

concentration ($\mu\text{g/mL}$)	% cell viability	
	SCES	SCWF
0.001	90.83 \pm 1.89	88.74 \pm 1.43
0.01	87.44 \pm 0.98	85.11 \pm 2.05
0.1	90.16 \pm 1.65	82.40 \pm 2.61
1	89.06 \pm 3.81	81.91 \pm 2.81
10	87.49 \pm 3.37	86.08 \pm 4.09
100	89.74 \pm 2.35	88.00 \pm 5.02

Table 16. The percentage of cell viability of TC at various concentrations for 24 h measured by MTT assay. Each value represented the mean \pm S.E.M. of three independent experiments. Each performed in triplicate.

concentration ($\mu\text{g}/\text{mL}$)	% cell viability	
	TCES	TCWS
0.001	88.17 \pm 1.97	81.9 \pm 2.95
0.01	84.00 \pm 4.95	78.13 \pm 3.75
0.1	81.57 \pm 4.68	75.87 \pm 4.48
1	82.85 \pm 7.28	76.85 \pm 2.09
10	85.55 \pm 6.16	79.32 \pm 4.78
100	86.78 \pm 8.84	81.13 \pm 8.51

Table 17. Time-dependent study of cell migration of APES with FBS for 6, 12 and 24 h measured by *in vitro* scratch assay. Each value represented the mean \pm S.E.M. of three independent experiments. Each performed in triplicate.

APES ($\mu\text{g}/\text{mL}$)	% wound closure		
	6 h	12 h	24 h
control	28.49 \pm 3.37	67.13 \pm 9.97	97.15 \pm 2.85
12.5	30.60 \pm 2.05	68.47 \pm 8.45	91.94 \pm 8.06
25	29.95 \pm 2.75	67.61 \pm 7.07	97.67 \pm 2.33
50	27.22 \pm 0.90	62.45 \pm 5.58	99.44 \pm 0.32
100	25.65 \pm 1.35	58.06 \pm 3.34	99.41 \pm 0.59
200	29.93 \pm 1.50	61.41 \pm 1.22	98.12 \pm 1.68

Table 18. Time-dependent study of cell migration of APES without FBS for 6, 12 and 24 h measured by *in vitro* scratch assay. Each value represented the mean \pm S.E.M. of three independent experiments. Each performed in triplicate. * $p < 0.05$ compared to the untreated control.

APES ($\mu\text{g/mL}$)	% wound closure		
	6 h	12 h	24 h
control	18.24 \pm 1.96	32.28 \pm 2.84	59.43 \pm 6.83
12.5	22.30 \pm 2.55	33.62 \pm 4.16	56.70 \pm 7.24
25	28.61 \pm 1.92*	40.19 \pm 2.46	60.26 \pm 8.86
50	27.41 \pm 1.69*	35.56 \pm 1.56	45.23 \pm 5.50
100	26.74 \pm 3.34*	31.18 \pm 4.68	33.00 \pm 10.13
200	14.30 \pm 0.60	17.28 \pm 1.20	18.17 \pm 1.30

Table 19. Time-dependent study of cell viability of APES with FBS for 6, 12 and 24 h measured by MTT assay. Each value represented the mean \pm S.E.M. of three independent experiments. Each performed in triplicate. * $p < 0.05$ compared to the untreated control.

APES ($\mu\text{g/mL}$)	% cell viability		
	6 h	12 h	24 h
control	100.00 \pm 0.00	100.00 \pm 0.00	100.00 \pm 0.00
12.5	95.93 \pm 2.64	105.16 \pm 1.97*	108.79 \pm 3.36*
25	99.51 \pm 3.57	105.37 \pm 0.92*	109.47 \pm 2.41*
50	100.22 \pm 2.27	104.57 \pm 0.27*	110.33 \pm 3.14*
100	98.54 \pm 2.36	106.55 \pm 1.00*	111.67 \pm 1.81*
200	102.11 \pm 2.30	104.46 \pm 1.38*	107.74 \pm 1.77*

Table 20. Time-dependent study of cell viability of APES without FBS for 6, 12 and 24 h measured by MTT assay. Each value represented the mean \pm S.E.M. of three independent experiments. Each performed in triplicate.

APES ($\mu\text{g/mL}$)	% wound closure		
	6 h	12 h	24 h
control	100.00 \pm 0.00	100.00 \pm 0.00	100.00 \pm 0.00
12.5	97.39 \pm 1.92	94.60 \pm 3.00	97.87 \pm 2.47
25	97.26 \pm 1.85	95.51 \pm 2.42	101.20 \pm 2.06
50	97.82 \pm 1.00	98.32 \pm 2.96	102.91 \pm 1.42
100	100.00 \pm 1.20	99.76 \pm 3.14	97.79 \pm 3.05
200	98.96 \pm 2.52	96.31 \pm 6.30	96.26 \pm 2.34

Table 21. The percentage of DCF fluorescence of APES at various concentrations for 6 h measured by DCFH-DA assay. Each value represented the mean \pm S.E.M. of three independent experiments. Each performed in triplicate. * $p < 0.05$ compared to the untreated control.

APES ($\mu\text{g/mL}$)	% DCF fluorescence
control	100.00 \pm 0.00
12.5	93.38 \pm 2.63
25	90.14 \pm 2.43*
50	87.87 \pm 1.74*
100	85.19 \pm 2.01*
200	85.35 \pm 1.17*

Table 22. Concentration-dependent study of APES on SOD activity in ECV304 cells for 6 h. Each value represented the mean \pm S.E.M. of three independent experiments. Each performed in triplicate. * $p < 0.05$ compared to the untreated control.

APES ($\mu\text{g/mL}$)	SOD activity (U/mg protein)
control	7.33 ± 0.22
25	$9.11 \pm 0.42^*$
50	8.38 ± 0.47
100	7.14 ± 0.41

Table 23. Calibration curve of NADPH. Each value represented the mean \pm S.E.M. of three independent experiments. Each performed in triplicate.

NADPH (nmol)	OD ₃₄₀
0	0.00 ± 0.00
20	0.23 ± 0.01
40	0.43 ± 0.02
60	0.64 ± 0.03
80	0.91 ± 0.04
100	1.09 ± 0.04

Table 24. Concentration-dependent study of APES on GPx activity in ECV304 cells for 6 h. Each value represented the mean \pm S.E.M. of three independent experiments. Each performed in triplicate.

APES ($\mu\text{g/mL}$)	GPx activity	
	(U)	(U/mg protein)
control	62.77 ± 3.32	6.98 ± 0.40
GPx Positive	127.51 ± 15.43	-
25	67.99 ± 2.93	7.83 ± 0.11
50	61.86 ± 3.43	8.10 ± 0.74
100	58.35 ± 1.59	7.01 ± 0.85

Table 25. Calibration curve of H_2O_2 . Each value represented the mean \pm S.E.M. of three independent experiments. Each performed in triplicate.

H_2O_2 (nmol)	OD_{570}
0	0.00 ± 0.00
20	0.21 ± 0.02
40	0.50 ± 0.02
60	0.75 ± 0.06
80	1.03 ± 0.05
100	1.25 ± 0.04

Table 26. Concentration-dependent study of APES on CAT activity in ECV304 cells for 6 h. Each value represented the mean \pm S.E.M. of three independent experiments. Each performed in triplicate.

APES ($\mu\text{g/mL}$)	CAT activity	
	(U)	(U/mg protein)
control	17.48 ± 2.19	1.91 ± 0.31
CAT Positive	30.96 ± 5.20	-
25	17.86 ± 2.48	2.09 ± 0.36
50	19.48 ± 2.63	2.25 ± 0.30
100	19.22 ± 2.51	2.22 ± 0.41

Table 27. Calibration curve of NO_2^- . Each value represented the mean \pm S.E.M. of three independent experiments. Each performed in triplicate.

NO_2^- (μM)	RFU 365 nm/ 450 nm
0	0.00 ± 0.00
0.125	5970.00 ± 93.76
0.25	9946.00 ± 181.01
0.5	14516.00 ± 884.46
1	26882.00 ± 631.62
2	51235.00 ± 1854.44

Table 28. Time-dependent study of APES on NO_2^- production for 0.5, 1, 2 and 6 h measured by DAN assay. Each value represented the mean \pm S.E.M. of three independent experiments. Each performed in triplicate.

APES ($\mu\text{g/mL}$)	NO_2^- (μM)			
	0.5	1	2	6
control	100.00 \pm 0.00	100.00 \pm 0.00	100.00 \pm 0.00	100.00 \pm 0.00
12.5	100.04 \pm 0.99	101.50 \pm 1.02	99.63 \pm 1.33	99.33 \pm 0.73
25	101.05 \pm 2.06	99.37 \pm 0.36	99.99 \pm 1.76	98.57 \pm 0.50
50	106.20 \pm 7.52	99.97 \pm 1.11	100.81 \pm 1.26	98.35 \pm 0.81
100	97.95 \pm 4.12	100.98 \pm 0.95	101.92 \pm 1.07	100.26 \pm 0.59
200	99.44 \pm 2.95	101.50 \pm 0.80	106.23 \pm 3.75	101.21 \pm 0.54

Table 29. Concentration-dependent study of APES on COX activity in ECV304 cells for 6 h. Each value represented the mean \pm S.E.M. of three independent experiments. Each performed in triplicate. * $p < 0.05$ compared to the untreated control.

APES ($\mu\text{g/mL}$)	COX activity (U/mg protein)
control	11.35 \pm 0.47
COX positive	72.11 \pm 2.85
25	9.75 \pm 0.98
50	14.34 \pm 1.17
100	19.42 \pm 0.53*

Table 30. Concentration-dependent study of APES on COX-1 and COX-2 activities in ECV304 cells for 6 h. Each value represented the mean \pm S.E.M. of three independent experiments. Each performed in triplicate. * $p < 0.05$ compared to the untreated control.

APES ($\mu\text{g/mL}$)	(U/mg protein)	
	COX-1	COX-2
control	2.49 ± 0.15	2.85 ± 0.23
25	1.82 ± 0.22	2.06 ± 0.24
50	2.07 ± 0.27	2.29 ± 0.25
100	$3.51 \pm 0.59^*$	$3.32 \pm 0.33^*$

APPENDIX C
FIGURE OF EXPERIMENTAL RESULTS

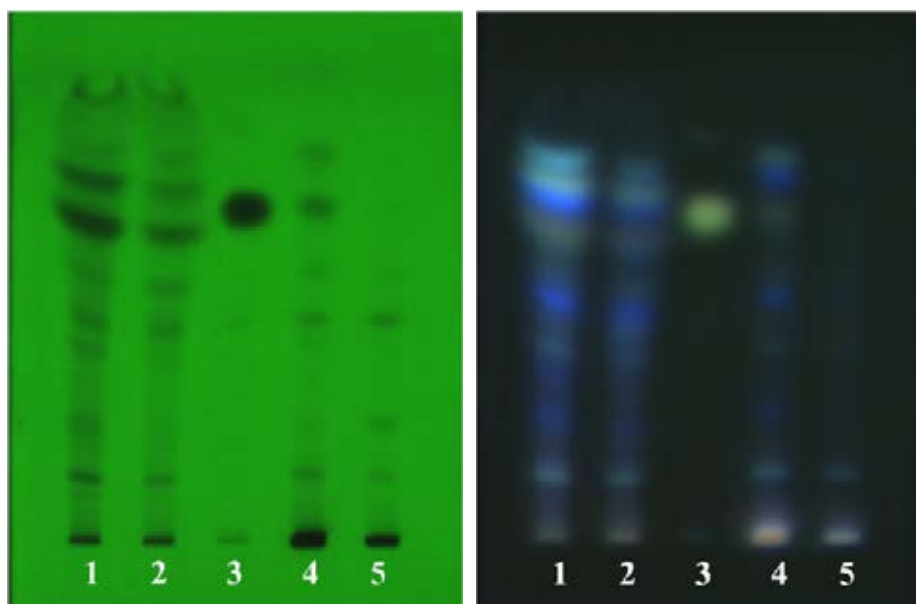


Figure 22. Thin-layer chromatograms of AD (left: detection under UV 254 nm, right: detection under UV 366 nm) stationary phase = silica gel 60 F254, mobile phase = toluene: ethyl acetate: acetic acid (75:25:5). Lane1 = sample of AD, 2 = Authentic sample of *Angelica dahurica* (Fish.) Benth. & Hook, 3 = standard of imperatorin, 4= ADES, 5 = ADWS

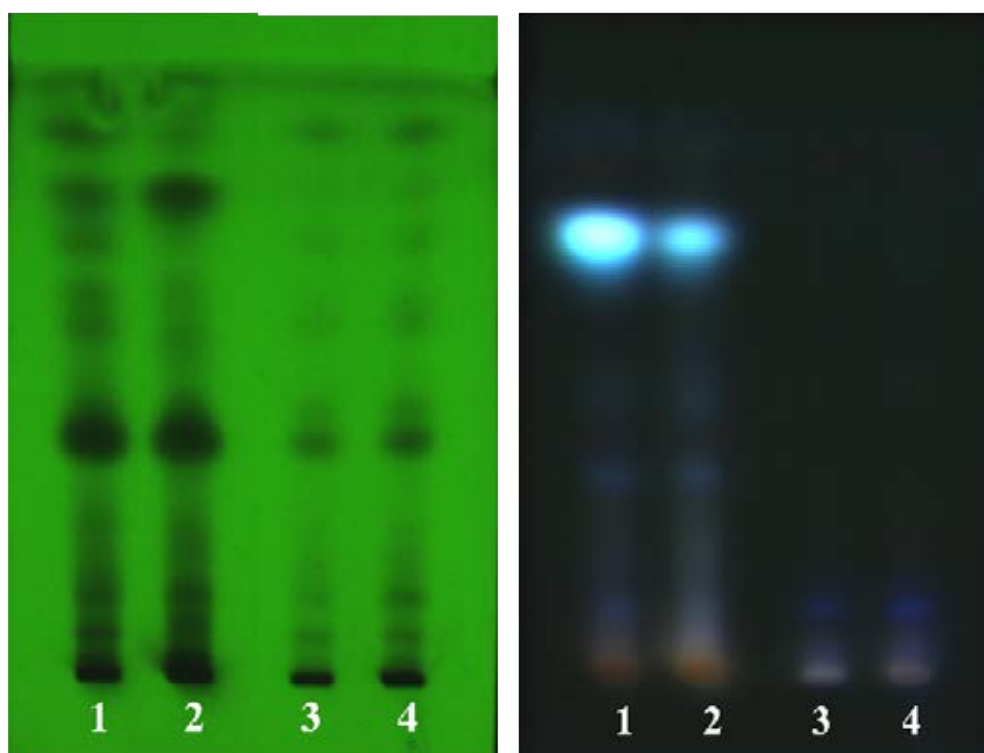


Figure 23. Thin-layer chromatograms of AL (left: detection under UV 254 nm, right: detection under UV 366 nm) stationary phase = silica gel 60 F254, mobile phase = hexane: ethyl acetate (58:42). Lane1 = sample of AL, 2 = Authentic sample of *Atractylodes lancea* (Thunb.) DC., 3 = ALES, 4 = ALWF

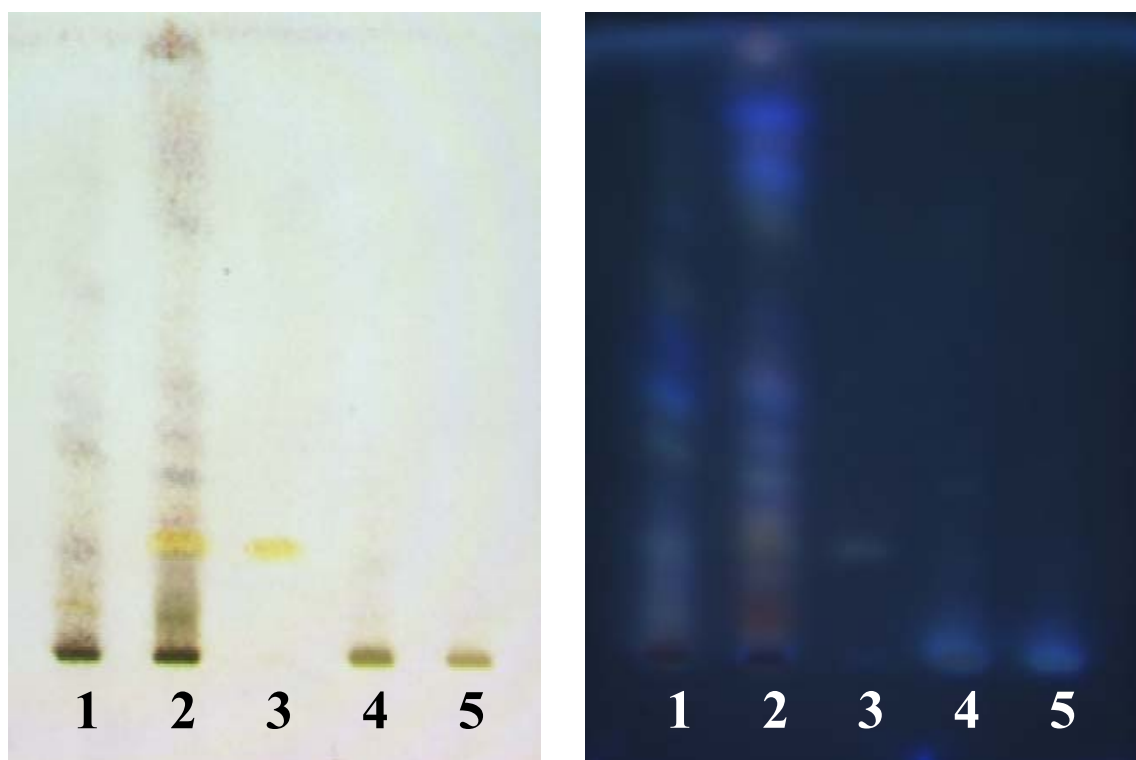


Figure 24. Thin-layer chromatograms of AP (left: detection with anisaldehyde – sulfuric acid, right: detection under UV 366 nm) stationary phase = silica gel 60 F254, mobile phase = hexane: acetone (56:44). Lane1 = sample of AP, 2 = Authentic sample of *Artemisia vulgaris* L., 3 = standard of arteminin, 4 = APES, 5 = APWS

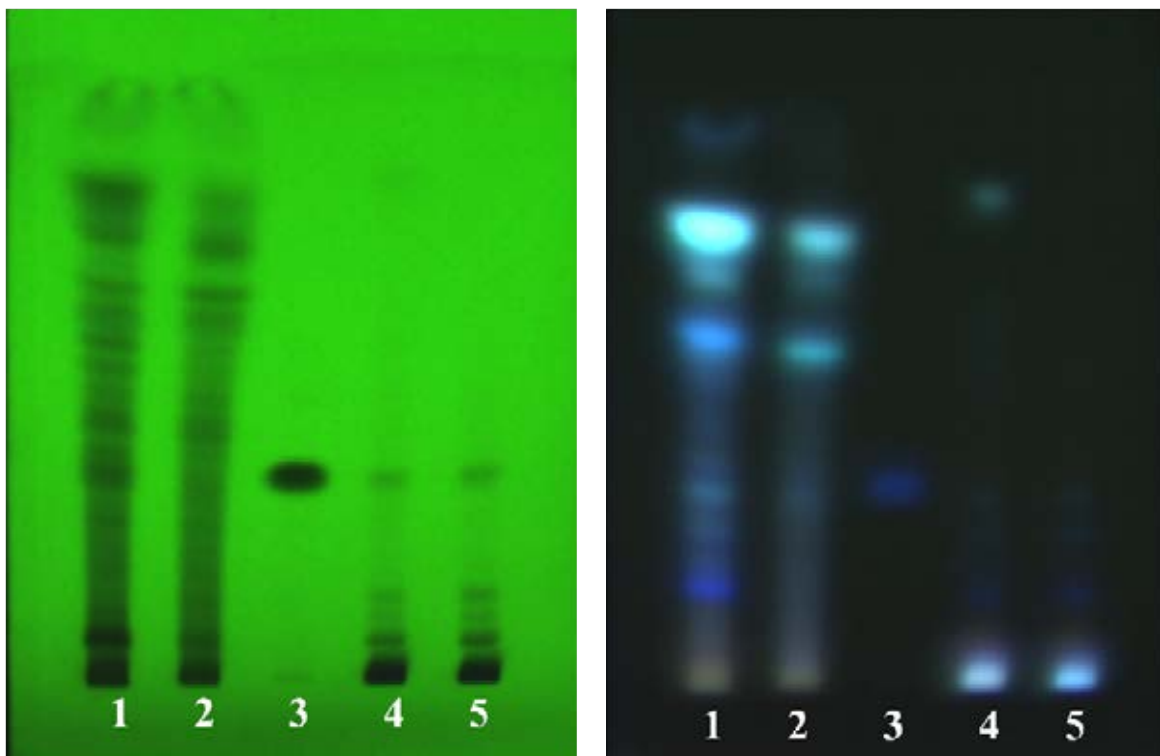


Figure 25. Thin-layer chromatograms of AS (left: detection under UV 254 nm, right: detection under UV 366 nm) stationary phase = silica gel 60 F254, mobile phase = toluene: ethyl acetate: formic acid (86:14:5). Lane1 = sample of AS, 2 = Authentic sample of *Angelica sinensis* (Oliv.) Diels, 3 = standard of ferulic acid, 4 = ASES, 5 = ASWS

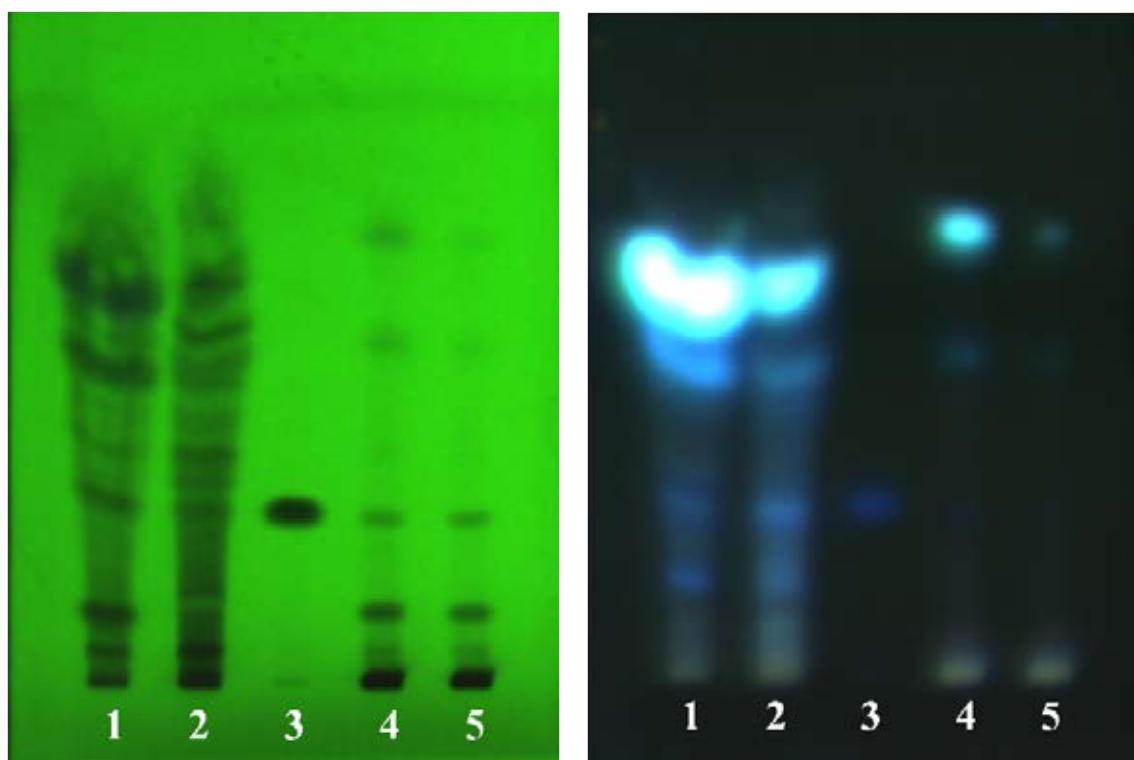


Figure 26. Thin-layer chromatograms of LC (left: detection under UV 254 nm, right: detection under UV 366 nm) stationary phase = silica gel 60 F254, mobile phase = toluene: ethyl acetate: formic acid (86:14:5). Lane1 = sample of LC, 2 = Authentic sample of *Ligusticum chuanxiong* Hort., 3 = standard of ferulic acid, 4 = LCES, 5 = LCWS

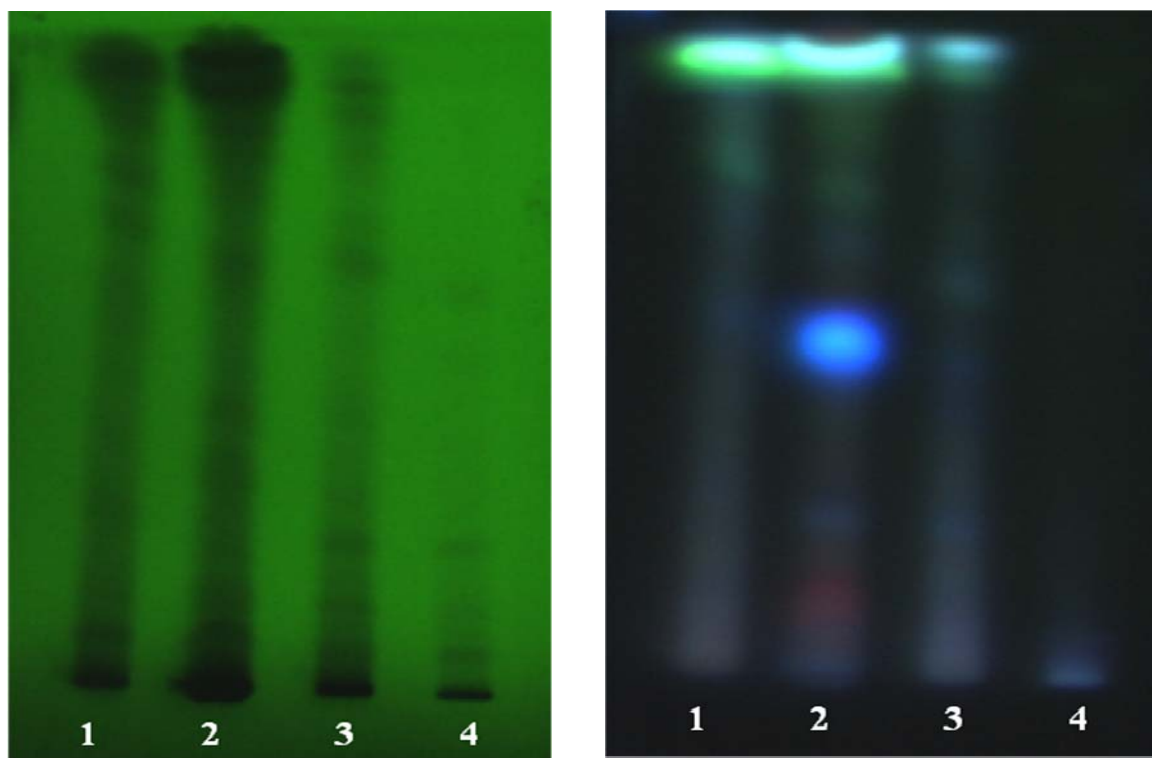


Figure 27. Thin-layer chromatograms of NJ (left: detection under UV 254 nm, right: detection under UV 366 nm) stationary phase = silica gel 60 F254, mobile phase = hexane: ethyl acetate: acetic acid (70:30:1). Lane1 = sample of NJ, 2 = Authentic sample of *Nardostachys jatamansi* (D. Don) DC., 3= NJEF, 4 = NJWF

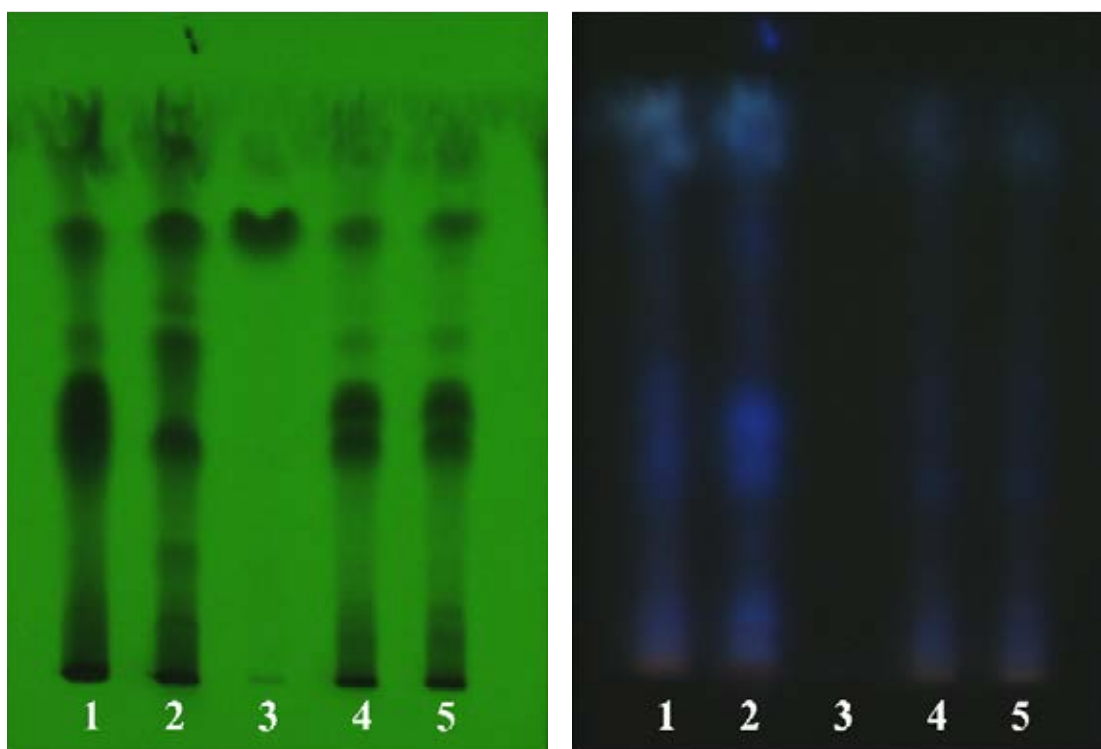


Figure 28. Thin-layer chromatograms of PK (left: detection under UV 254 nm, right: detection under UV 366 nm) stationary phase = silica gel 60 F254, mobile phase = chloroform: ethyl acetate: methanol: ammonia (50:30:20:1). Lane 1 = sample of PK, 2 = Authentic sample of *Picrorhiza kurrooa* Royle ex Benth., 3 = standard of vanillic acid, 4 = PKES, 5 = PKWS

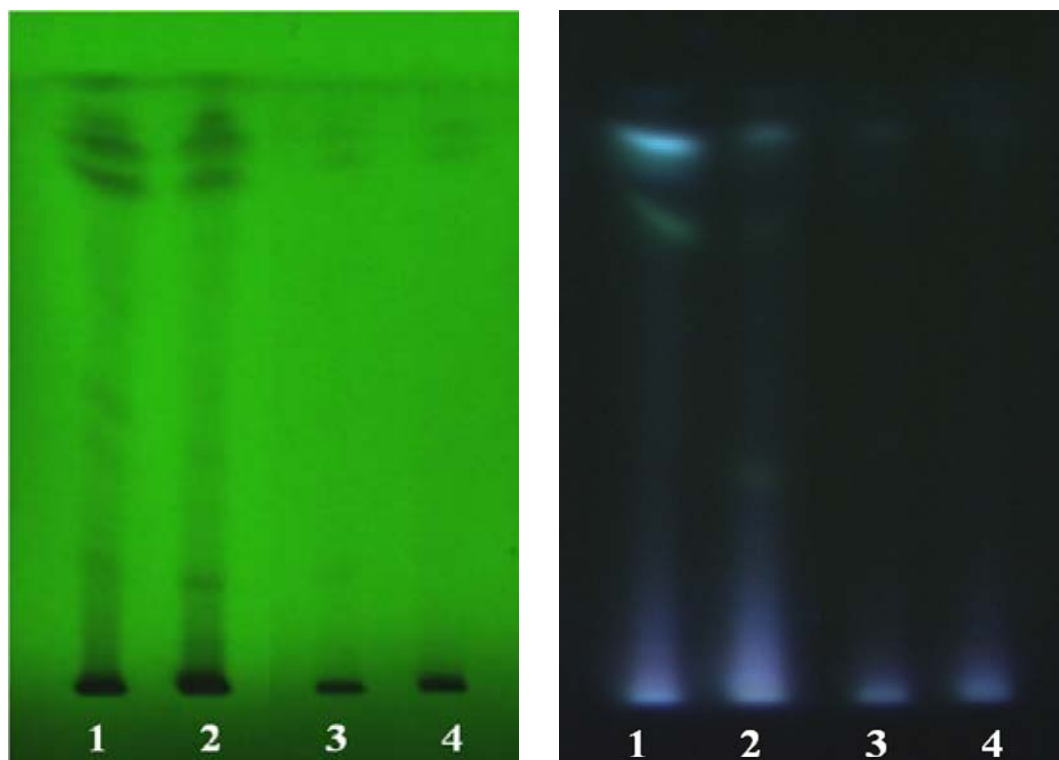


Figure 29. Thin-layer chromatograms of SC (left: detection under UV 254 nm, right: detection under UV 366 nm) stationary phase = silica gel 60 F254, mobile phase = dichloromethane: ethylacetate: methanol: ammonia (60:20:20:2). Lane1 = sample of SC, 2 = Authentic sample of *Saussurea costus* (Falc.) Lipsch., 3 = SCES, 4 = SCWF

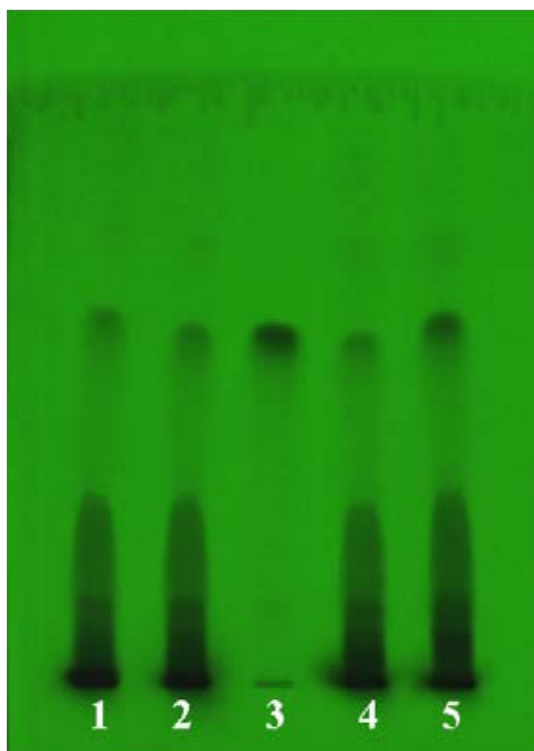
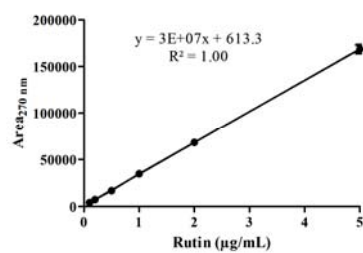
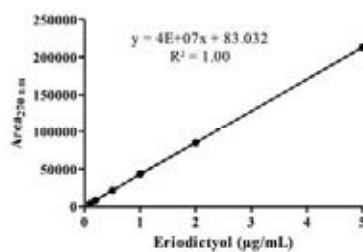


Figure 30. Thin-layer chromatograms of TC (detection under UV 254 nm) stationary phase = silica gel 60 F254, mobile phase = hexane: ethyl acetate: acetic acid (70:30:1). Lane1 = sample of TC, 2 = Authentic sample of *Terminalia chebula* Retz. var chebula, 3 = standard of gallic acid, 4 = TCES, 5 = TCWS

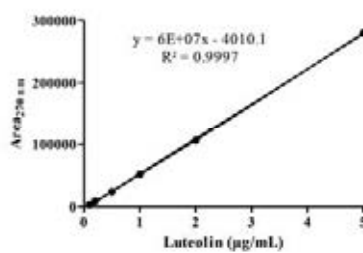
(A)



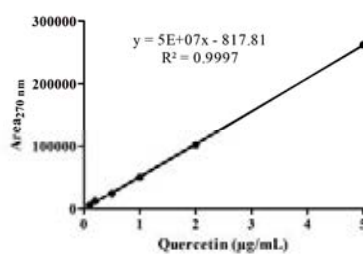
(B)



(C)



(D)



(E)

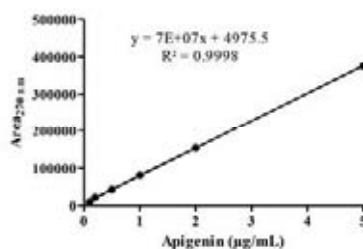


Figure 31. Calibration curve of (A) rutin, (B) eriodictyol, (C) luteolin, (D) quercetin and (E) apigenin. Results were expressed as mean \pm S.E.M. (N = 3, each performed in triplicate).

VITA

Miss Sarunya Tongumpai was born on July 24, 1986 in NakhonPathom, Thailand. In 2009, she recieved Bachelor of Science Program in Medical Sciences from the Faculty of Medical Science, Naresuan University.